

Intelligent Signal Processing

Non-Linear PCA and ICA

Angelo Ciaramella

Principal Component Analysis

- Principal Component Analysis (PCA) is a statistical technique
 - Dimensionality reduction
 - Lossy data compression
 - Feature extraction
 - Data visualization
- It is also known as the *Karhunen-Loeve* transform
- PCA can be defined as the principal subspace such that the variance of the projected data is maximized

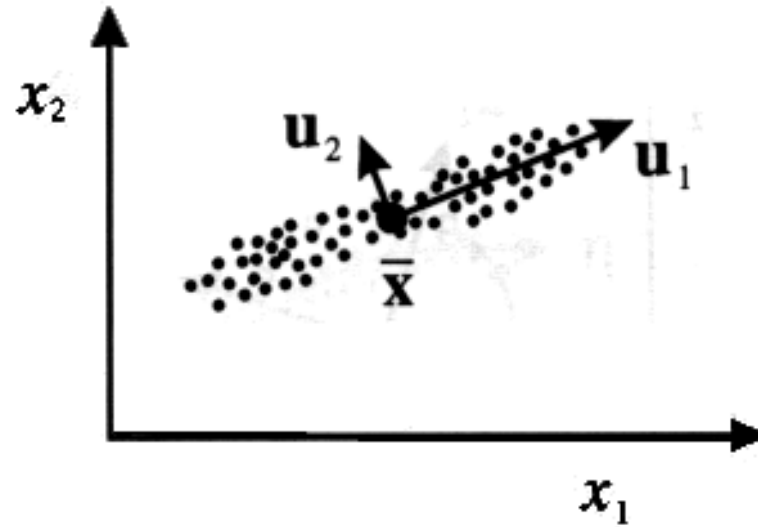


Second-Order methods

- The **second-order methods** are the most popular methods to find a **linear transformation**
- This methods find the representation using only the information contained in the **covariance matrix** of the data vector \mathbf{x}
- **PCA** is widely used in signal processing, statistics, and neural computing



Principal Components



In a linear projection down to one dimension, the optimum choice of projection, in the sense of minimizing the sum-of-squares error, is obtained first subtracting off the mean of the data set, and then projecting onto the first eigenvector \mathbf{u}_1 of the covariance matrix.



Projection error minimization

- We introduce a complete orthonormal set of D -dimensional basis vectors ($i=1, \dots, D$)

$$\mathbf{u}_i^T \mathbf{u}_j = \delta_{ij}$$

- Because this basis is complete, each data point can be represented by a linear combination of the basis vectors

$$\mathbf{x}_n = \sum_{i=1}^D \alpha_{ni} \mathbf{u}_i$$



Projection error minimization

- We can write also that

$$\mathbf{x}_n = \sum_{i=1}^D (\mathbf{x}_n^T \mathbf{u}_i) \mathbf{u}_i \quad \leftarrow \quad \alpha_{nj} = \mathbf{x}_n^T \mathbf{u}_j$$

- Our goal is to **approximate** this data point using a representation involving a restricted number $M < D$ of variables corresponding to a **projection** onto a lower-dimensional subspace

$$\tilde{\mathbf{x}}_n = \sum_{i=1}^M z_{ni} \mathbf{u}_i + \sum_{i=M+1}^D b_i \mathbf{u}_i$$



Projection error minimization

- As our distortion measure we shall use the **squared distance** between the original point and its approximation averaged over the data set so that our goal is to minimize

$$J = \frac{1}{N} \sum_{n=1}^N \|\mathbf{x}_n - \tilde{\mathbf{x}}_n\|^2$$

- The **general solution** is obtained by choosing the basis to be eigenvectors of the covariance matrix given by

$$\mathbf{S}\mathbf{u}_i = \lambda_i \mathbf{u}_i$$



Projection error minimization

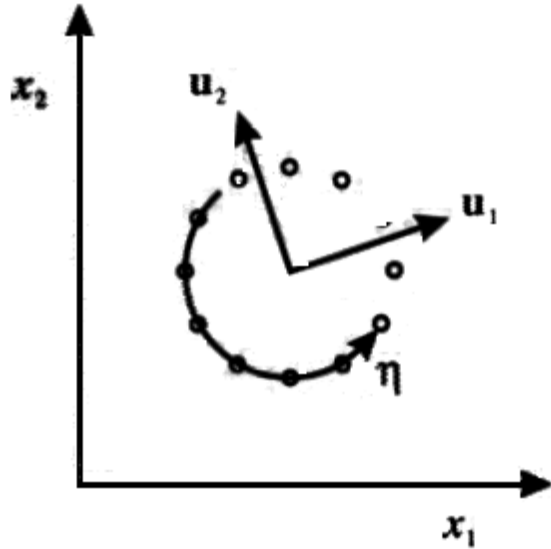
- The corresponding value of the **distortion measure** is then given by

$$J = \sum_{i=M+1}^D \lambda_i$$

- We **minimize** this error selecting the **eigenvectors** defining the principal subspace are those corresponding to the M largest eigenvalues

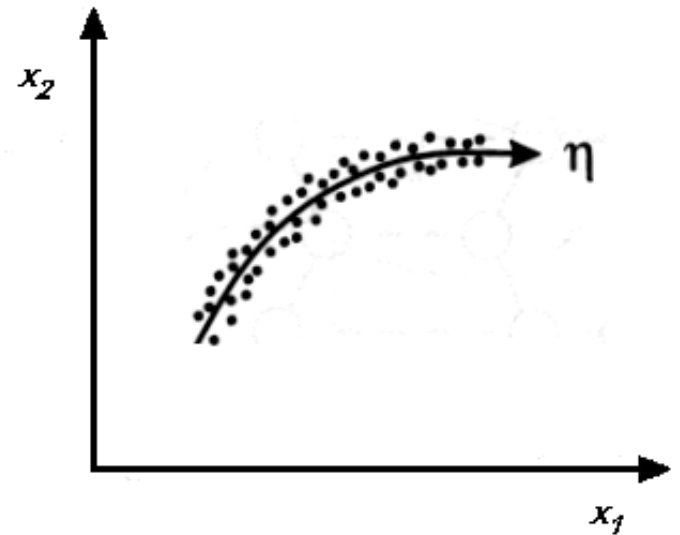


Complex distributions



A linear dimensionality reduce technique, such as PCA, is unable to detect the lower dimensionality. In this case PCA gives two eigenvectors with equal eigenvalues. The data can be described by a single eigenvalue

Addition of a small level of noise to data having an intrinsic dimensionality of 1 can increase its intrinsic dimensionality to 2. The data can be represented to a good approximation by a single variable η and can be regarded as having an intrinsic dimensionality of 1.

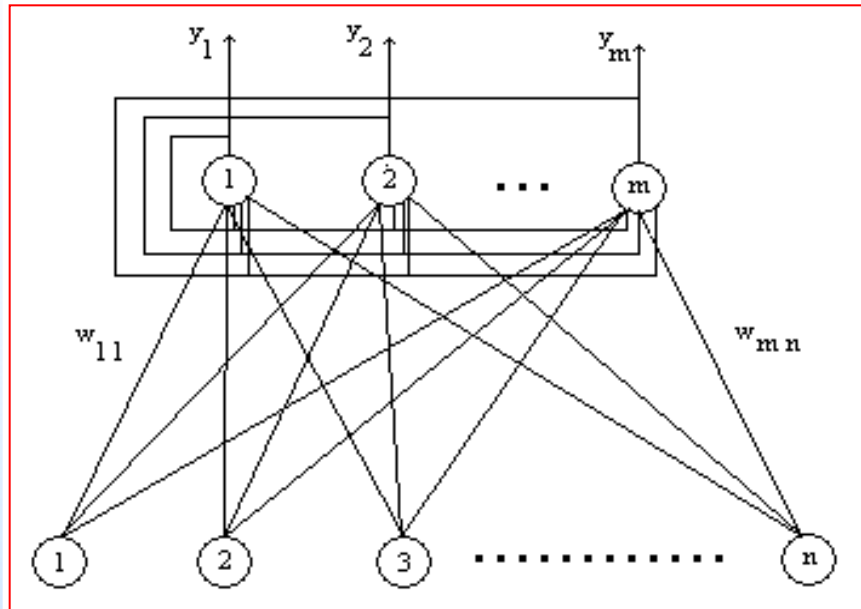


Unsupervised Neural Networks

- Typically **Hebbian** type **learning** rules are used
- There are two type of NN able to extract the Principal Components:
 - **Symmetric** (Oja, 1989)
 - **Hierarchical** (Sanger, 1989)



PCA and Unsupervised Neural Network

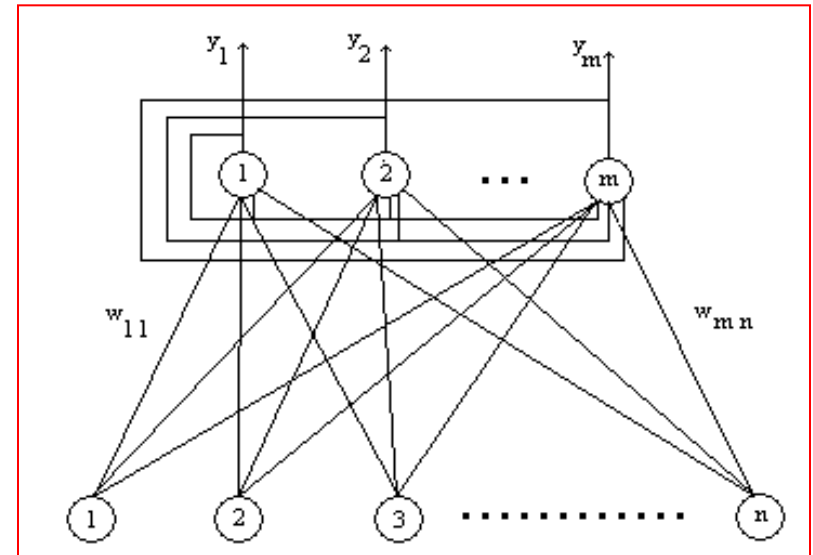


Symmetric PCA NN

$$E[\mathbf{y}^2] = E[(\mathbf{w}^T \mathbf{x})^2]$$

Objective function

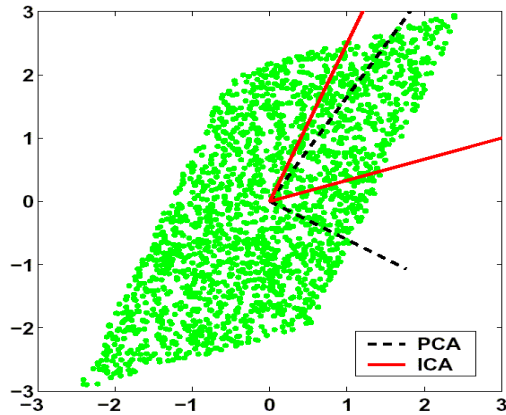
Single layer Neural Network



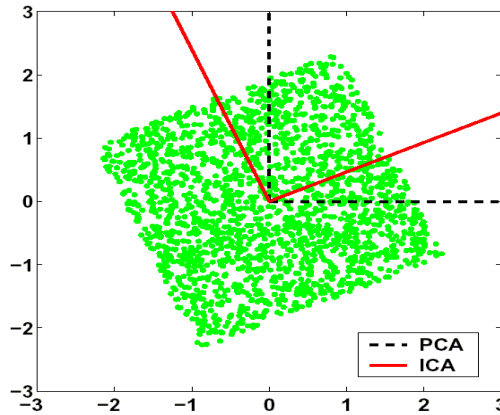
Hierarchical PCA NN



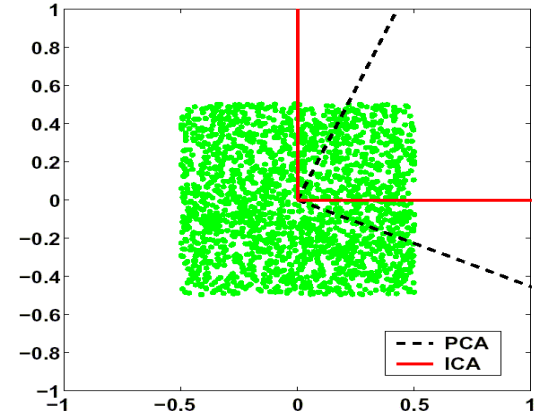
ICA versus PCA



(a) Original



(b) After PCA pre-whitening

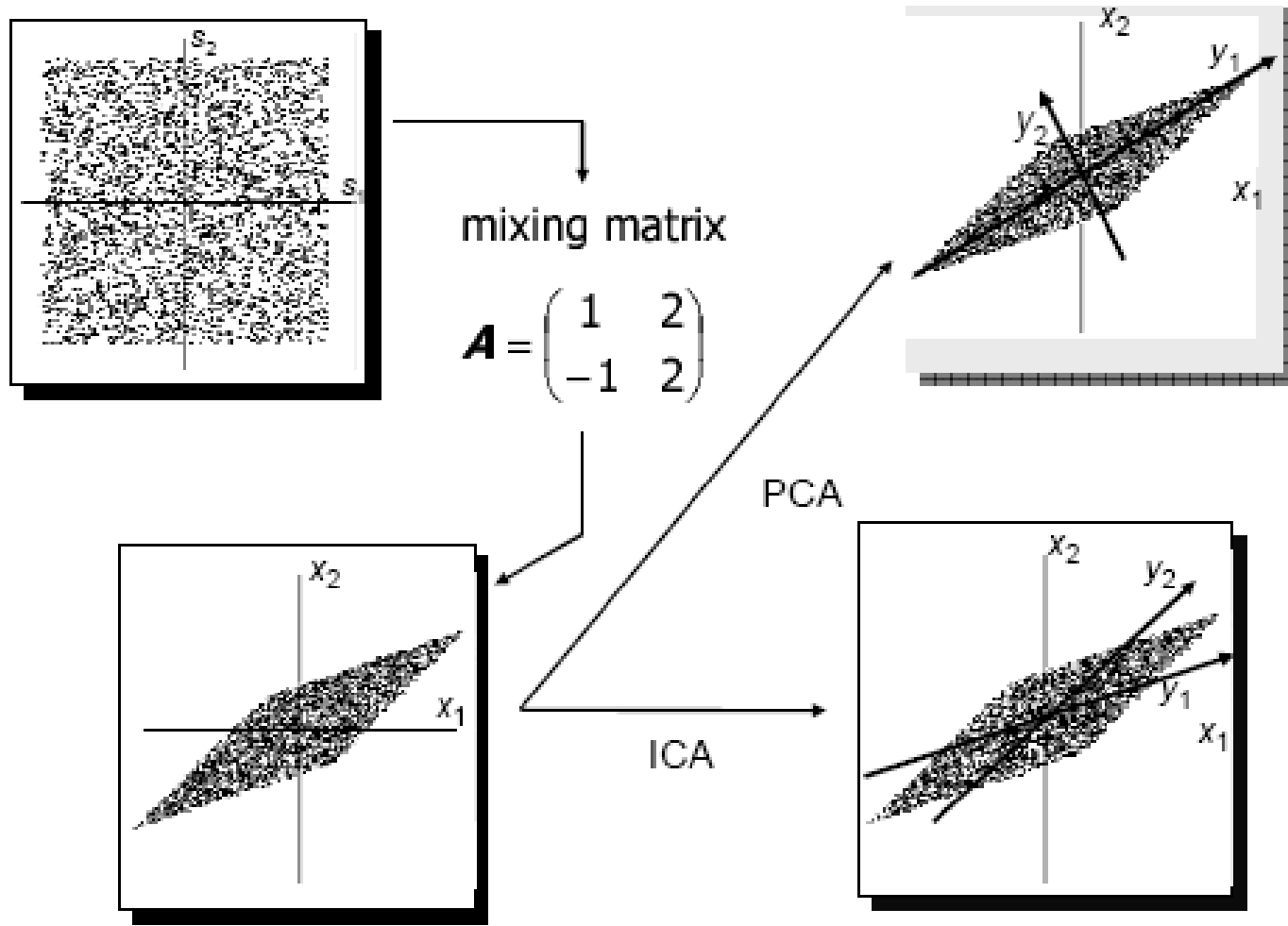


(c) After ICA projection

PCA maximises the variance and projections onto the basis vectors are mixtures. ICA correctly finds the two vectors onto which the *projections are independent*.



Mixing matrix



Non-linear objective function

Maximization

$$\mathbf{x} \xrightarrow{\mathbf{w} \text{ (weights)}} E \{ f(\mathbf{w}^T \mathbf{x}) \}$$

L-dimensional vector

where E is the expectation with respect to the (unknown) density of \mathbf{x} and $f(\cdot)$ is a continue function (e.g. $\ln \cosh(\cdot)$)

Taylor series

$$\ln \cosh(y) = \frac{1}{2} y^2 - \frac{1}{12} y^4 + \frac{1}{45} y^6 + O(y^8)$$

$$E \{ \ln \cosh(y) \} = \frac{1}{2} E \{ (w^T x)^2 \} - \frac{1}{12} E \{ (w^T x)^4 \} + \frac{1}{45} E \{ (w^T x)^6 \} + E \{ O((w^T x)^2) \}$$

$$C = I \quad \text{and} \quad \frac{1}{2} E \{ (w^T x)^2 \} = \frac{1}{2}$$

$$-\frac{1}{12} E \{ (w^T x)^4 \}$$

That is dominating, and the kurtosis is optimized



Unsupervised Neural Network

Robust PCA

$$J_1(\mathbf{w}) = E[f(\mathbf{x}^T \mathbf{w})] + \sum_{j=1}^{I(i)} \lambda_{ij} [\mathbf{w}_i^T \mathbf{w}_j - \delta_{ij}]$$

$$\mathbf{w}(k+1) = \mathbf{w}(k) + \mu_k g(\mathbf{y}_i(k)) e_i(k)$$

$$e(k) = \mathbf{x}_k - \sum_{j=1}^{I(i)} \mathbf{y}_j(k) \mathbf{w}_j(k)$$

Standard PCA

$$E[\mathbf{y}^2] = E[(\mathbf{w}^T \mathbf{x})^2]$$

$$J_2(e_i) = 1^T E[f(\mathbf{x} - \hat{\mathbf{x}}_i)]$$

$$\mathbf{w}(k+1) = \mathbf{w}(k) + \mu_k \left(\mathbf{w}_i(k)^T g(e_i(k)) \mathbf{x}_k + \mathbf{x}_k^T \mathbf{w}_i(k) g(e_k(i)) \right)$$

Nonlinear PCA

$$E[|b_i(k)|^2]$$

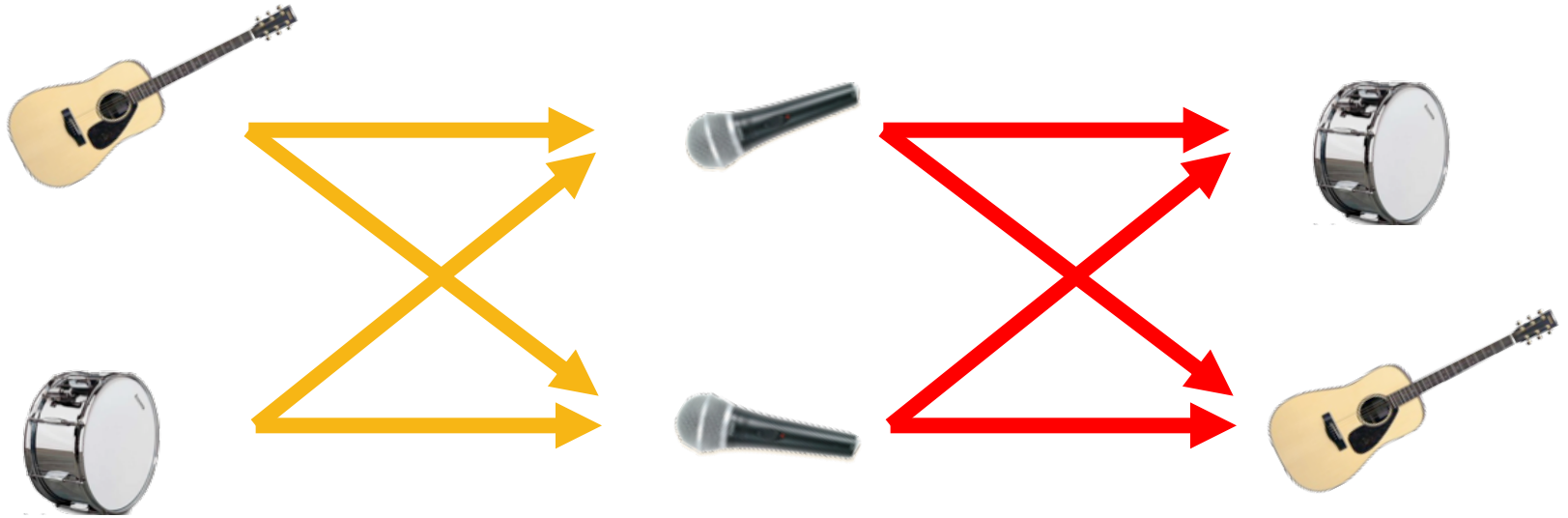
$$b_i(k) = \mathbf{x}_k - \sum_{j=1}^{I(i)} g(\mathbf{y}_j(k)) \mathbf{w}_j(k)$$

$$\mathbf{w}_i(k+1) = \mathbf{w}_i(k) + \mu g(\mathbf{y}_i(k)) b_i(k)$$

Descent gradient algorithm



Cocktail party



Sources

Mixtures

Estimated-Sources

s

A

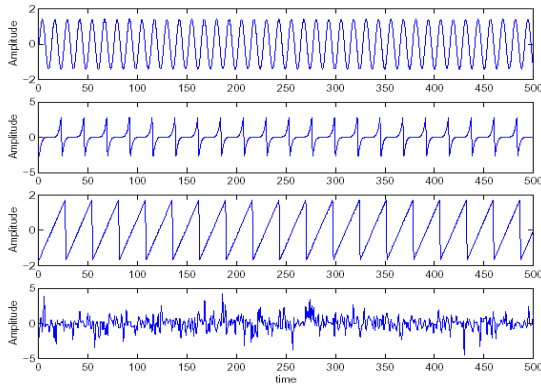
x

W

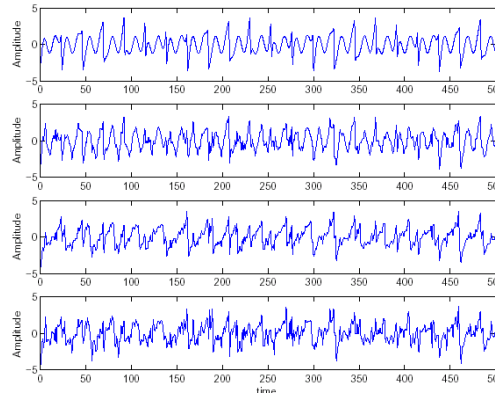
y



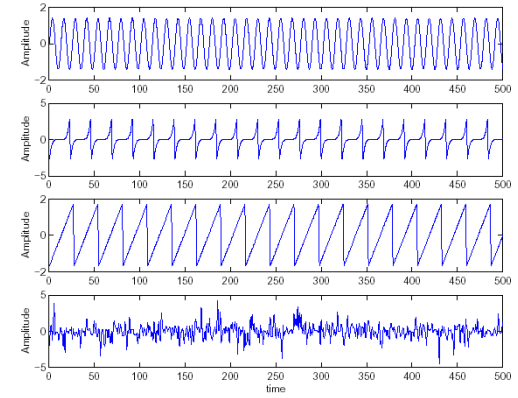
Source estimation



Source signals



Mixed signals



Estimated signals

$$\begin{aligned}x_1(t) &= a_{11}s_1(t) + a_{12}s_2(t) + a_{13}s_3(t) \\x_2(t) &= a_{21}s_1(t) + a_{22}s_2(t) + a_{23}s_3(t) \\x_3(t) &= a_{31}s_1(t) + a_{32}s_2(t) + a_{33}s_3(t)\end{aligned}$$

$$\begin{aligned}y_1(t) &= w_{11}x_1(t) + w_{12}x_2(t) + w_{13}x_3(t) \\y_2(t) &= w_{21}x_1(t) + w_{22}x_2(t) + w_{23}x_3(t) \\y_3(t) &= w_{31}x_1(t) + w_{32}x_2(t) + w_{33}x_3(t)\end{aligned}$$

$x_1(t), x_2(t), x_3(t)$ are the observed signals,
 $s_1(t), s_2(t), s_3(t)$ the source signals

$y_1(t), y_2(t), y_3(t)$ are the separated signals



Independent Component Analysis

- Independent Component Analysis (ICA)
 - statistical and computational technique for revealing hidden factors that underlie sets of random variables, measurements, or signals
- ICA can be seen an extension of **Principal Component Analysis (PCA)** and **Factor Analysis (FA)**
- The technique of ICA was firstly introduced in early 1980s in the context of the **Neural Networks (NNs)** modeling
- ICA is becoming one of the exciting new topics, both in the field of NNs, mainly unsupervised learning, and in advanced statistics and signal processing



Probability distributions and densities

- **random variable (rv)** or **stochastic variable** is a variable whose value results from a measurement on some type of random process
- The **cumulative distribution function (cdf)** F_x of a random variable x at point $x = x_0$ is defined as the probability

$$F_x(x_0) = P(x \leq x_0)$$

- For continuous rv the cdf is a nonnegative, nondecreasing continuous function

$$0 \leq F_x(x_0) \leq 1$$



Probability distributions and densities

- The **probability density function (pdf)** $p_x(x)$ is obtained as the derivative of its cumulative distribution function

$$p_x(x_0) = \left. \frac{dF_x(x)}{dx} \right|_{x=x_0}$$

- The cdf is computed by using

$$F_x(x_0) = \int_{-\infty}^{x_0} p_x(\xi) d\xi$$



Distribution of a random vector

- Assume now that \mathbf{x} is a n-dimensional **random vector** of continuous random variables

$$\mathbf{x} = (x_1, x_2, \dots, x_n)^T$$

- The cdf is computed by using

$$F_{\mathbf{x}}(\mathbf{x}_0) = P(\mathbf{x} \leq \mathbf{x}_0)$$

$$p_{\mathbf{x}}(\mathbf{x}_0) = \frac{\partial}{\partial x_1} \frac{\partial}{\partial x_2} \dots \frac{\partial}{\partial x_n} F_{\mathbf{x}}(\mathbf{x}) \Big|_{\mathbf{x}=\mathbf{x}_0}$$



Joint and marginal distributions

- The cdf called the **joint distribution function** of \mathbf{x} and \mathbf{y} is

$$F_{\mathbf{x},\mathbf{y}}(\mathbf{x}_0, \mathbf{y}_0) = P(\mathbf{x} \leq \mathbf{x}_0, \mathbf{y} \leq \mathbf{y}_0)$$

- The **joint density function** $p_{\mathbf{x},\mathbf{y}}(\mathbf{x}, \mathbf{y})$ is defined by differentiating the joint distribution function
- The **marginal densities** are (e.g. on \mathbf{x})

$$p_{\mathbf{x}}(\mathbf{x}) = \int_{-\infty}^{\infty} p_{\mathbf{x},\mathbf{y}}(\mathbf{x}, \eta) d\eta$$



Expectation and moments

- Let $\mathbf{g}(\mathbf{x})$ denote any quantity derived from the random vector \mathbf{x} the **expectation** of $\mathbf{g}(\mathbf{x})$ is

$$E\{\mathbf{g}(\mathbf{x})\} = \int_{-\infty}^{\infty} \mathbf{g}(\mathbf{x}) p_{\mathbf{x}}(\mathbf{x}) d\mathbf{x}$$

- Moments** are expectations used to characterize a random vector. The **mean vector** is

$$\mathbf{m}_{\mathbf{x}} = E\{\mathbf{x}\} = \int_{-\infty}^{\infty} \mathbf{x} p_{\mathbf{x}}(\mathbf{x}) d\mathbf{x}$$

- The **$n \times n$ correlation matrix** is

$$\mathbf{R}_{\mathbf{x}} = E\{\mathbf{x}\mathbf{x}^T\} = \mathbf{C}_{\mathbf{x}} + \mathbf{m}_{\mathbf{x}}\mathbf{m}_{\mathbf{x}}^T$$

$$\mathbf{C}_{\mathbf{x}} = E\{(\mathbf{x} - \mathbf{m}_{\mathbf{x}})(\mathbf{x} - \mathbf{m}_{\mathbf{x}})^T\}$$

Covariance matrix



Uncorrelatedness and independence

- Two random vectors \mathbf{x} and \mathbf{y} are **uncorrelated** if their cross-covariance matrix is a zero matrix

$$\mathbf{C}_{xy} = E\{(\mathbf{x} - \mathbf{m}_x)(\mathbf{y} - \mathbf{m}_y)^T\} = \mathbf{0}$$

- The rvs x and y are said **independent** if and only if

$$p_{x,y}(x, y) = p_x(x)p_y(y)$$

- For random vectors is

$$p_{\mathbf{x},\mathbf{y},\mathbf{z},\dots}(\mathbf{x}, \mathbf{y}, \mathbf{z}, \dots) = p_{\mathbf{x}}(\mathbf{x})p_{\mathbf{y}}(\mathbf{y})p_{\mathbf{z}}(\mathbf{z})\dots$$

- Uncorrelated Gaussian rvs are also independent. This property is not shared by other distributions in general



Higher-order statistics

- Consider a scalar rv x , the j -th moment is defined as ($j=1,2,\dots$)

$$\alpha_j = E\{x^j\} = \int_{-\infty}^{\infty} \xi^j p_x(\xi) d\xi$$

- The j -th central moment

$$\mu_j = E\{(x - \alpha_1)^j\} = \int_{-\infty}^{\infty} (\xi - m_x)^j p_x(\xi) d\xi$$



Skewness

- The third central moment is called the **skewness** (asymmetry of the pdf)

$$\mu_3 = E\{(x - m_x)^3\}$$

- The **4-th moment and central moment** are applied in ICA



Kurtosis

- Usually the 4-order statistic (i.e. cumulants) is employed and it is called **Kurtosis**

$$\mathbf{kurt}(x) = E\{x^4\} - 3[E\{x^2\}]^2$$

- A distribution having kurtosis
 - **Zero** is called **mesocurtic**
 - **Negative platykurtic** (subgaussian)
 - **Positive leptokurtic** (supergaussian)



Differential entropy

- The **differential entropy** of a rv is defined as

$$H(x) = -\int p_x(\xi) \log p_x(\xi) d\xi = -E\{\log p_x(x)\}$$

- Can be interpreted as a **measure of randomness**.
If the rv is concentrated on certain small intervals, its differential entropy is small



Mutual Information

- **Mutual information** is a measure of the information that members of a set of random variables have on other random variables in the set

$$I(x_1, x_2, \dots, x_n) = \sum_{i=1}^n H(x_i) - H(\mathbf{x})$$

where \mathbf{x} is the vector containing all the x_i

- If x_i are independent they give no information on each other



Kullback-Leibler divergence

- Mutual information can be considered a distance using the **Kullback-Leibler divergence**

$$\delta(p^1, p^2) = \int p^1(\xi) \log \frac{p^1(\xi)}{p^2(\xi)} d\xi$$

- Can be considered as a distance between pdfs
 - Is always nonnegative
 - Is zero if and only if the two distributions are equal
 - Can be symmetrized



Negentropy

- The **Negentropy** is a measure that is zero for a Gaussian variable and always nonnegative

$$J(\mathbf{x}) = H(\mathbf{x}_{Gauss}) - H(\mathbf{x})$$

- A **simple approximation** is (standardized rv)

$$J(x) \approx \frac{1}{12} E\{x^3\}^2 + \frac{1}{48} \mathbf{kurt}(x)^2$$



Negentropy

- A more robust approximation is

$$J(x) \approx k_1 \left(E\{G^1(x)\} \right)^2 + k_2 \left(E\{G^2(x)\} - E\{G^2(v)\} \right)^2$$

where k_1 and k_2 are positive constants, G^1 and G^2 are odd and even function, respectively (e.g. $G^1(x) = x^3$ and $G^2(x) = x^4$)



Newton's method

- **Newton's method** is one of the most efficient ways for function minimization $F(\mathbf{w})$
- The updating rule is (by using the gradient and the *Hessian*)

$$\Delta \mathbf{w} = - \left[\frac{\partial^2 F(\mathbf{w})}{\partial \mathbf{w}^2} \right]^{-1} \frac{\partial F(\mathbf{w})}{\partial \mathbf{w}}$$

- The convergence of the Newton's method is quadratic



The Lagrange method

- In many cases we have **constrained optimizations**

$$\begin{aligned} \min F(\mathbf{w}) \\ \text{subject to } H_i(\mathbf{w}) = 0, \quad i = 1, \dots, k \end{aligned}$$

- The most used way to take the constraints into account is the method of **Lagrange multipliers** $(\lambda_1, \dots, \lambda_k)$

- We form the **Lagrange function**

$$L(\mathbf{w}, \lambda_1, \dots, \lambda_k) = F(\mathbf{w}) + \sum_{i=1}^k \lambda_i H_i(\mathbf{w})$$



$$\frac{\partial L(\mathbf{w}, \lambda_1, \dots, \lambda_k)}{\partial \mathbf{w}} = 0$$



- We want to maximize the negentropy using this approximation

$$J_G(\mathbf{w}) = \left[E\{G(\mathbf{w}^T \mathbf{x})\} - E\{G(v)\} \right]^2$$

- The multi-unit problem is

$$\max \sum_{i=1}^n J_G(\mathbf{w}_i) \quad \mathbf{w}_i, i = 1, \dots, n$$

such that $E\{(\mathbf{w}_k^T \mathbf{x})(\mathbf{w}_j^T \mathbf{x})\} = \delta_{jk}$

- A fixed point algorithm is obtained by applying the **Newton's** method to the **Lagrangian** of this optimization problem (**FastICA**)



- In many cases we have **constrained optimizations**

$$G(y) = \frac{1}{a_1} \log \cosh a_1 y$$

$$G(y) = -\exp(-y^2 / 2)$$

$$G(y) = y^4$$

$$g(y) = \tanh(a_1 y)$$

$$g(y) = y \exp(-y^2 / 2)$$

$$g(y) = y^3$$

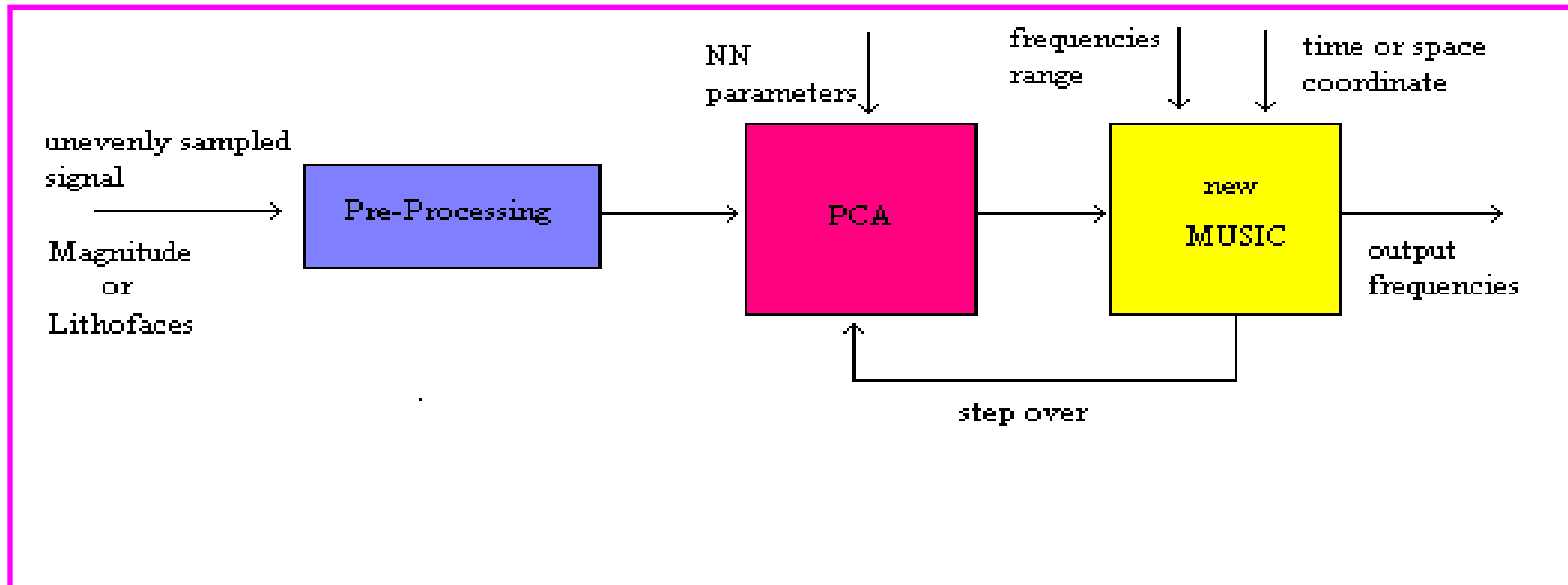


Frequency estimator

- Approach
 - Reformulation of the MUSIC (MULTI Signal Classifier) frequency estimator for unevenly sampled data
 - Robust PCA Neural Network to extract signal information
- Periodicities estimation
 - Light curves
 - W UMa-system (e.g. U Pegasi), Cepheid (e.g. Su Cygni), blazars, ecc.
 - Stratigraphic sequences
 - Tobenna, Raggeto, San Lorenzello mountains



STIMA approach



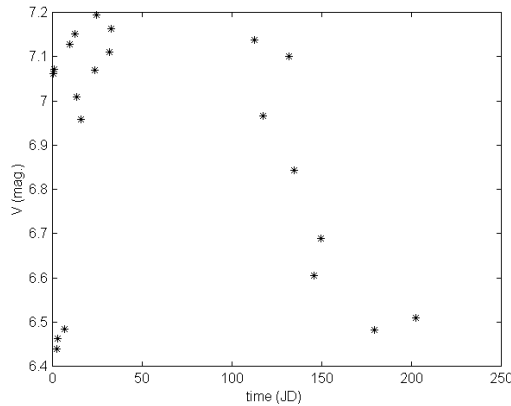
$$P_M = \frac{1}{M - \sum_{i=1}^M |e_f^H w(i)|^2}$$

MUSIC estimator for unevenly sampled data

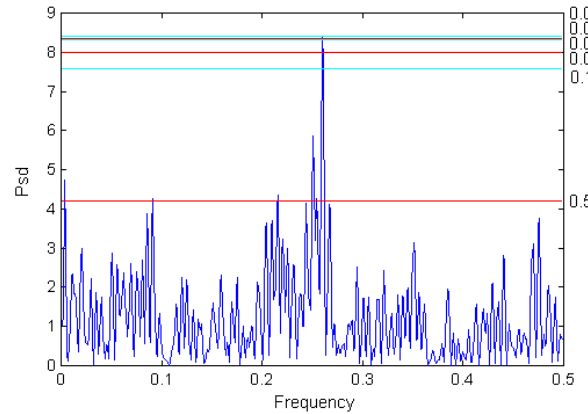
$$e_f^H = [e_f^{t_0}, e_f^{t_1}, \dots, e_f^{t_{L-1}}]^H$$



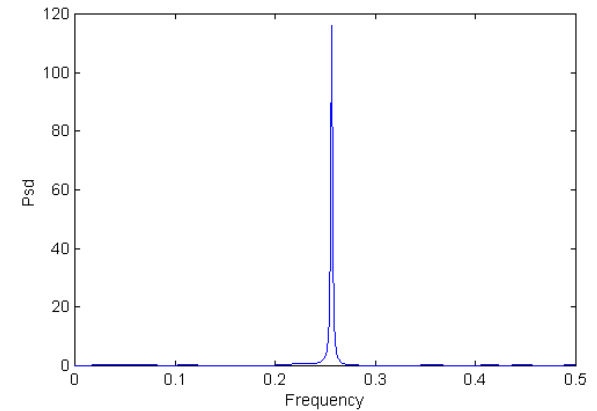
Light curve SU Cygni



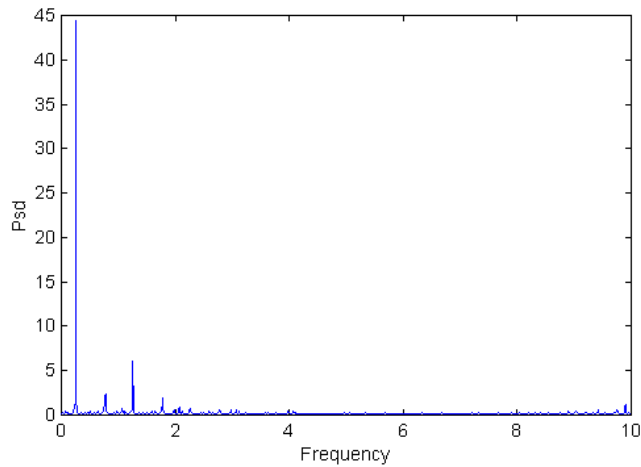
Light curve



Lomb's Periodogram

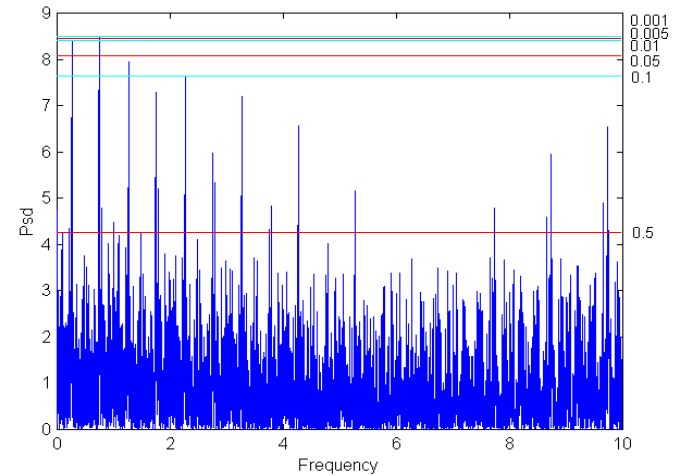


STIMA approach



STIMA approach

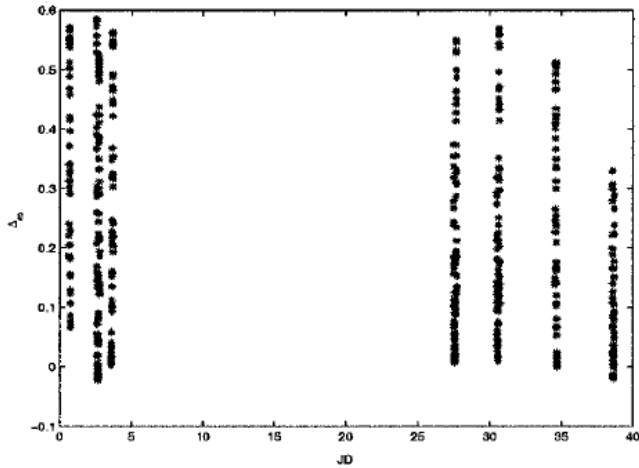
Frequency variation



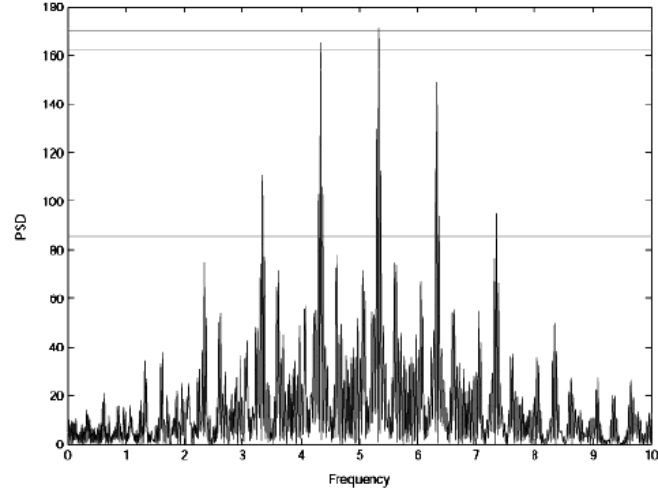
Scargle's Periodogram



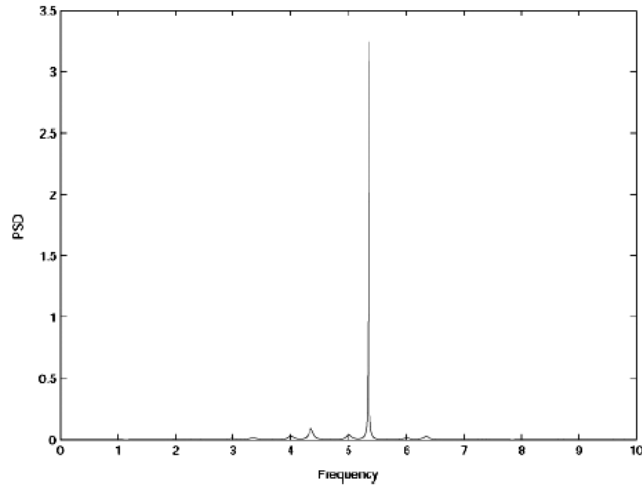
Light curve U Pegasi (I data set)



Light curve



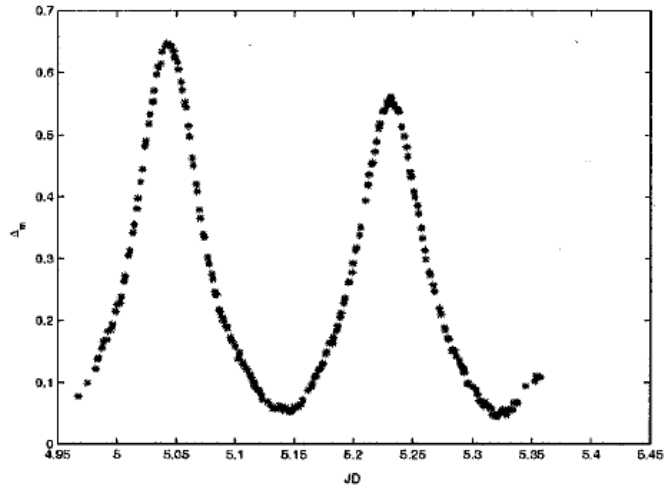
Lomb's Periodogram



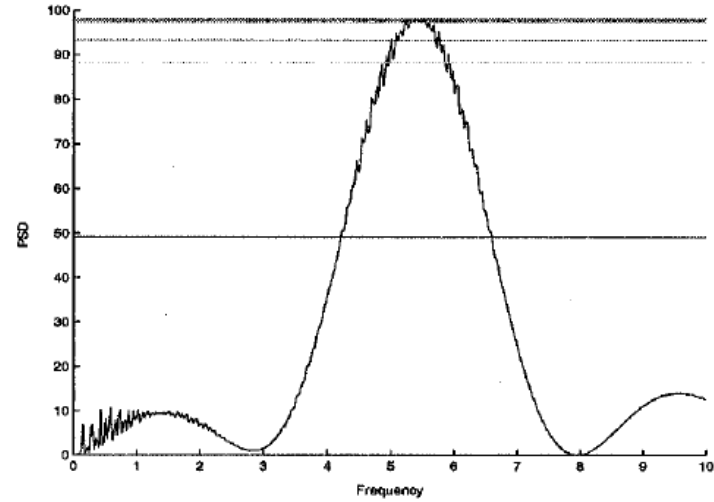
STIMA approach



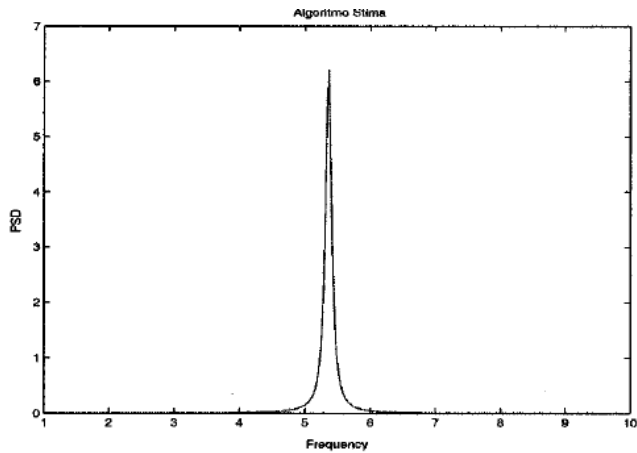
Light curve U Pegasi (II data set)



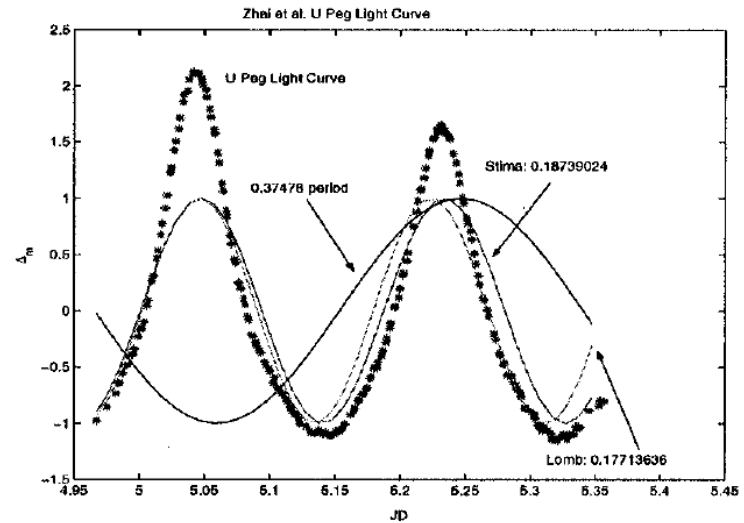
Light curve



Lomb's Periodogram



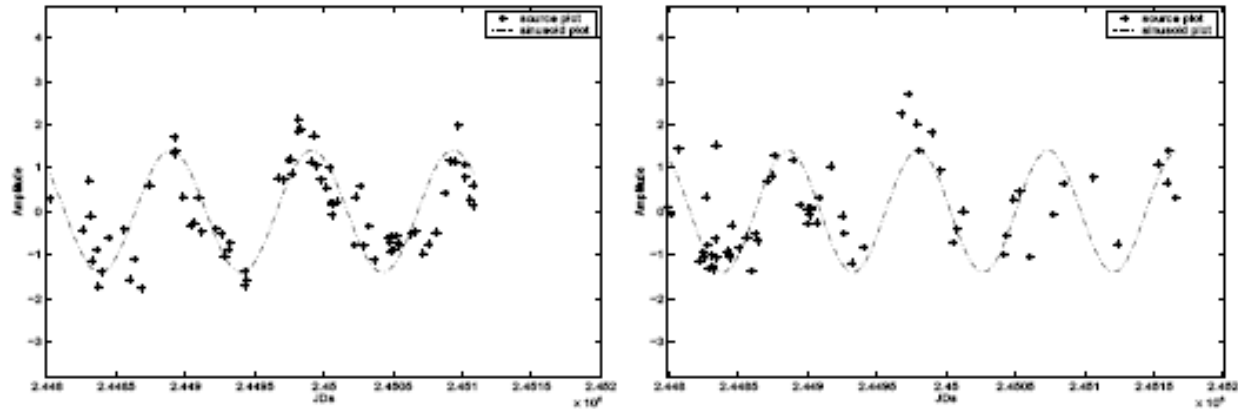
STIMA approach



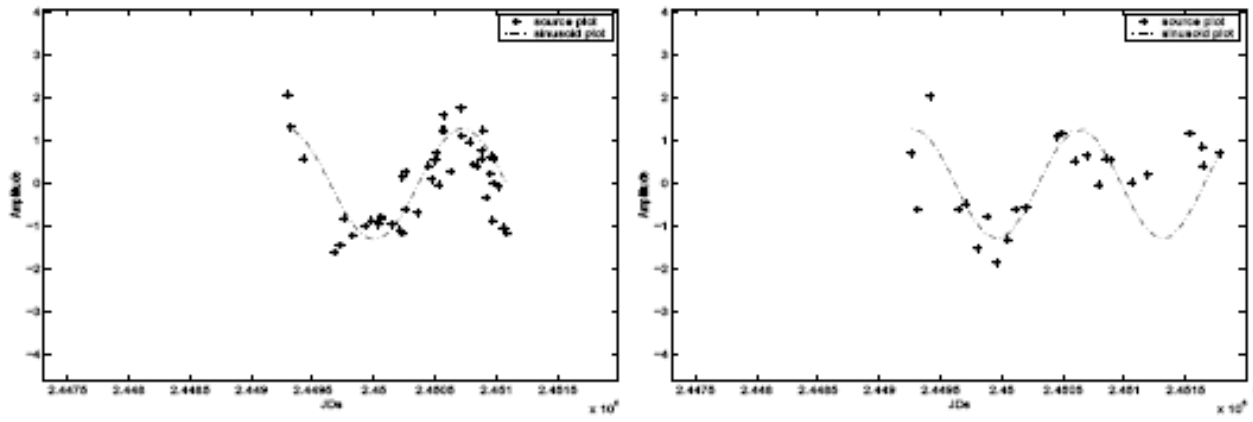
Comparison



Radio variability of blazars



A0224+671. Results for the 22 GHz (left panel) and 37 (right panel), daily averaged datasets. Sinusoids with a period equal to those provided by STIMA

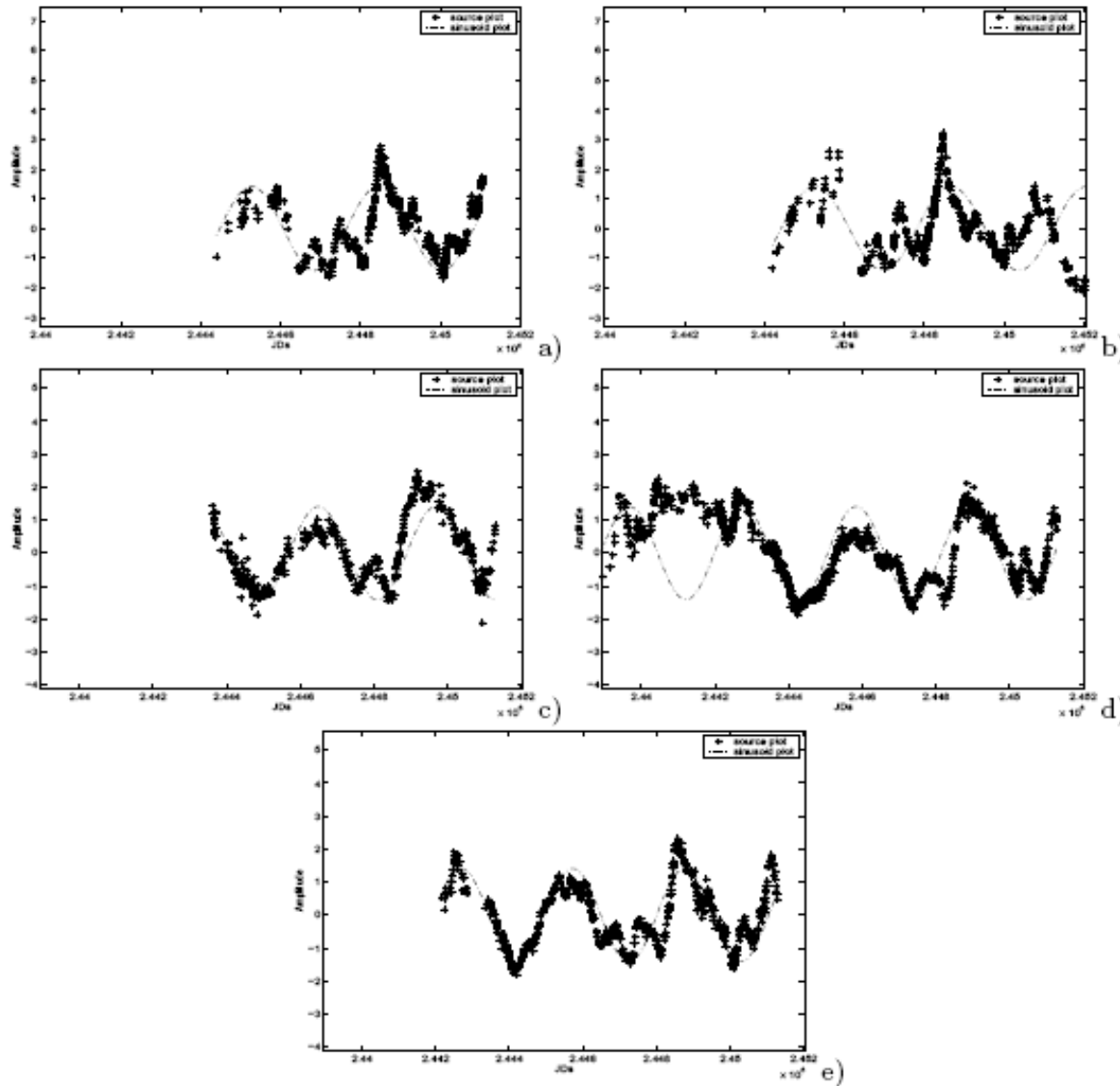


0945 + 408. Results for the 22 (left) and 37 GHz (right)

Collaboration with the Department of Physics of University of Naples “Federico II”, Astronomic Observatory of Padova, Dept. Of Astronomy of the University of Michigan, Metsahovi Radio Observatory, Kylmala, Finland



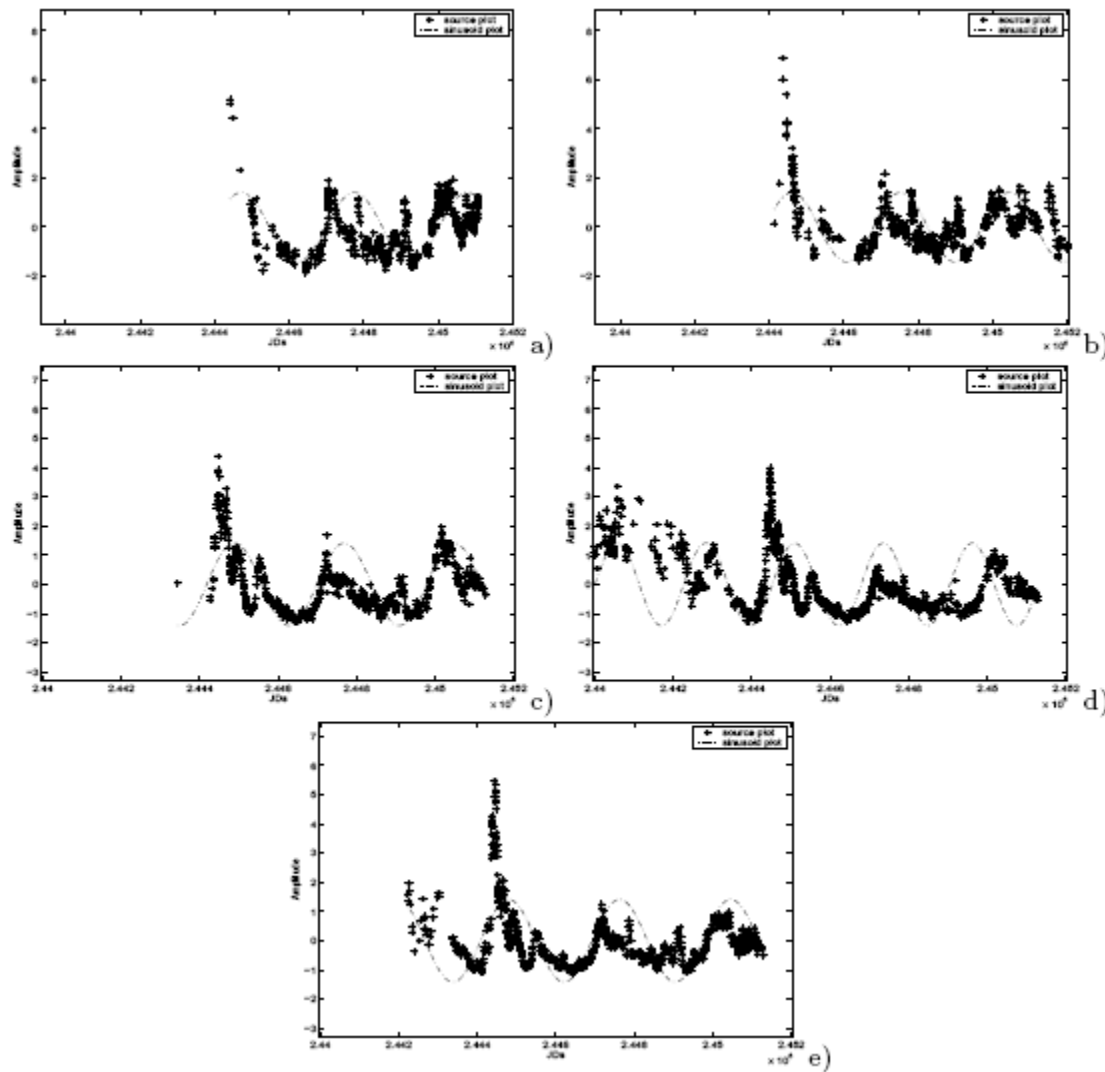
Radio variability of blazars



1226+023. Panels a and b: results for the 22 GHz and the 37 GHz daily averaged radio curves, respectively. Panels c, d and e: the same for the 4.8, 8 and 14.5 GHz data, respectively



Radio variability of blazars



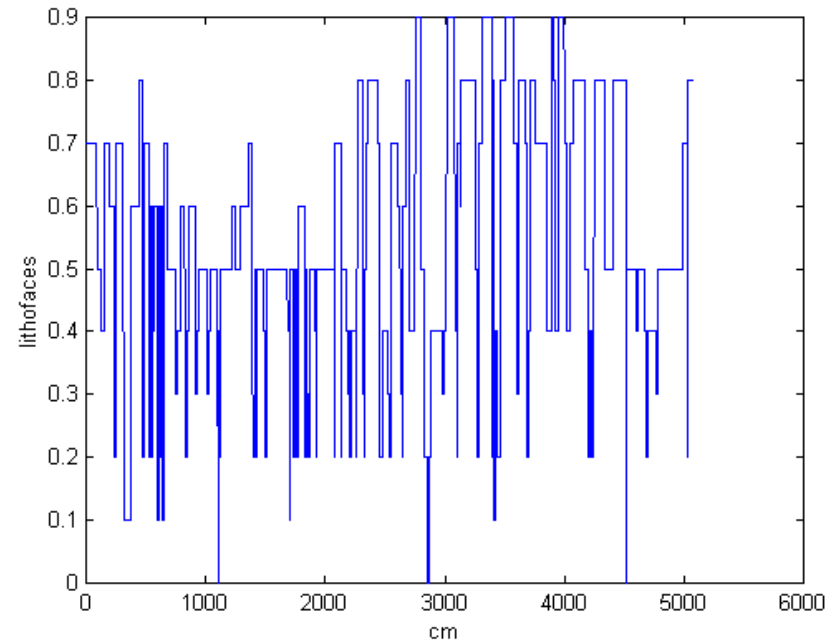
2200 + 420. Panels have the same meaning as in the previous figure



Stratigraphic sequences



An example of stratigraphy in a mountain

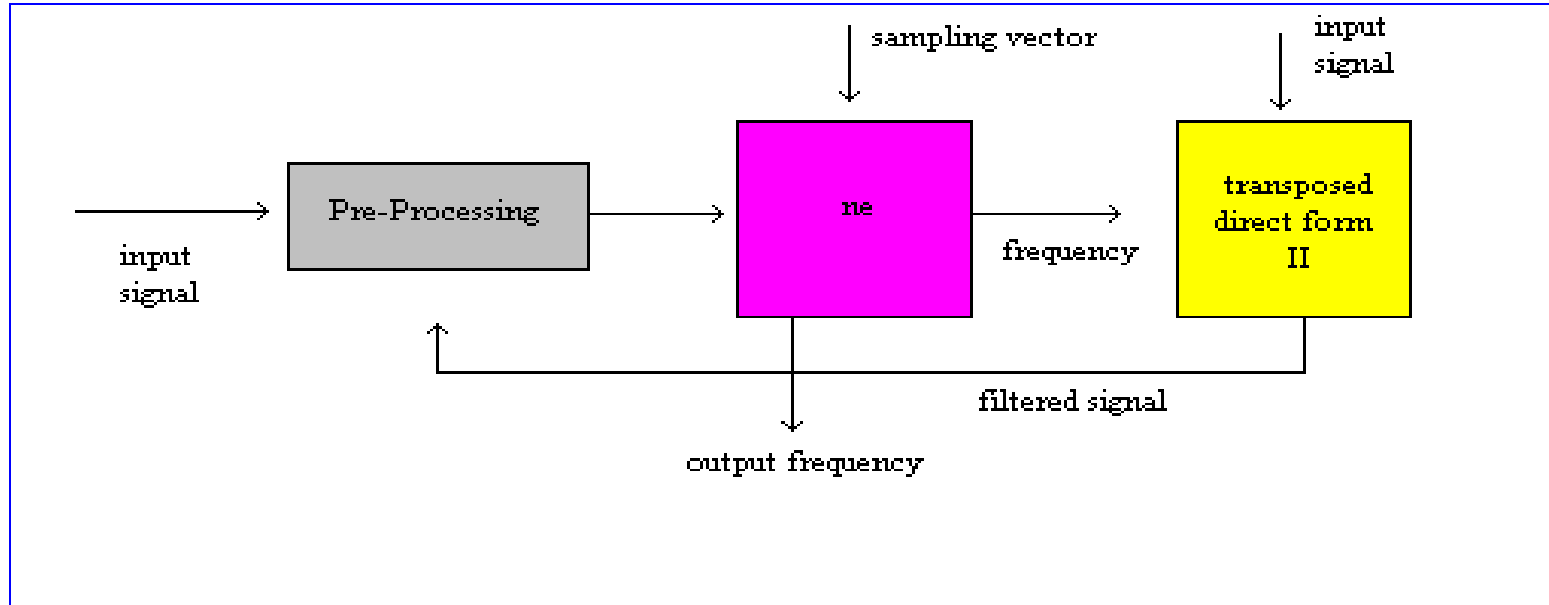


Mount San Lorenzello stratigraphic sequence

Collaboration with the Istituto Geomare (NA)



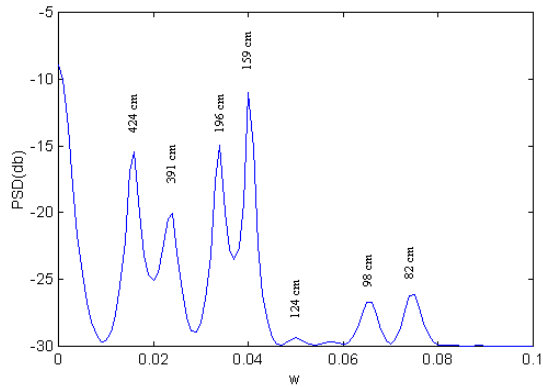
Estimation process



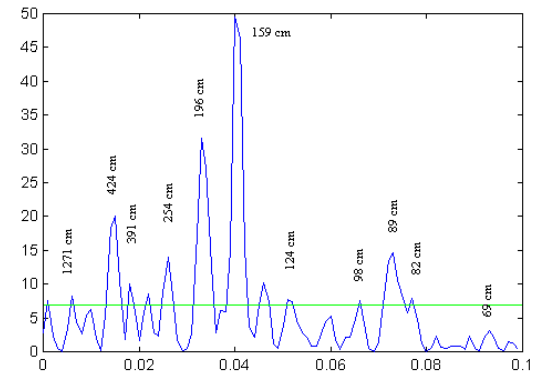
The method is the most powerful tool because it accurately finds the real spectral features, comprehensive of frequencies which the others methods do not find or confuse with the noise. They also require low computing time.



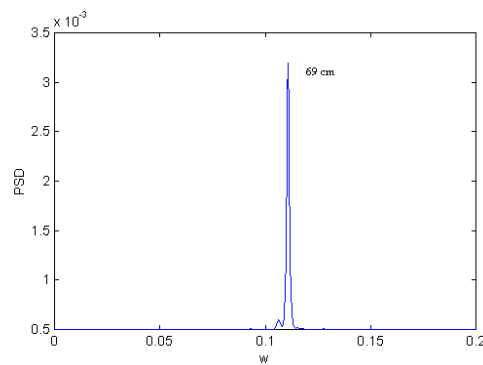
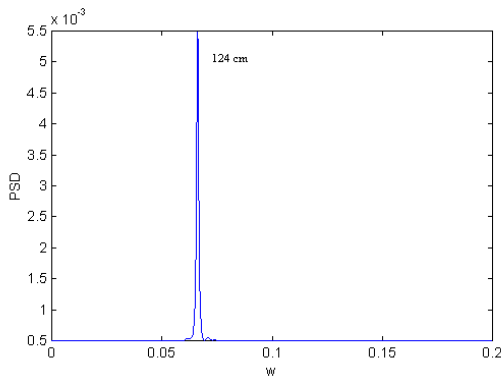
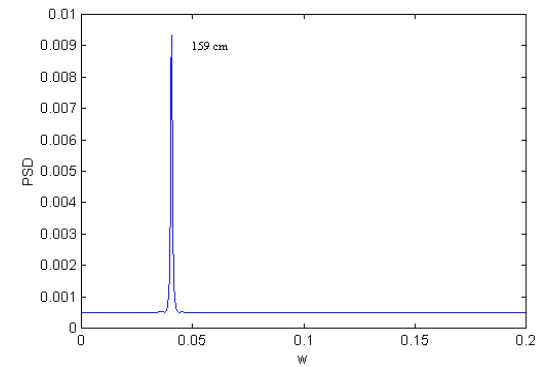
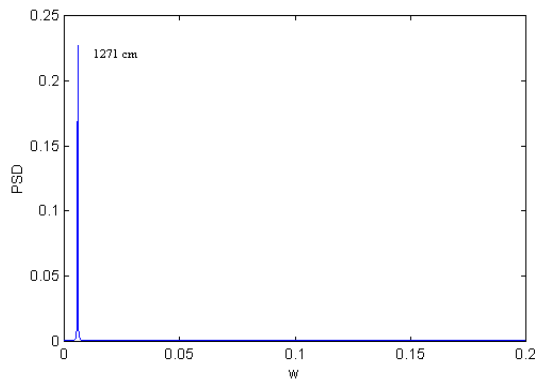
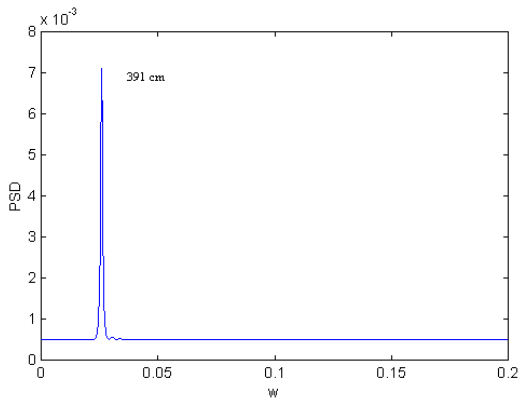
Periodicities estimation



STIMA approach



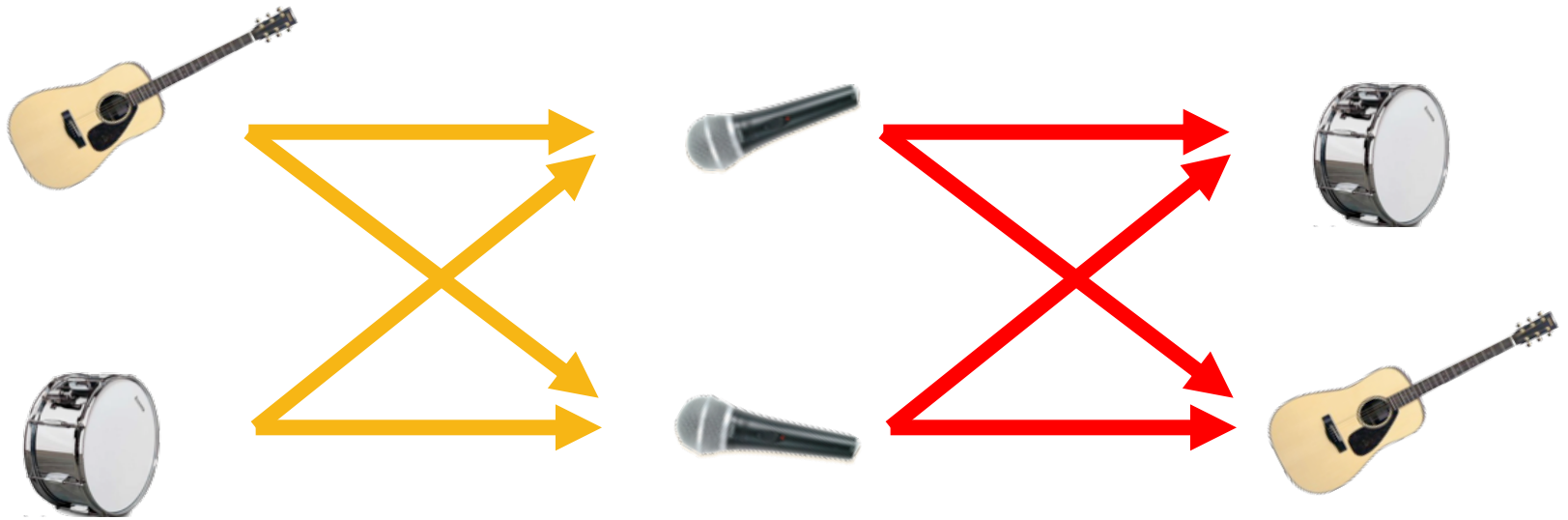
Scargle's Periodogram estimation



STIMA and filtering



Cocktail party



Sources

Mixtures

Estimated-Sources

s

A

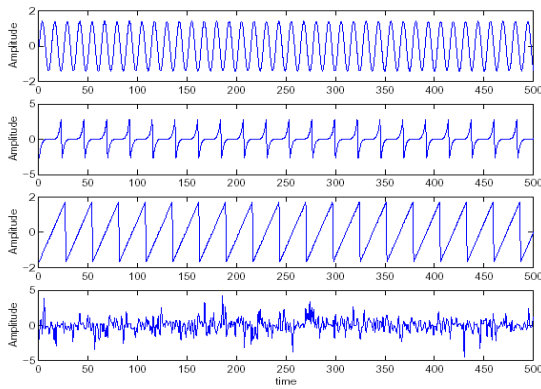
x

W

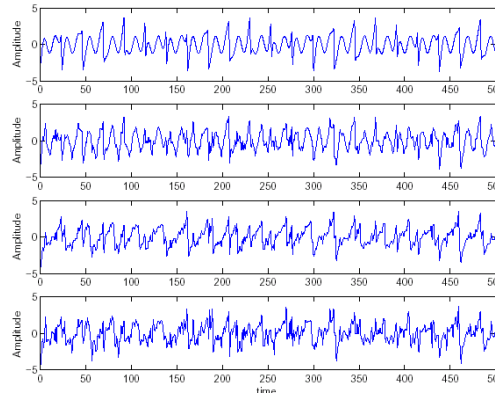
y



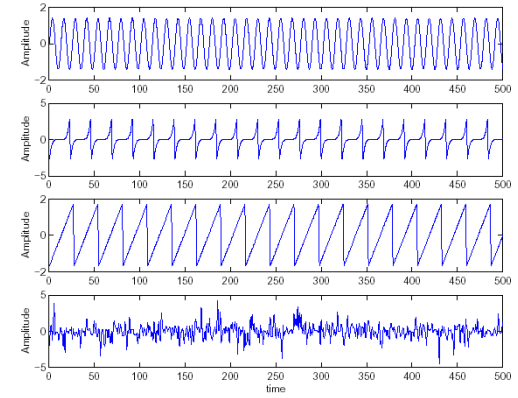
Source estimation



Source signals



Mixed signals



Estimated signals

$$\begin{aligned}x_1(t) &= a_{11}s_1(t) + a_{12}s_2(t) + a_{13}s_3(t) \\x_2(t) &= a_{21}s_1(t) + a_{22}s_2(t) + a_{23}s_3(t) \\x_3(t) &= a_{31}s_1(t) + a_{32}s_2(t) + a_{33}s_3(t)\end{aligned}$$

$$\begin{aligned}y_1(t) &= w_{11}x_1(t) + w_{12}x_2(t) + w_{13}x_3(t) \\y_2(t) &= w_{21}x_1(t) + w_{22}x_2(t) + w_{23}x_3(t) \\y_3(t) &= w_{31}x_1(t) + w_{32}x_2(t) + w_{33}x_3(t)\end{aligned}$$

$x_1(t), x_2(t), x_3(t)$ are the observed signals,
 $s_1(t), s_2(t), s_3(t)$ the source signals

$y_1(t), y_2(t), y_3(t)$ are the separated signals

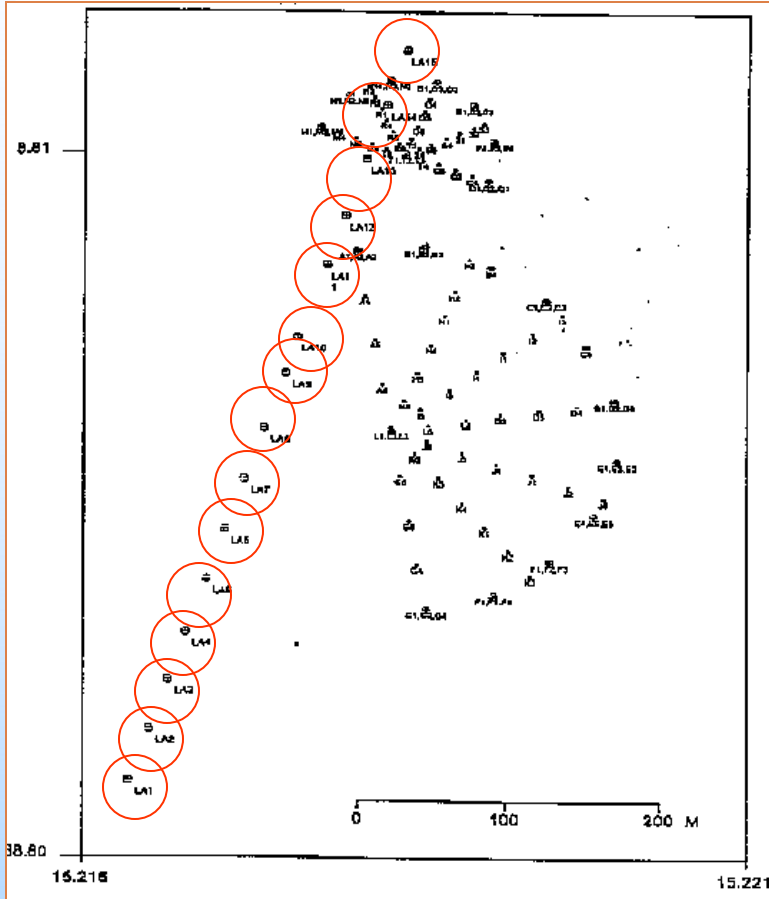


ICA and seismic signals

- ICA is used to analyze the **seismic signals** produced by explosions of the **Stromboli volcano**
- It has been experimentally proved that it is possible to extract the *most significant components* from seismometer recorders
- In particular, the signal, eventually thought **as generated by the source**, is corresponding to the higher power spectrum, isolated by our analysis
- Furthermore, the *amplitude of the source signals has been found* by using a simple trick and so overcoming, for this specific case, the classical problem of ICA regarding the amplitude loss of the separated signals

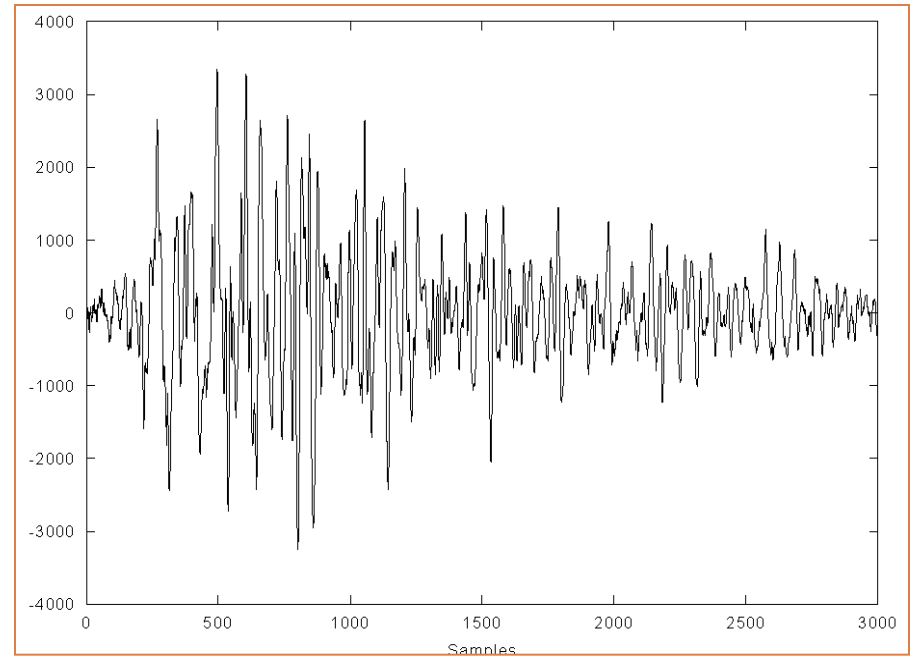


Seismic signals

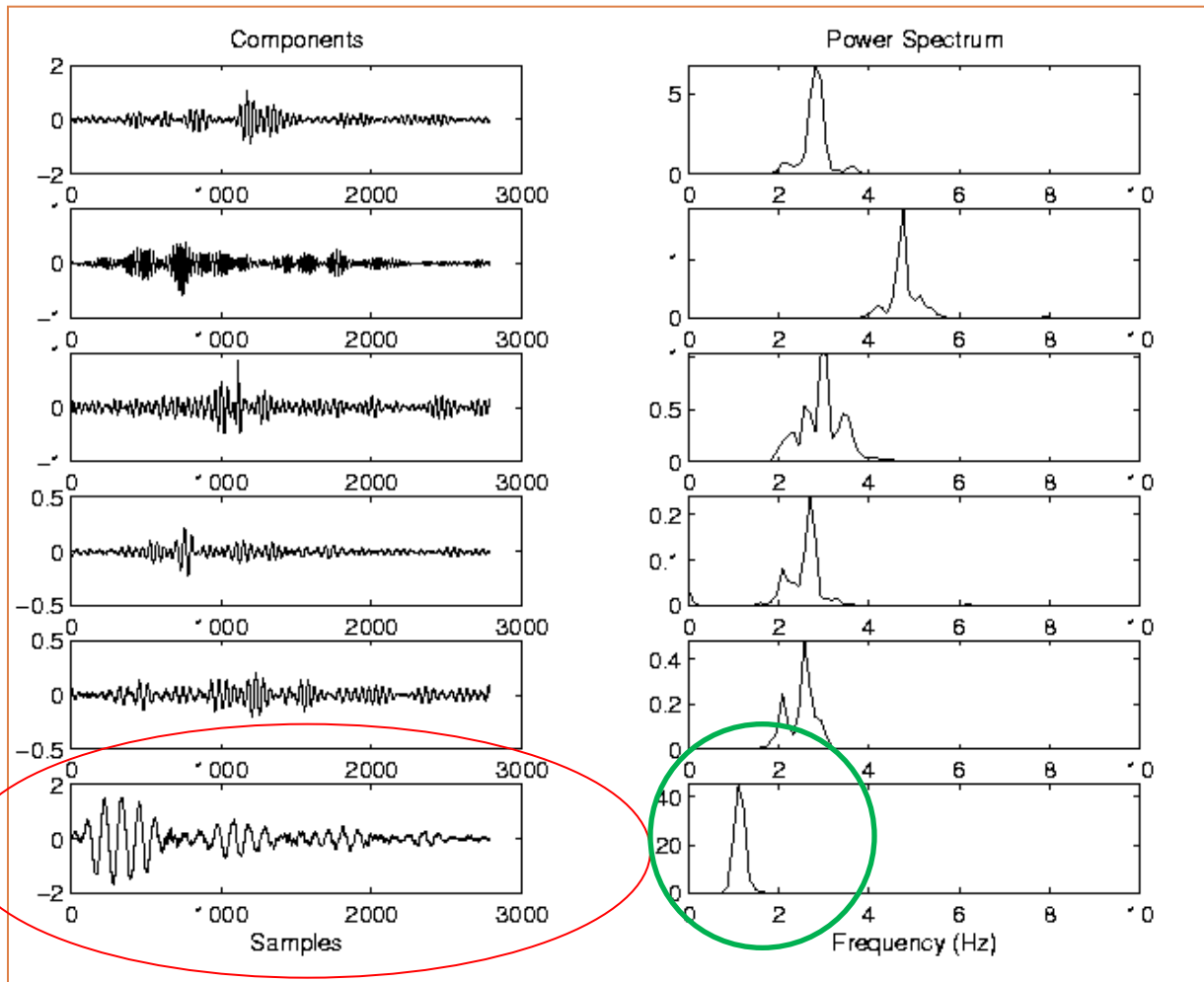


Array position

An example of explosion-quake



Source estimation



Radial separated signals



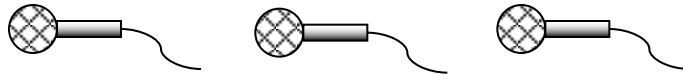
ICA and pipe organ sound

- The aim of this work is to **analyze** and to **resynthesize** acoustic signals emitted by **organ pipes** recorded in real environments
- By applying ICA to the recordings, we have established that a **single note** is itself composed of **three self-oscillating signals** (**Andronov oscillator**) with well defined frequencies
 - the pipe acoustic signals can be described by a mixture of non-linear oscillations obtained by a self-sustained feedback system
 - Considering this non-linear system, an **additive synthesis** model is proposed
- Suitable **analogical and integrate circuit models**, able to reproduce the registered waveform and sound in listening, have been designed



Pipe organ

C-E-G



mixtures

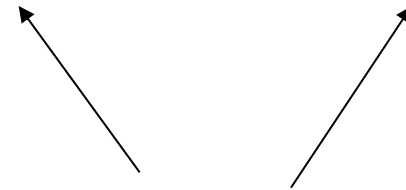
Do



Mi

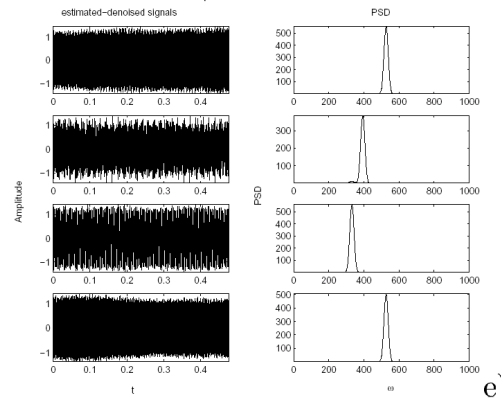
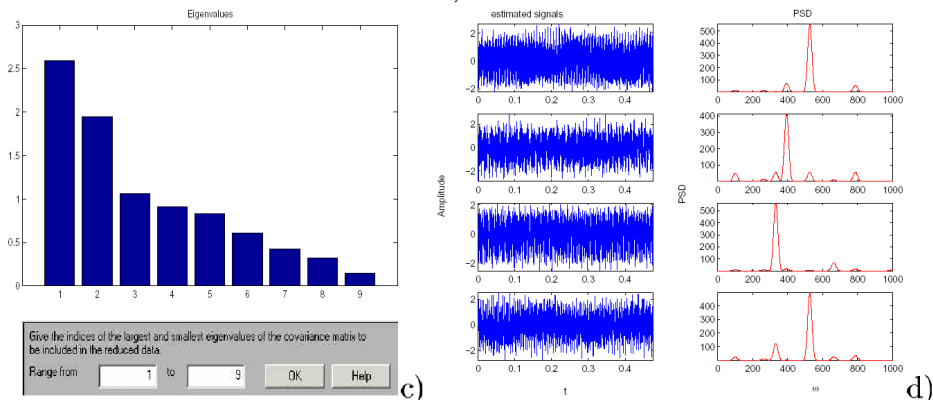
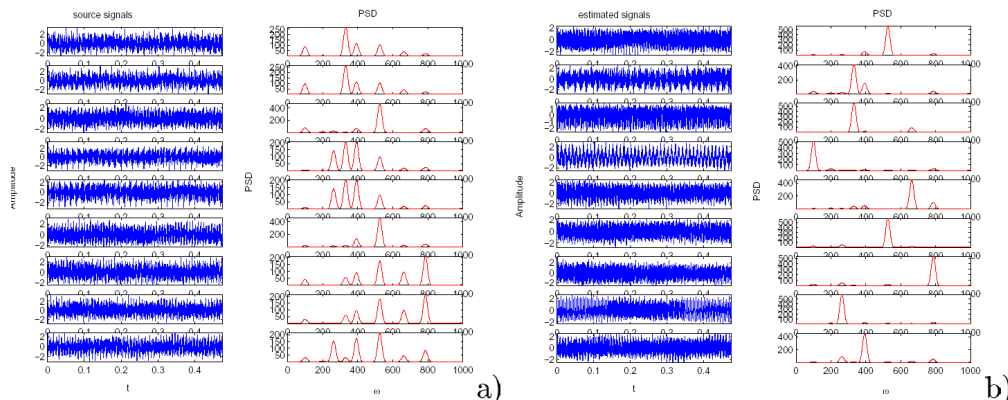


Sol

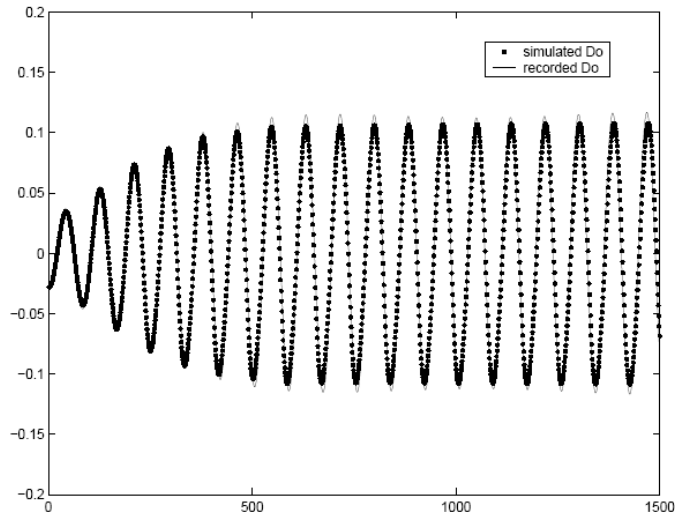


Source estimation

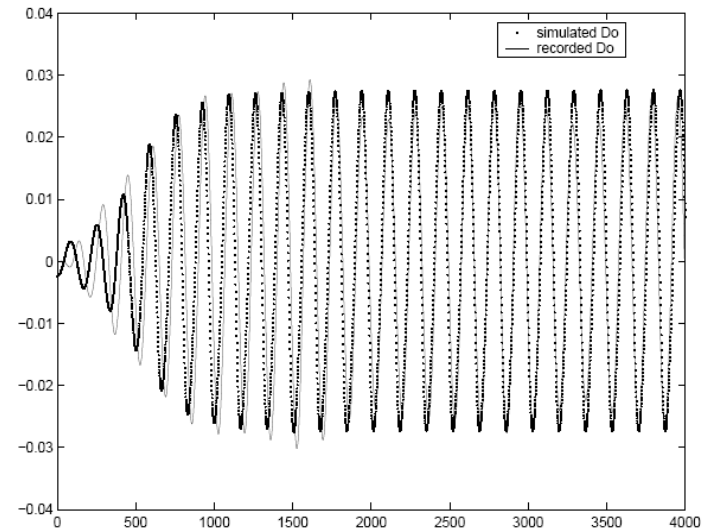
- a) C-E-G chord signals and their PSD;
- b) FastICA separation;
- c) Principal components of the covariance matrix;
- d) FastICA separation with four components
- e) Estimated signals after denoising



Simulated notes



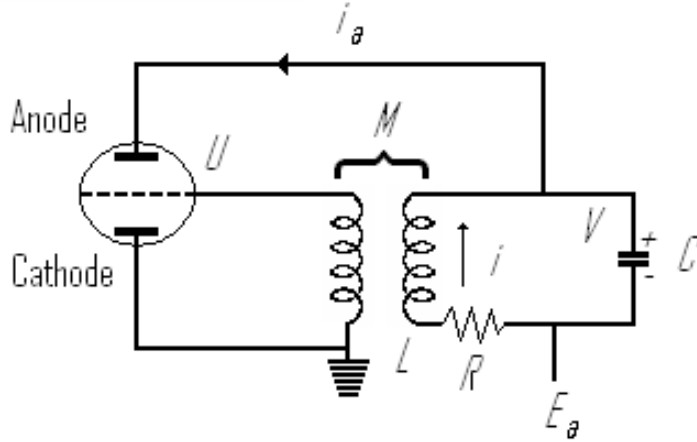
Comparison between simulated and real C note (523 Hz)



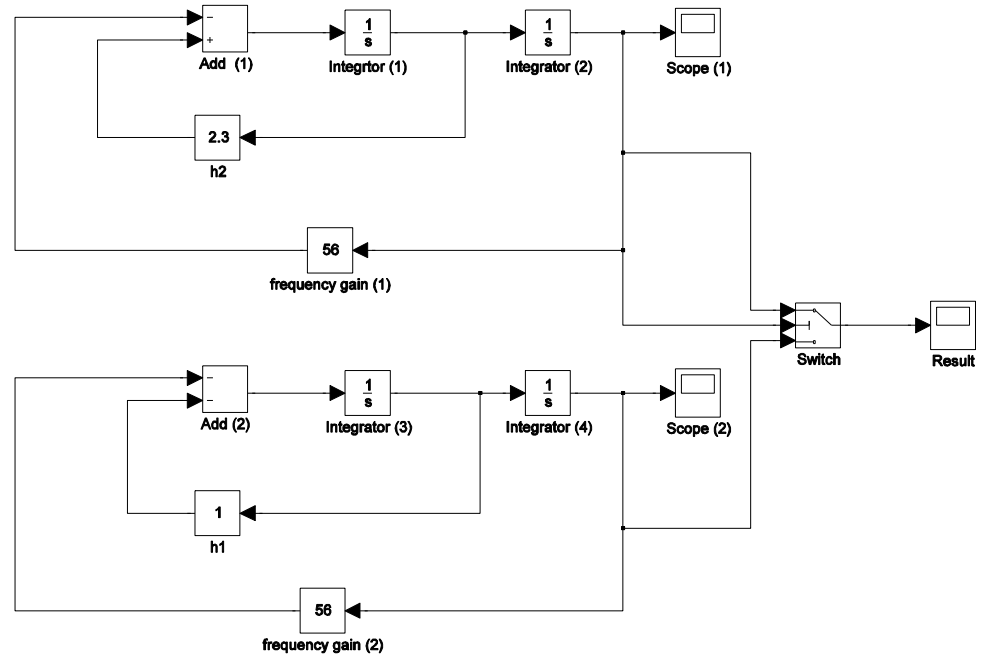
Comparison between simulated and real C note (263 Hz)



Analogi circuit



Andronov analogical circuit



Andronov system by using Matlab Simulink

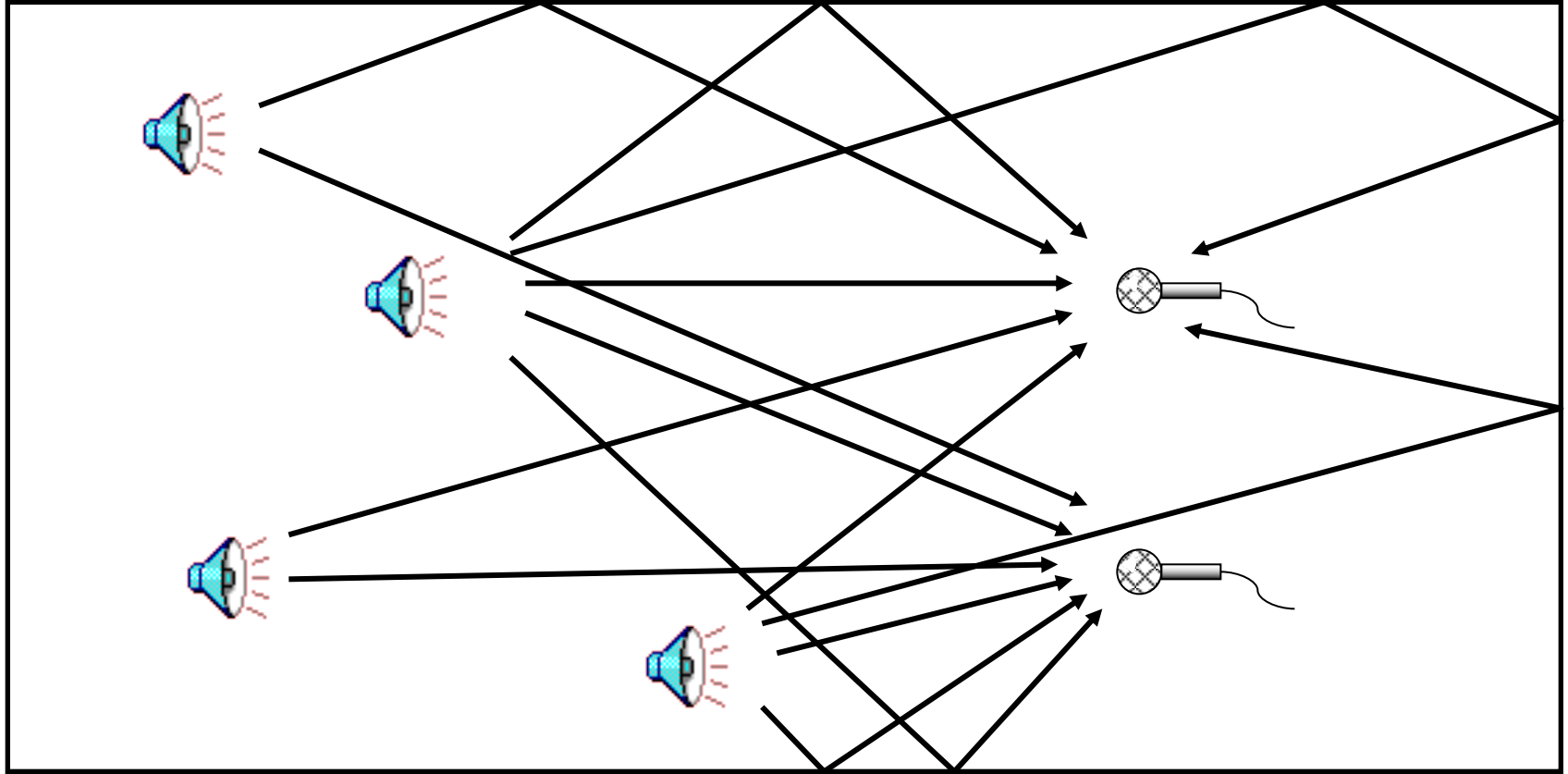


ICA and real environment

- Now we consider a novel approach to solve the **permutation indeterminacy** in the separation of **convolved mixtures** in frequency domain
- These are obtained applying a **Short Time Fourier Transform** on a set of fixed frames
- To solve the **ambiguity** of the amplitude dilation, a simple disassemble method is proposed
- The **permutation indeterminacy** is solved using an approach based on the *Hungarian algorithm* that solves an **Assignment Problem** and an algorithm of **Dynamic Programming**
 - To obtain the distances in the Assignment Problem, a **Kullback-Leibler** divergence is adopted



Real environment



In real cases we have to consider the reverberation and delay



Convolved mixtures

$$x_i(t) = \sum_{j=1}^n \sum_k a_{ikj} s_j(t - k) \quad \text{for } i = 1, \dots, n$$

Convolved mixtures
(FIR filter)

$$y_i(t) = \sum_{j=1}^n \sum_k w_{ikj} x_j(t - k) \quad \text{for } i = 1, \dots, n$$

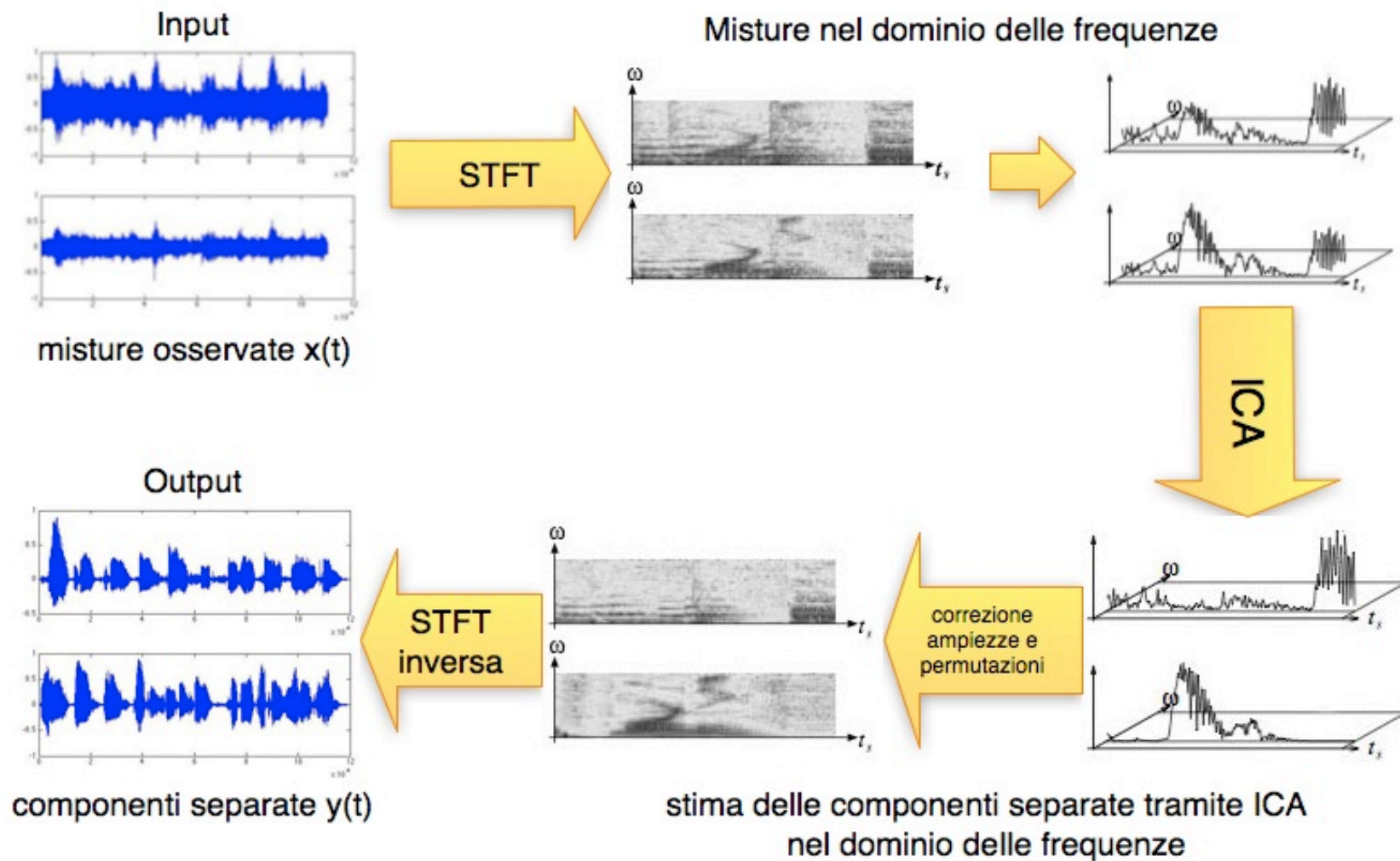
Estimate sources
(FIR filter)

$$X_i(\omega) = \sum_{j=1}^m A_{ij}(\omega) S_j(\omega), \quad \text{for } i = 1, \dots, n$$

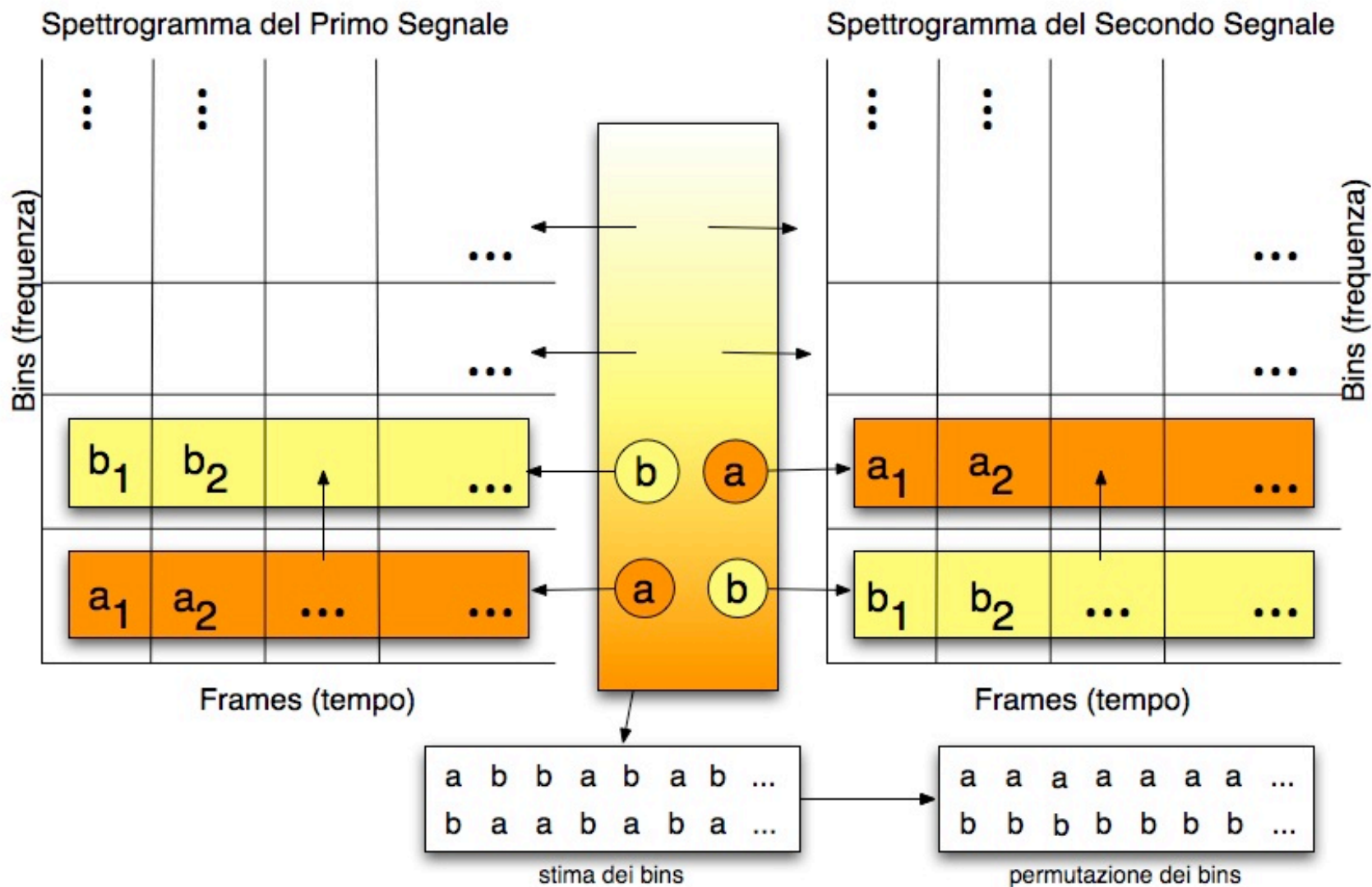
Product in frequency domain (STFT)



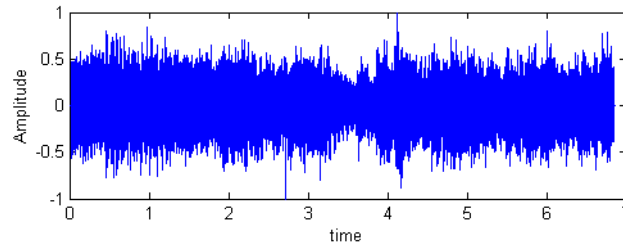
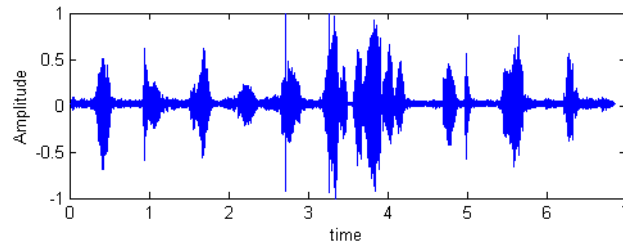
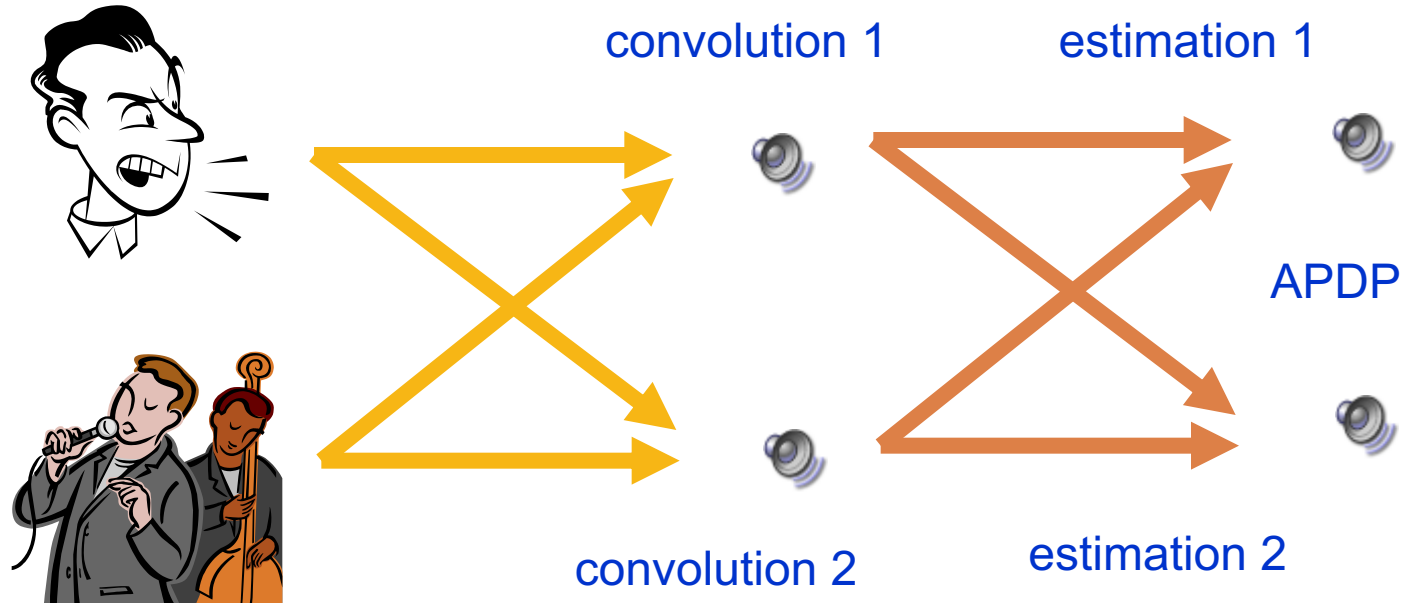
Convolved mixtures



Permutation



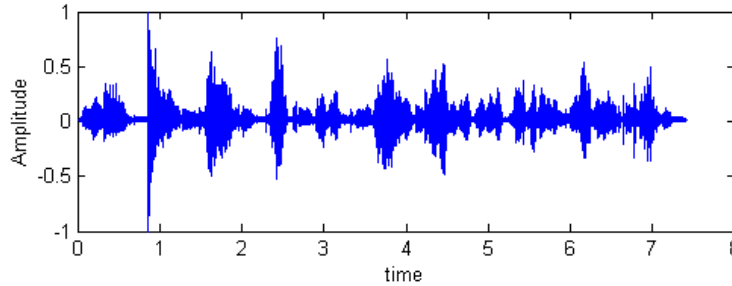
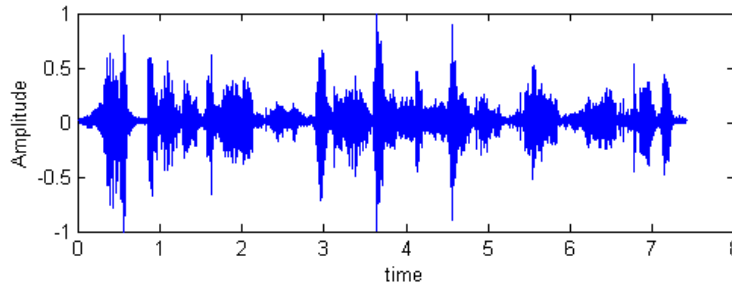
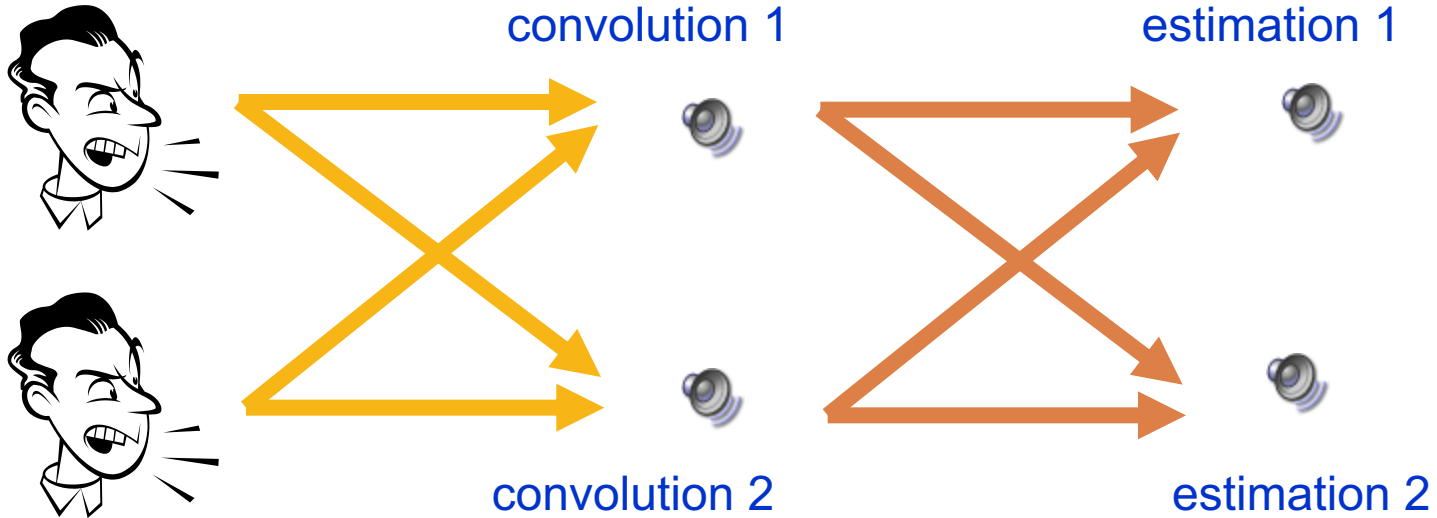
Speech-Music



Separated signals



Speech-Speech



Separated signals

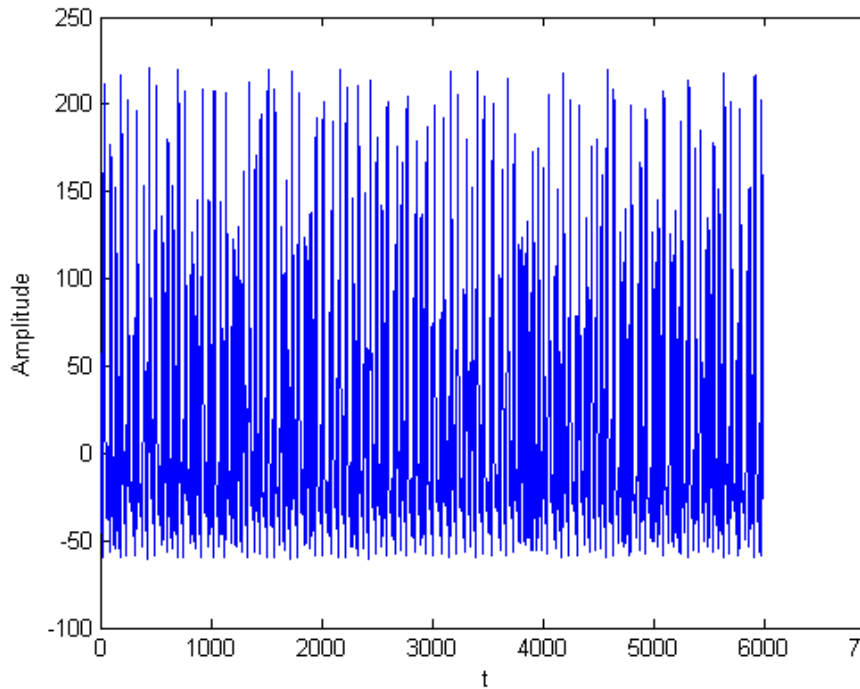


Single channel music transcription

- Extracting multiple source signals from a single channel mixture is an open problem and a challenging research field with several applications
- We present a method based on the **phase space reconstruction** of the mixture
 - we estimate the **embedding dimension** and the **time lag** of a mixture
 - we use the estimated parameters to obtain the **architecture** (input and output neurons) of a **Robust PCA (RPCA) Neural Network**

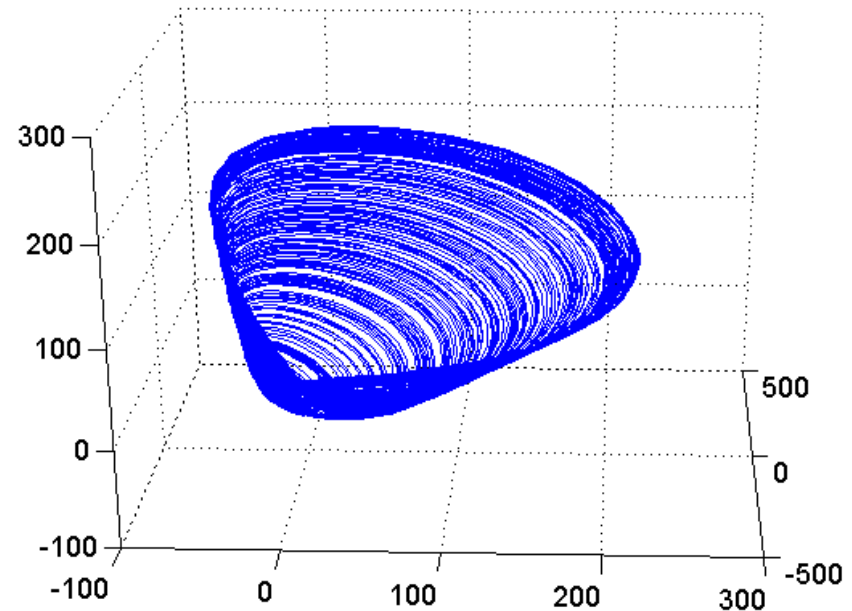


Chaotic features

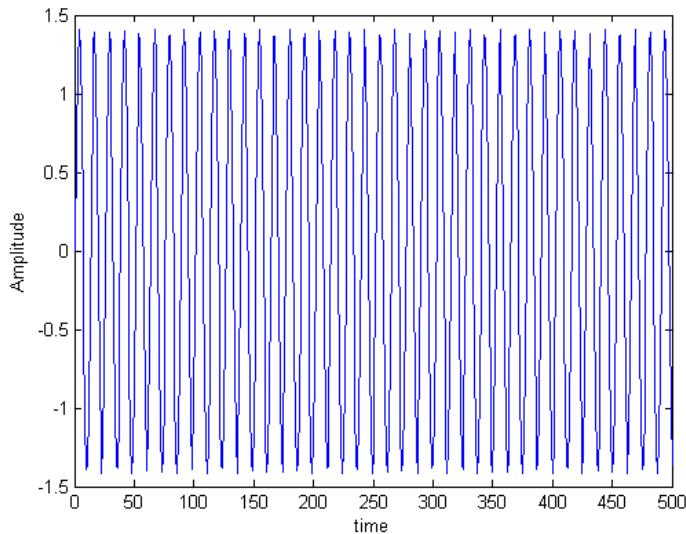


Time-series generated by an electrical Colpitts circuit that oscillates chaotically.

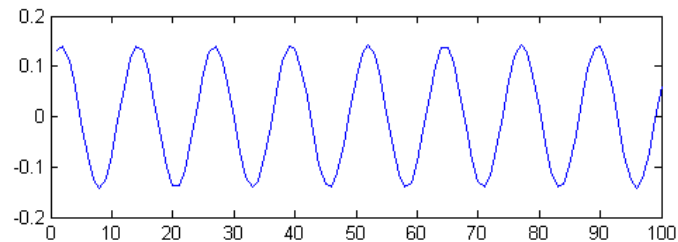
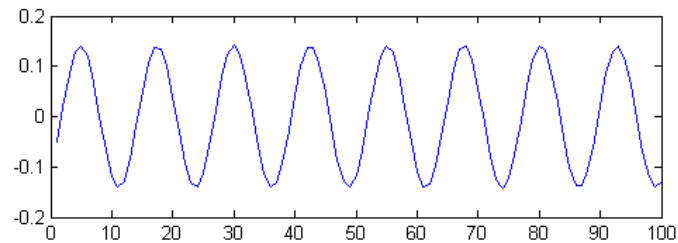
Phase space representation with $\tau = 4$ and embedding dimension = 3



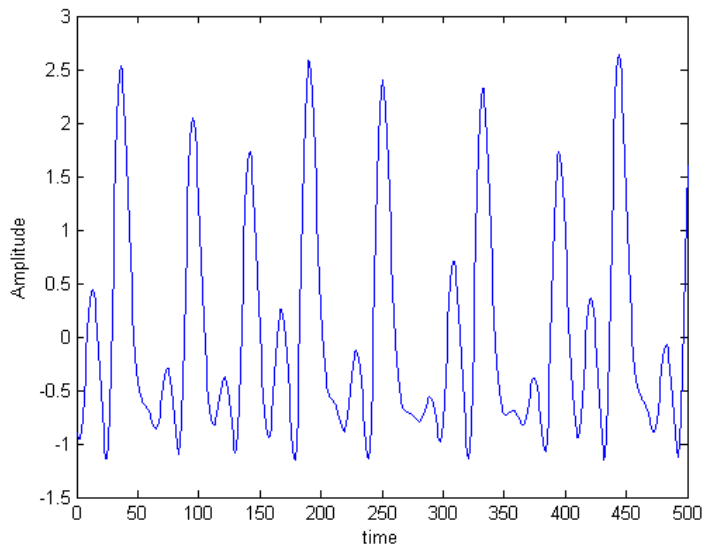
Oscillator and collpits



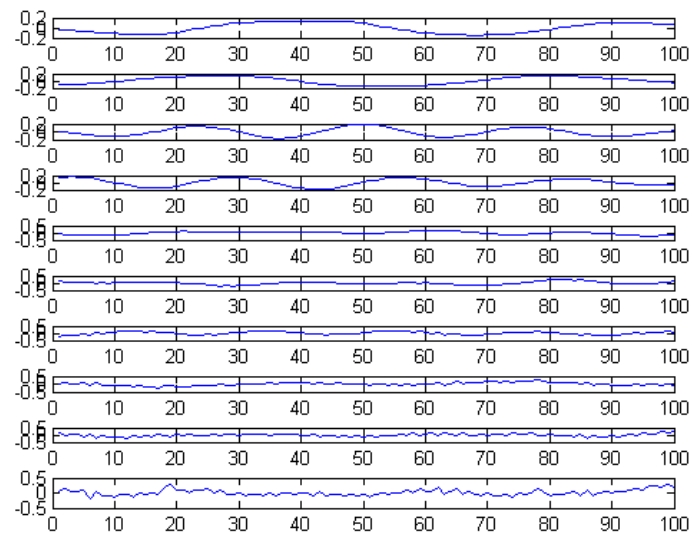
Harmonic oscillator



Independent basis obtained by using RPCA



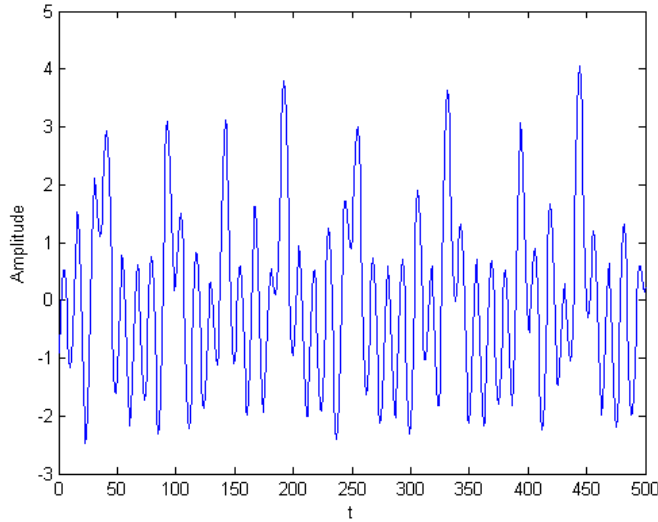
Colpitts time series



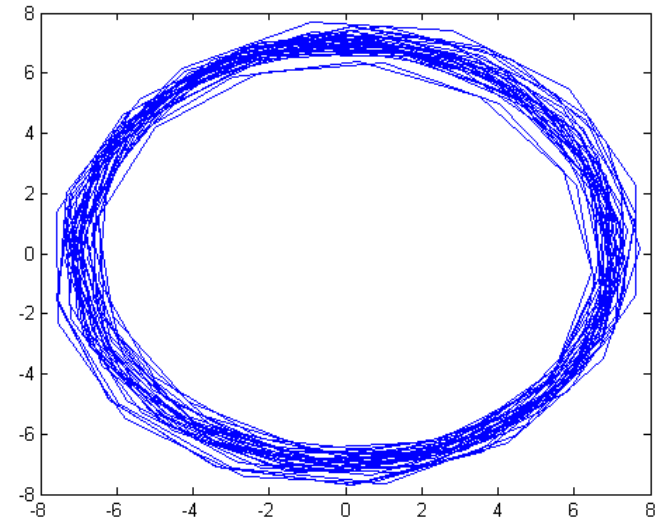
Independent basis obtained by using RPCA



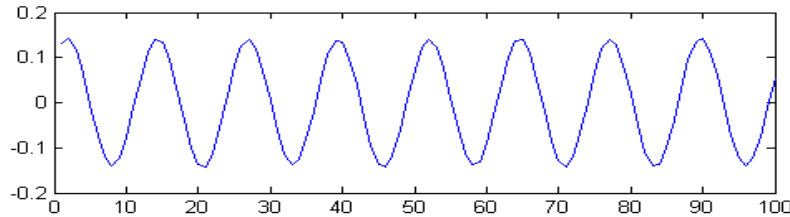
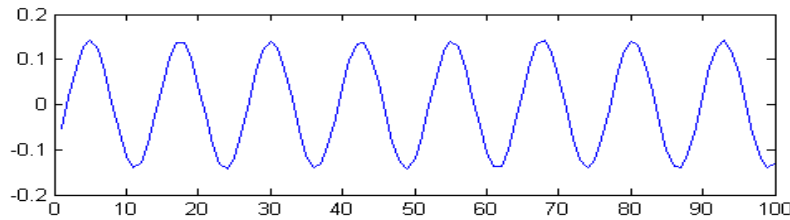
Oscillator



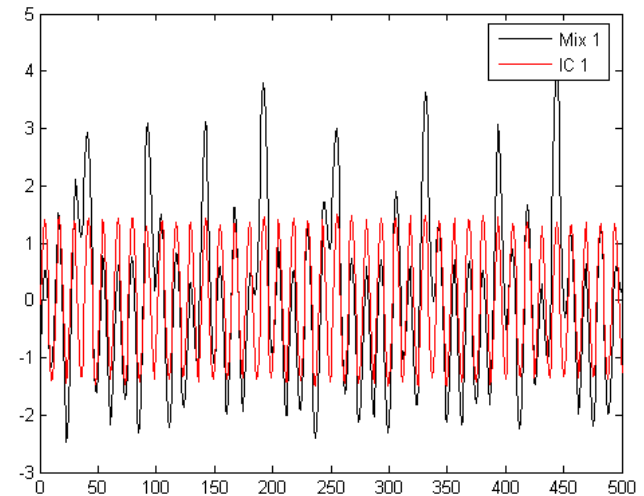
Mixture



Phase space on the first two components



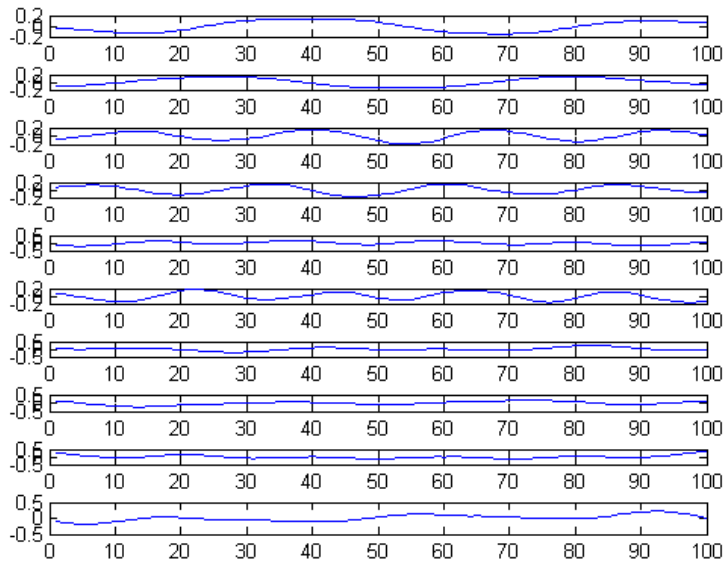
First two independent basis



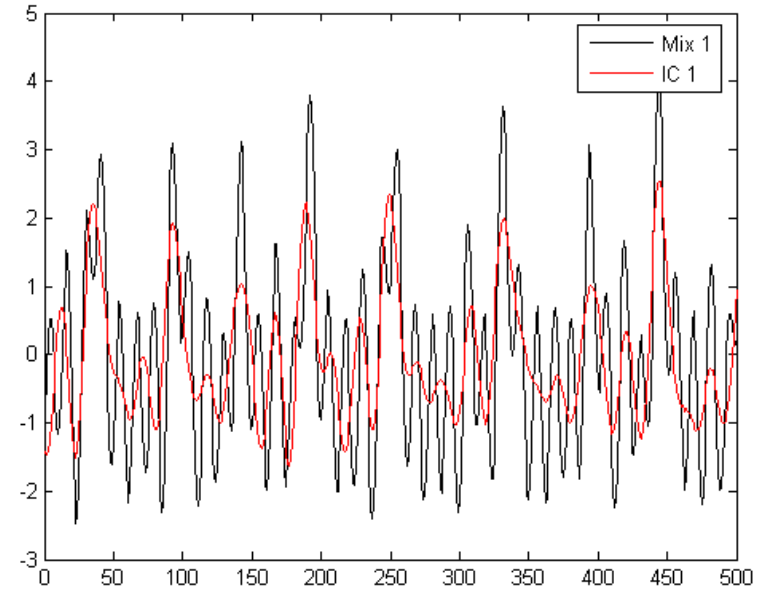
Comparison between the mixture and the reconstructed signal



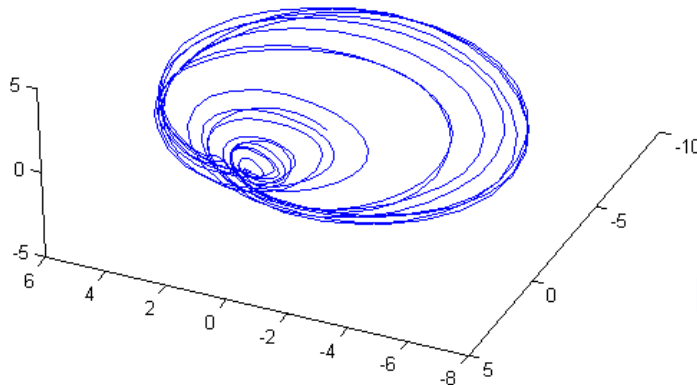
Colpitts



10 independent basis components



Comparison between the mixture and reconstructed signal



Phase space reconstruction on 3 of the 10 estimated components

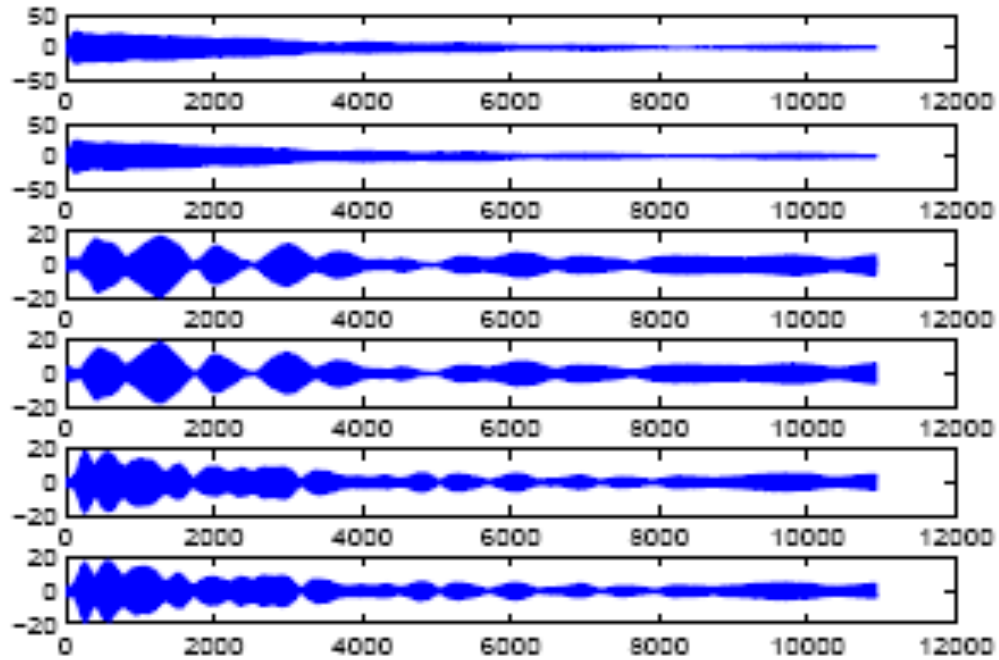


Transcription

- It is based on
 - Robust PCA
 - data base of features
 - Kullback-Leibler
 - MUSIC frequency estimator
- Several results are proposed
 - Synthetic
 - Piano and trumpet
 - Real recording
 - Blue room – Chet Baker
 - Real recording in a real environment
 - Shadows – Kismet



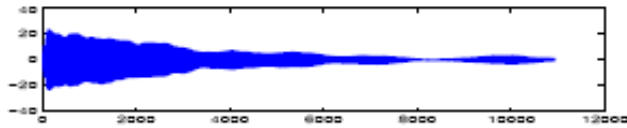
Experimental results



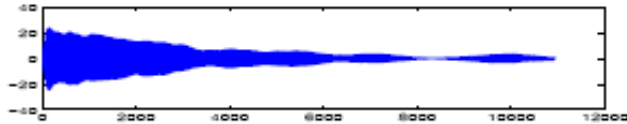
Non-linear PCA separated sources



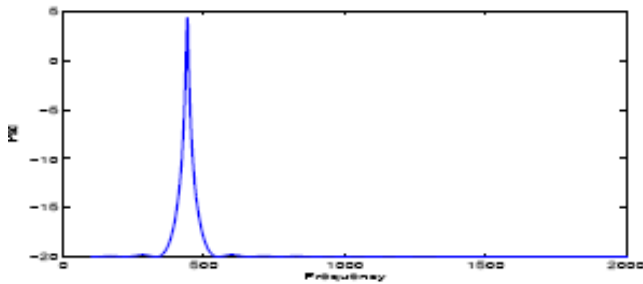
Experimental results



Piano classified components

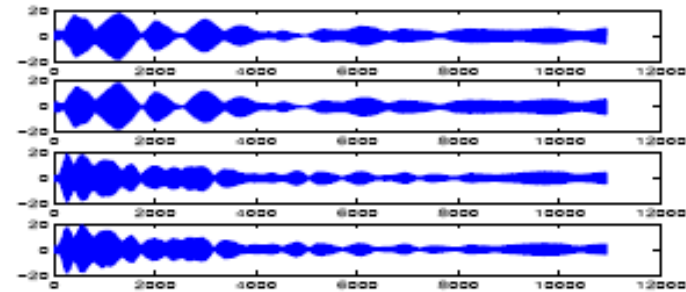


Time domain



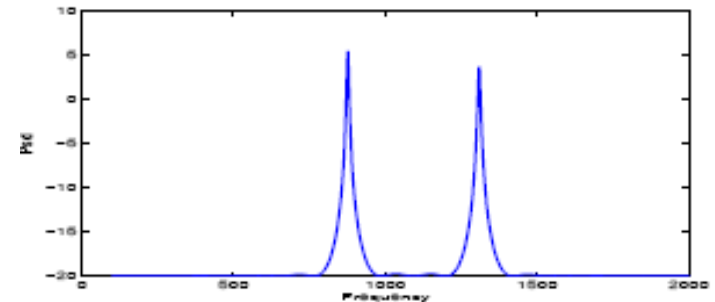
MUSIC frequency estimation

trumpet classified components

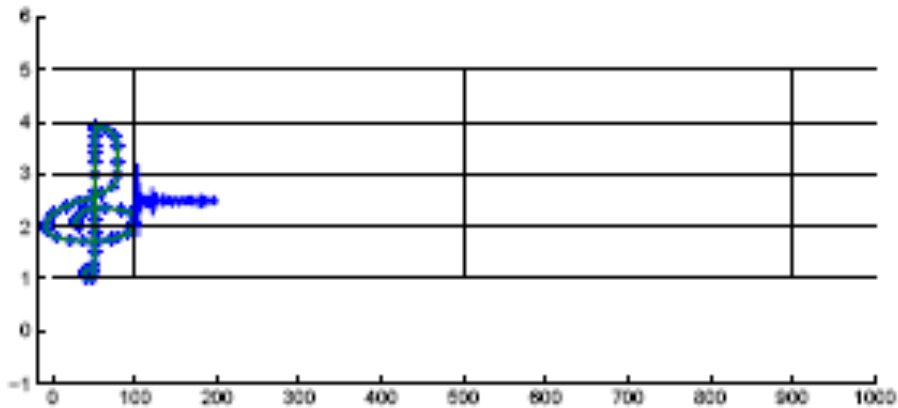


Time domain

MUSIC frequency estimation

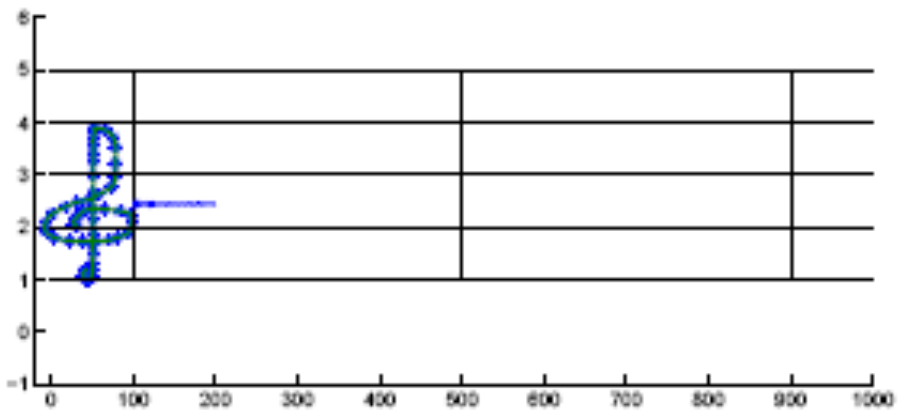


Experimental results



Transcription

piano



Trumpet

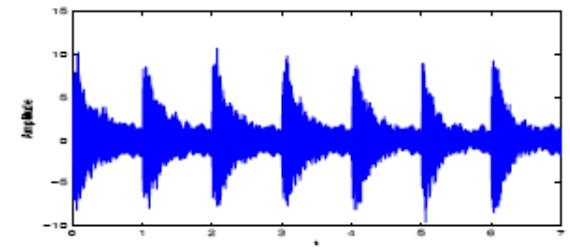


Experimental results

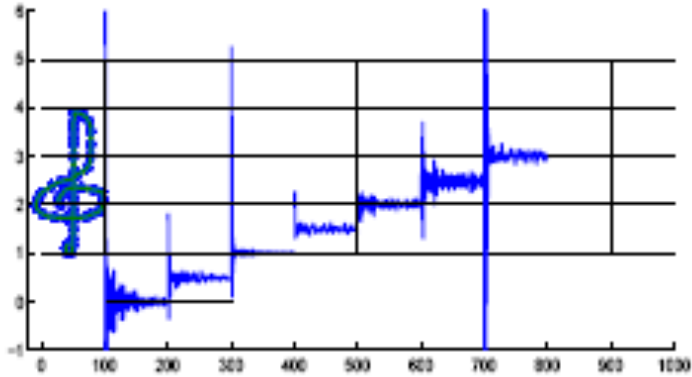
- We consider different notes for the piano (A_4 , G_4 , C_4 , D_4 , E_4 , F_4 , B_4) and the single note A_4 for the trumpet
- Aim of this experiment is to show that we can obtain a perfect separation also varying the fundamental frequency of the waveform



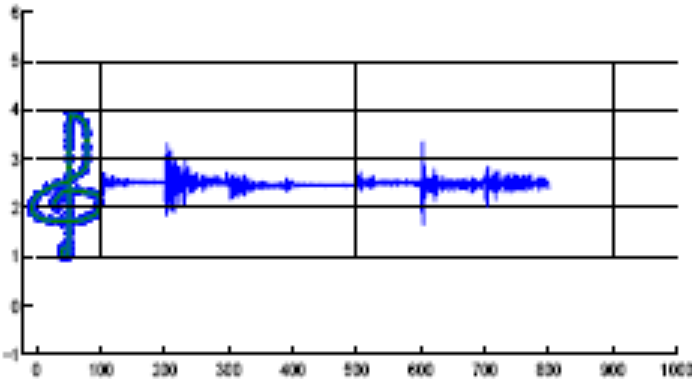
Experimental results



Transcription



piano



trumpet

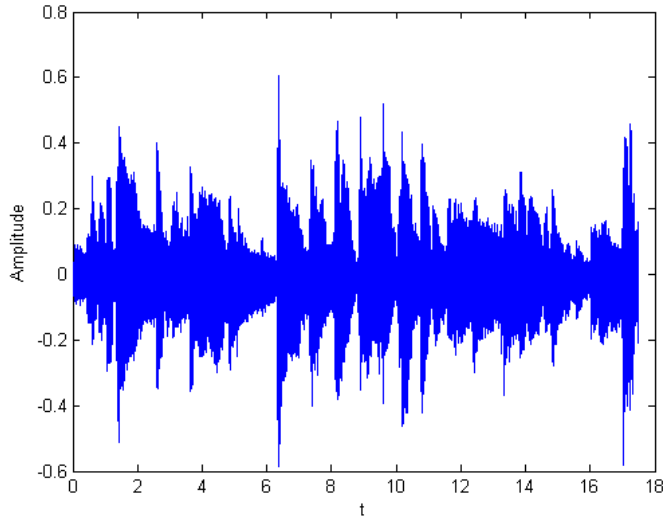


Experimental results

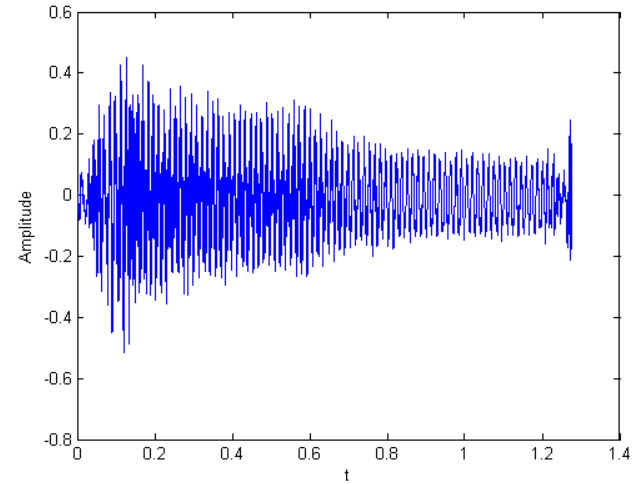
- We consider a real recorded song
- Blue Room song played by Chet Baker
 - Drum (shuffle)
 - Piano
 - Bass
 - Trumpet
- We present the extraction of the trumpet score



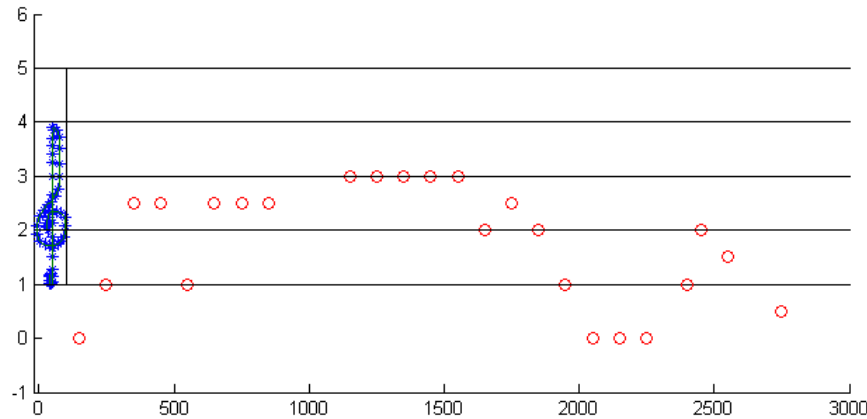
Experimental results



Solo sequence



Waveform in the database



score

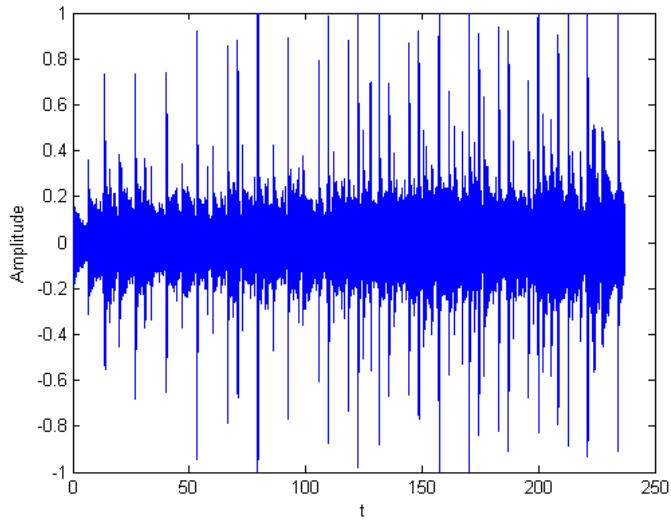


Experimental results

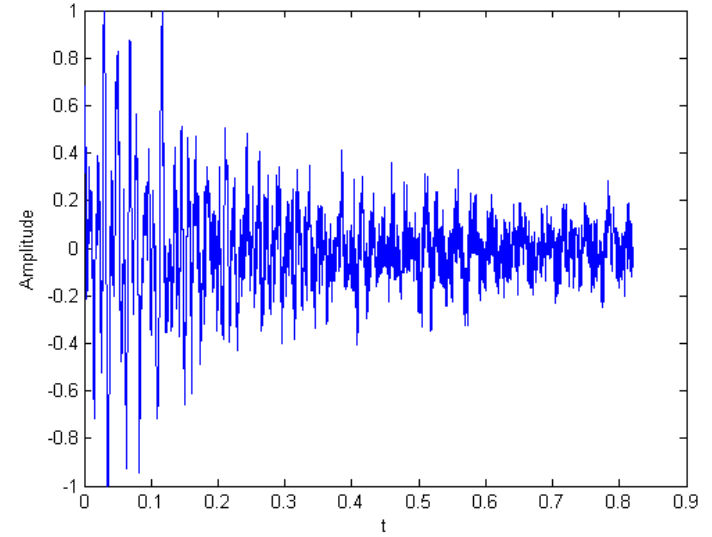
- We consider a song recorded in a real environment
- Shadows song played by Kismet
 - One drum
 - Bass
 - 2 Guitars (accompaniment and solo)
 - Voice
- We present the extraction of the **snare** and the **kick bass** drum scores



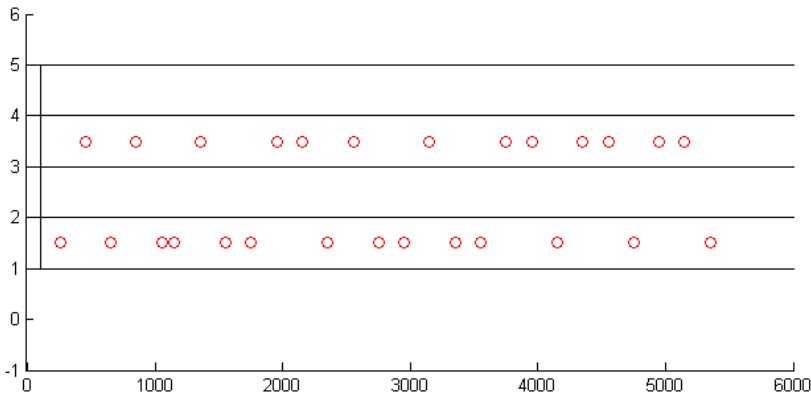
Experimental results



snare

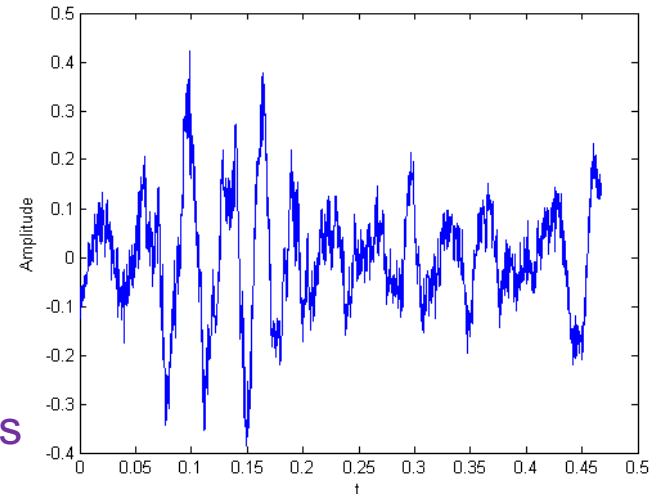


Waveforms in the database



score

kick bass



NEgentropy based Clustering (NEC)

- The proposed approach divides the clustering phase in several steps
 - Pre-processing
 - Robust PCA for unevenly sampled data
 - Pre-clustering
 - Competitive learning (Winner Take All, Self Organizing Maps, Probabilistic Principal Surfaces, ecc.)
 - Agglomerative clustering
 - Hierarchical agglomerative clustering based on Fisher and Negentropy information
 - Visual and interactive data exploration
 - Multi-Dimensional Scaling (MDS)



Fisher's Linear Discriminant

- Fisher's linear discriminant is a classification method that project high-dimensional data onto a line
- The projection maximizes the distance between the means of the two classes while minimizing the variance within each class



NEC approach

- We agglomerate the regions using the following objective function

$$J_{NEC}(\mathbf{x}) \propto \alpha_F J_F(\mathbf{x}) + \alpha_N J_N(\mathbf{x})$$

Fisher

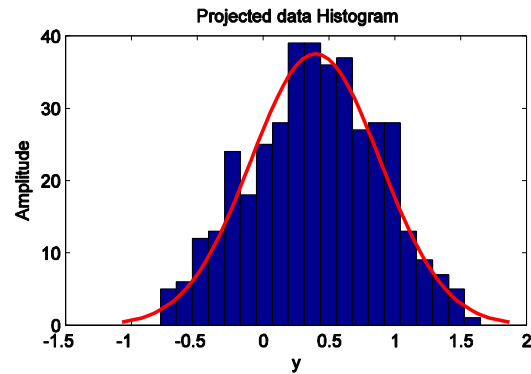
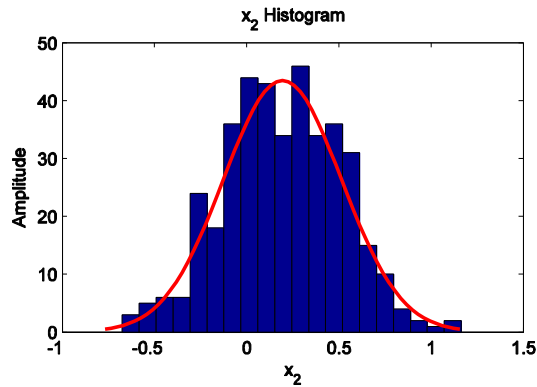
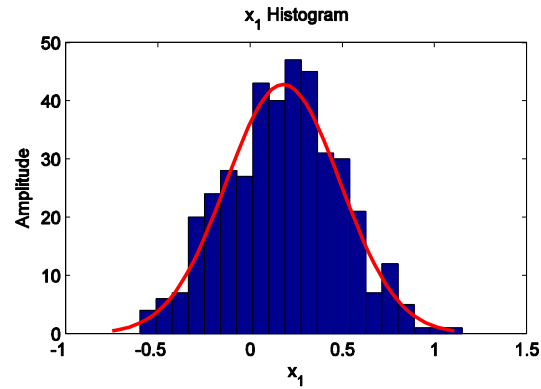
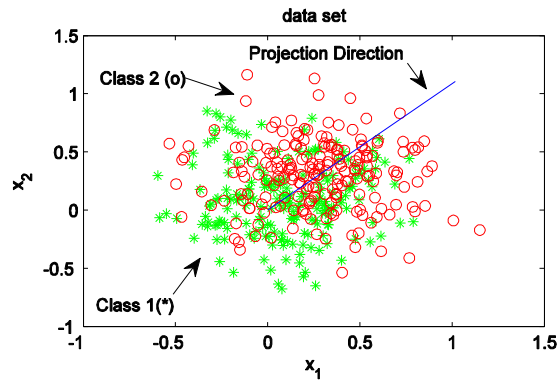
$$J_F(\mathbf{x}) = \frac{\mathbf{w}^T \mathbf{S}_B \mathbf{w}}{\mathbf{w}^T \mathbf{S}_W \mathbf{w}}$$

Negentropy

$$J_N(\mathbf{x}) \propto k_1 E\{\mathbf{x} \exp(-\mathbf{x}^2 / 2)\}^2 + k_2^a \left(E\{|\mathbf{x}|\} - \sqrt{2/\pi} \right)^2$$
$$J_N(\mathbf{x}) \propto k_1 E\{\mathbf{x} \exp(-\mathbf{x}^2 / 2)\}^2 + k_2^b \left(E\{\exp(-\mathbf{x}^2 / 2)\} - \sqrt{1/2} \right)^2$$



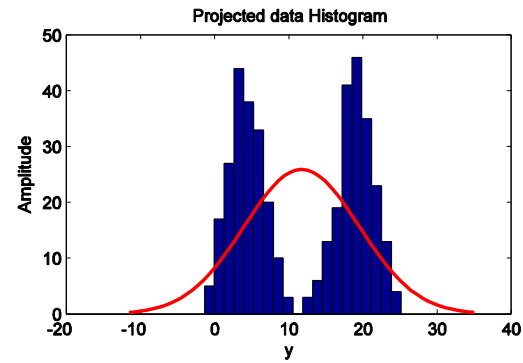
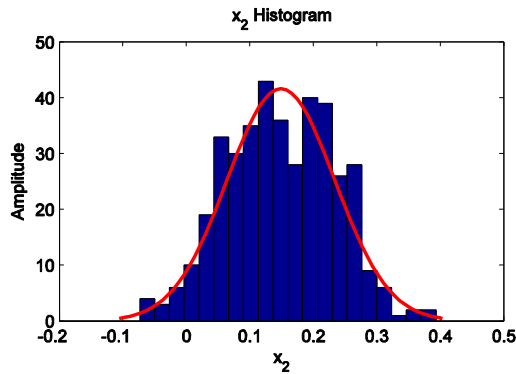
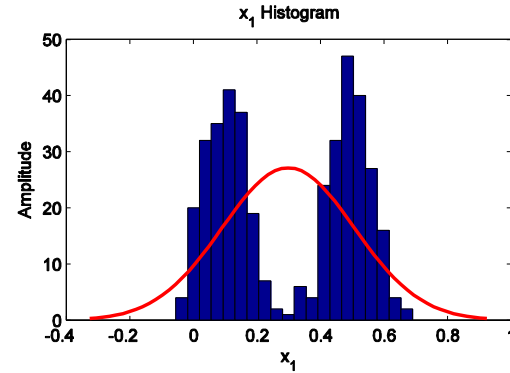
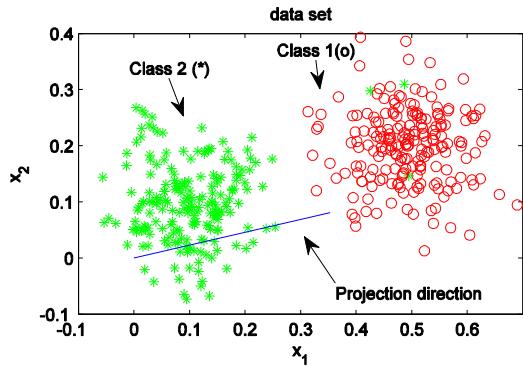
NEC approach



In this case we obtain $J_{NEC} = 0.0079$ in which $\alpha_F J_F = 0.0040$ and $\alpha_N J_N = 9.73 \times 10^{-4} + 0.0029$



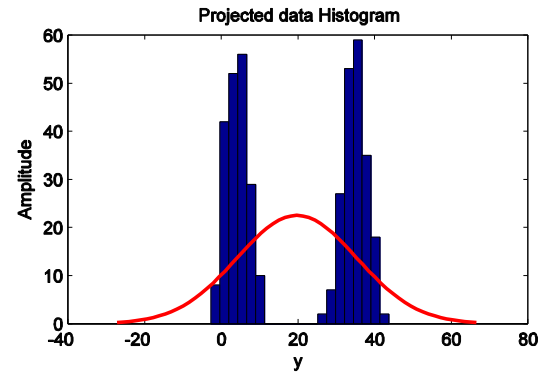
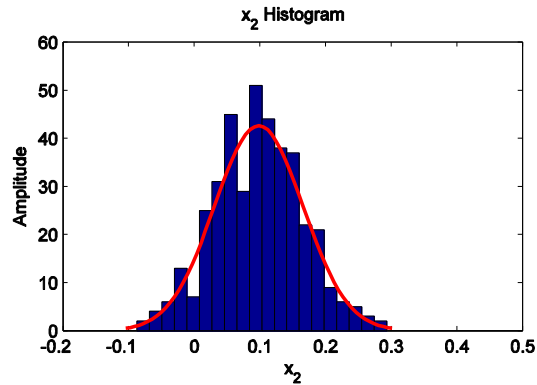
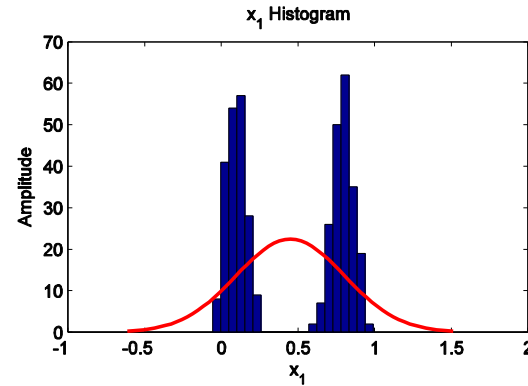
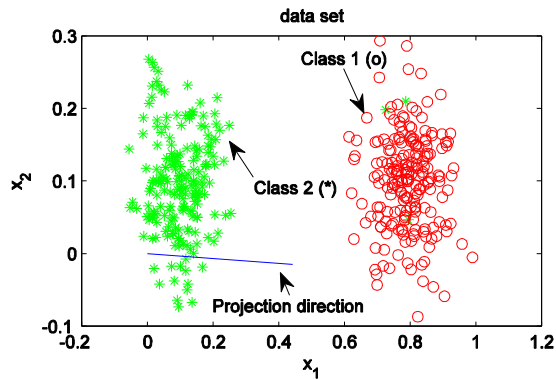
NEC approach



In this case we obtain $J_{NEC} = 0.4064$ in which $\alpha_F J_F = 0.1455$ and $\alpha_N J_N = 1.39 \times 10^{-4} + 0.2669$



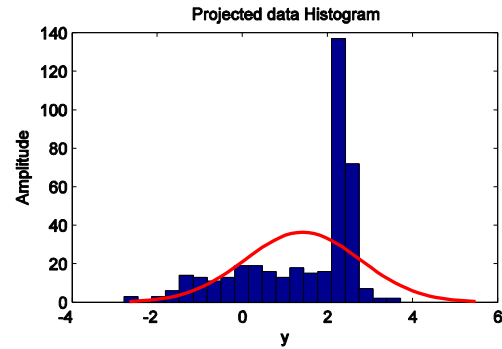
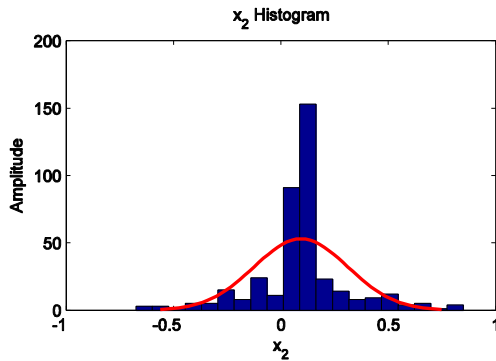
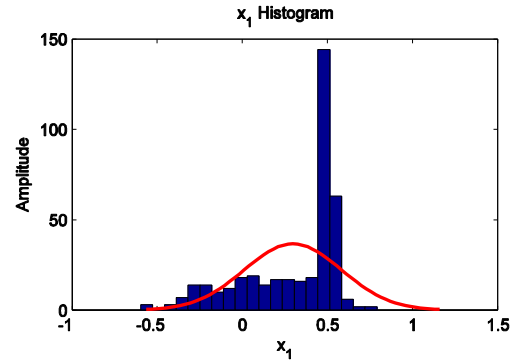
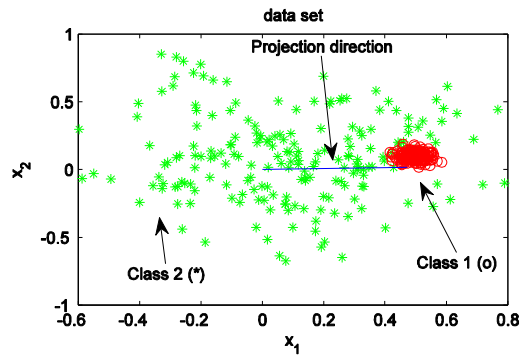
NEC approach



In this case we have two classes with the same direction on the y axes.
We obtain $J_{NEC} = 0.6794$ in which $\alpha_F J_F = 0.3027$ and $\alpha_N J_N = 3.49 \times 10^{-4} + 0.3763$



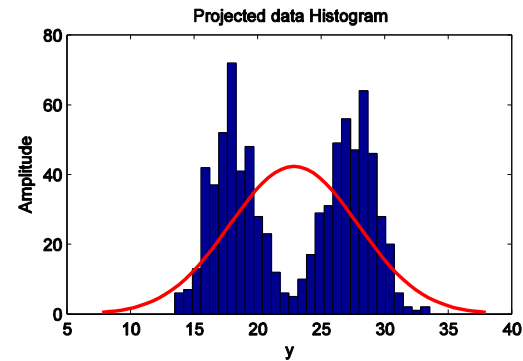
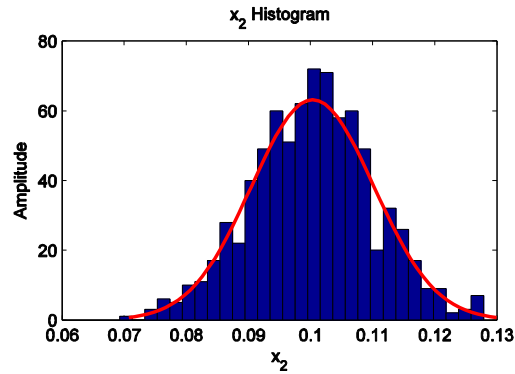
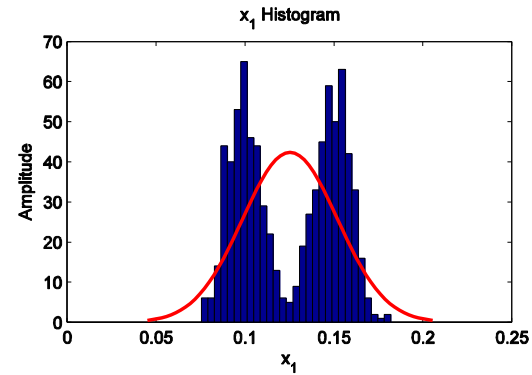
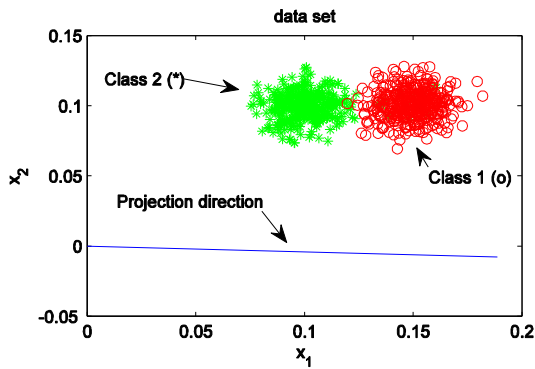
NEC approach



In this case we have two complete overlapped classes. We obtain $J_{NEC} = 0.26603$ in which $\alpha_F J_F = 0.0188$ and $\alpha_N J_N = 0.2196 + 0.0275$. We note that the information is high since the asymmetry information is high.



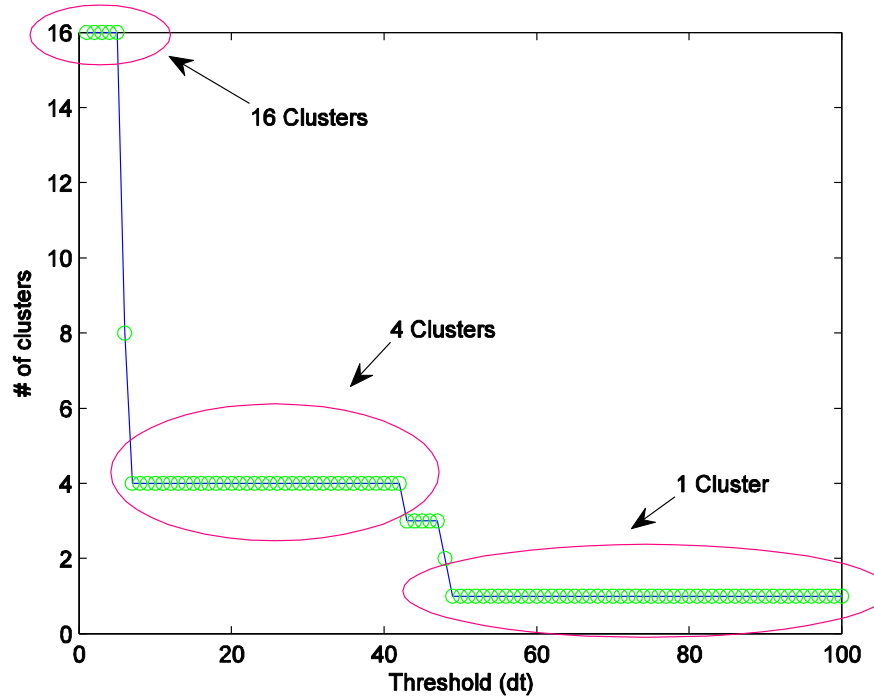
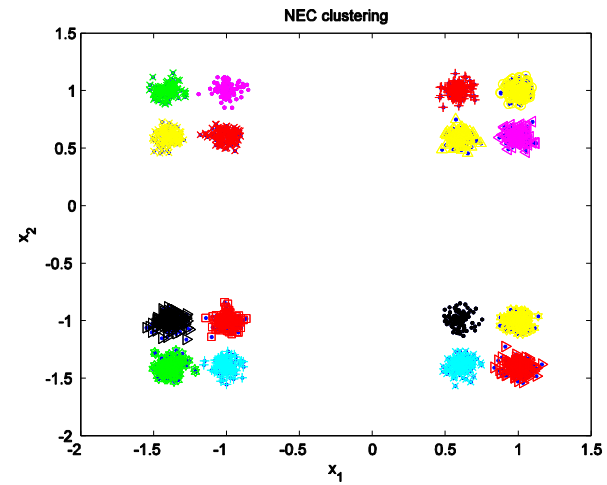
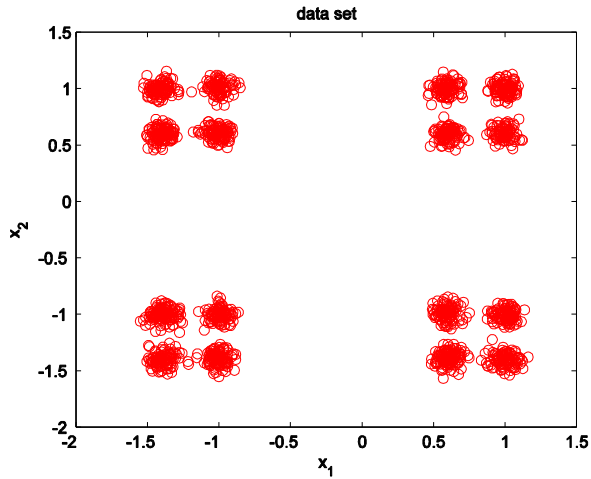
NEC approach



In this case we have two overlapped classes. We obtain $J_{NEC} = 0.2861$ in which $\alpha_F J_F = 0.0910$ and $\alpha_N J_N = 3.64 \times 10^{-4} + 0.194876$. We note that the information is high since the bimodality/sparsity information is higher than the other information.



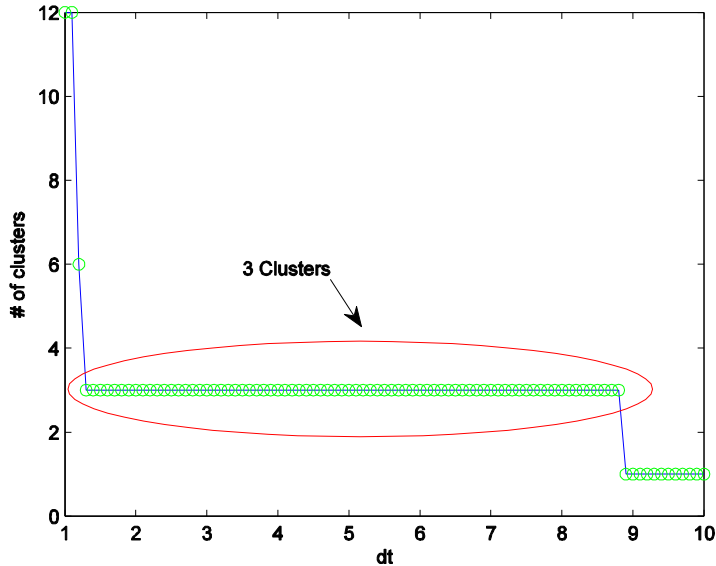
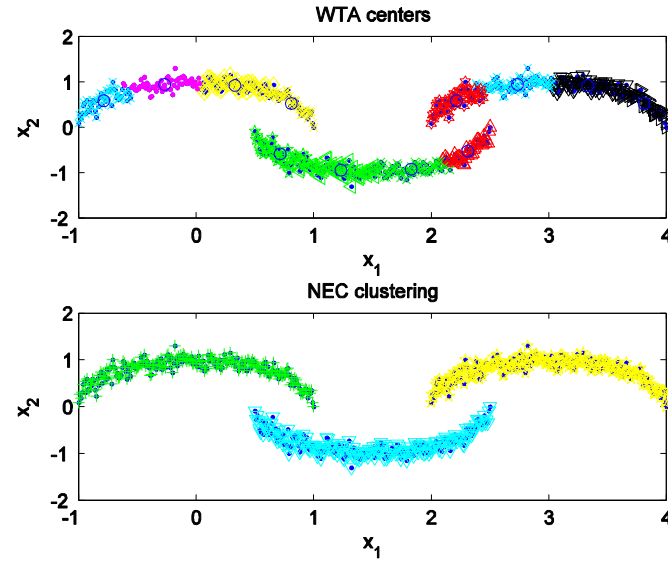
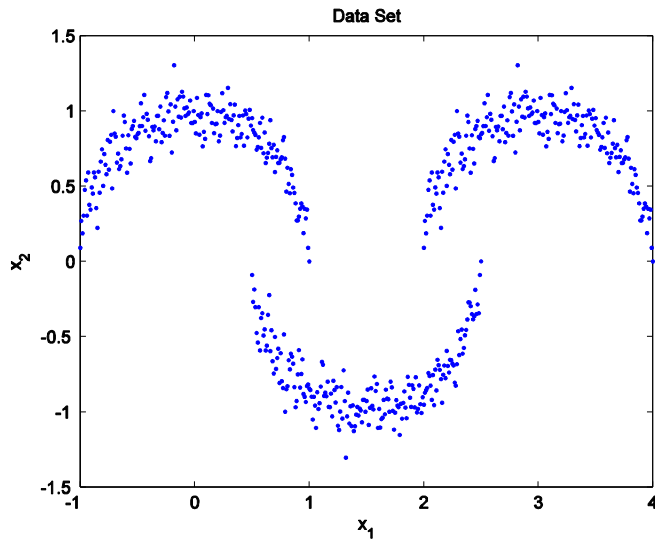
NEC approach



The clusters obtained varying the threshold (dt)



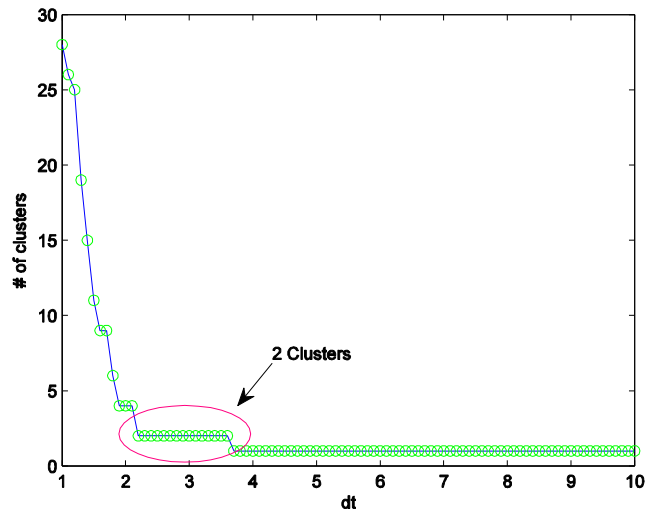
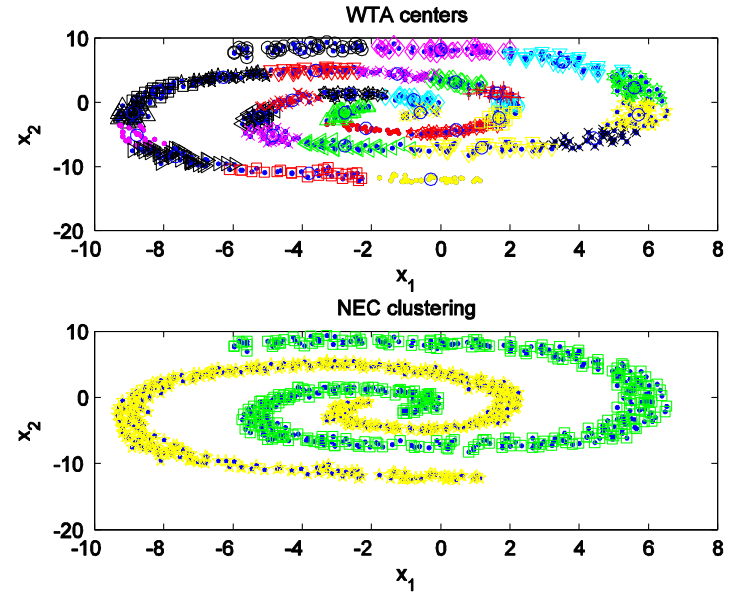
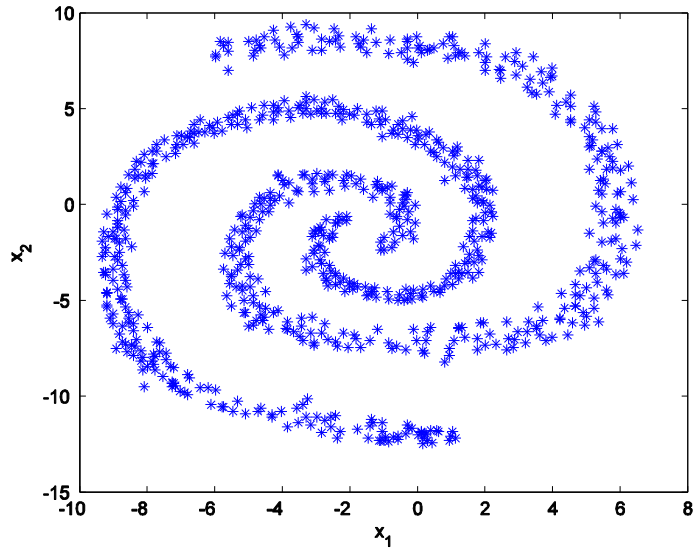
NEC approach



The clusters obtained varying the threshold (dt)



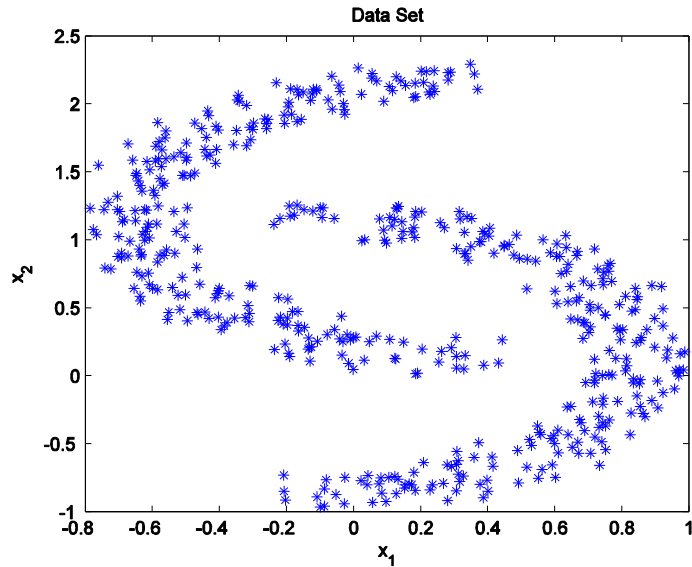
NEC approach



The clusters obtained varying the threshold (dt)

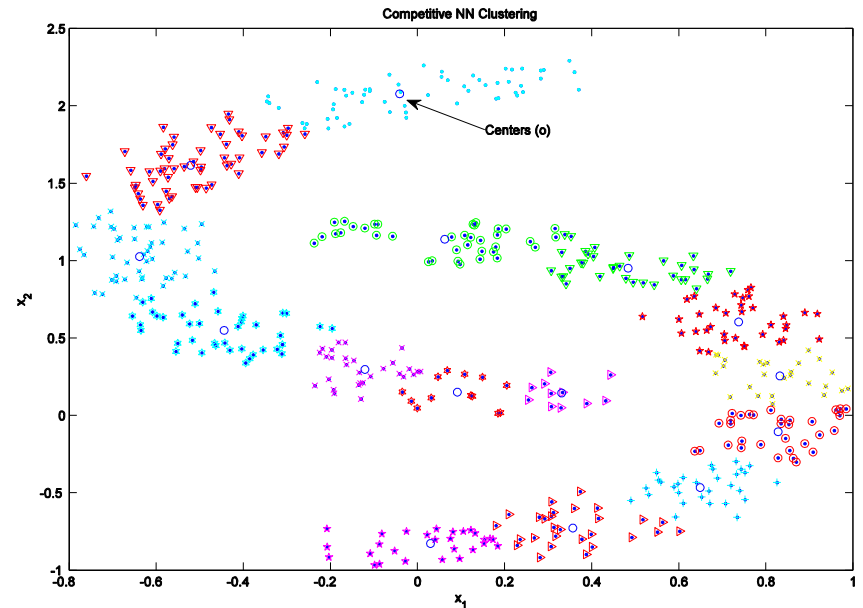


Clustering and Negentropy

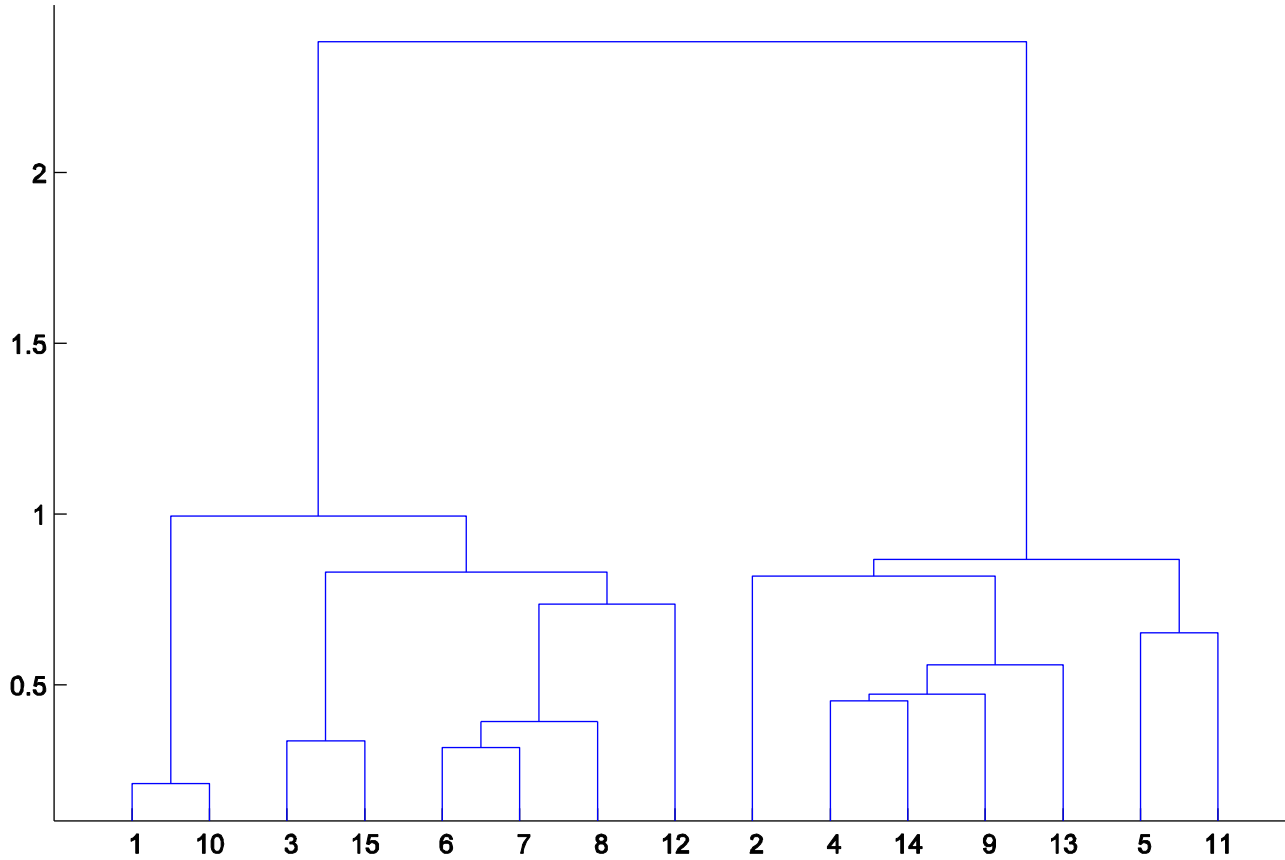


In this case we consider a 2-dimensional data set composed by two separated classes

Clusters obtained by using unsupervised clustering



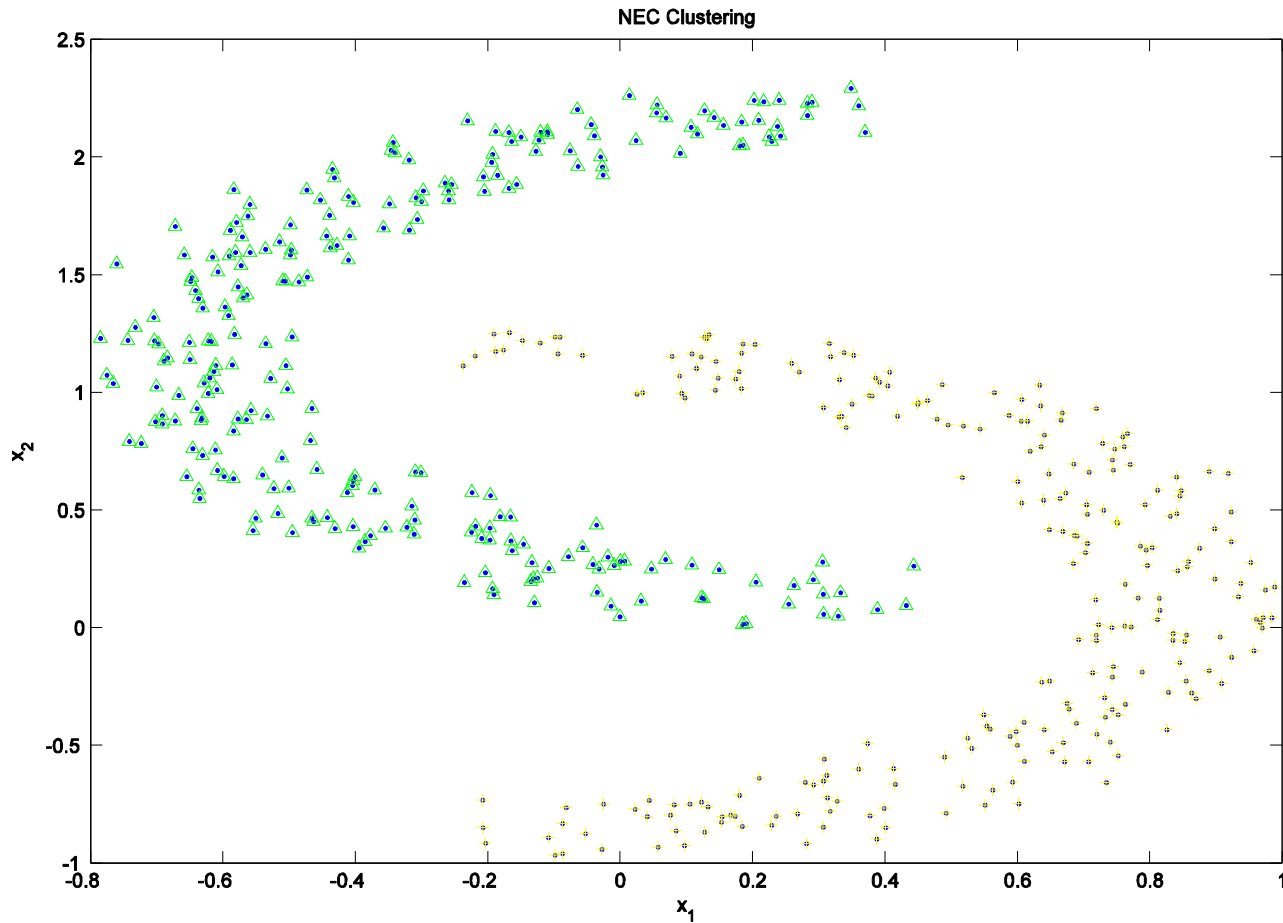
Dendrogram



Dendrogram obtained by using the NEC approach



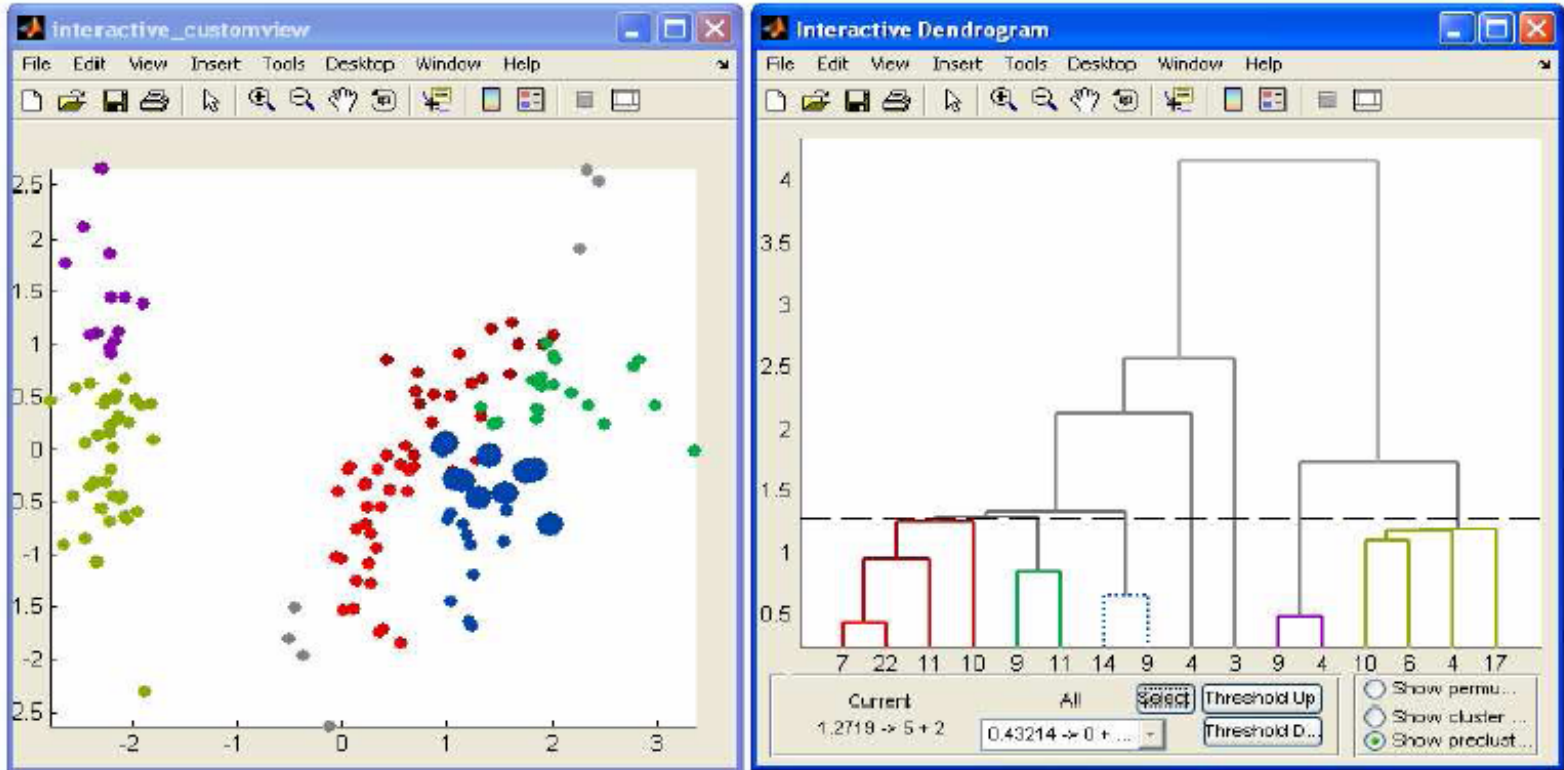
Dendrogram and clusterization



Clusters obtained by using the NEC approach



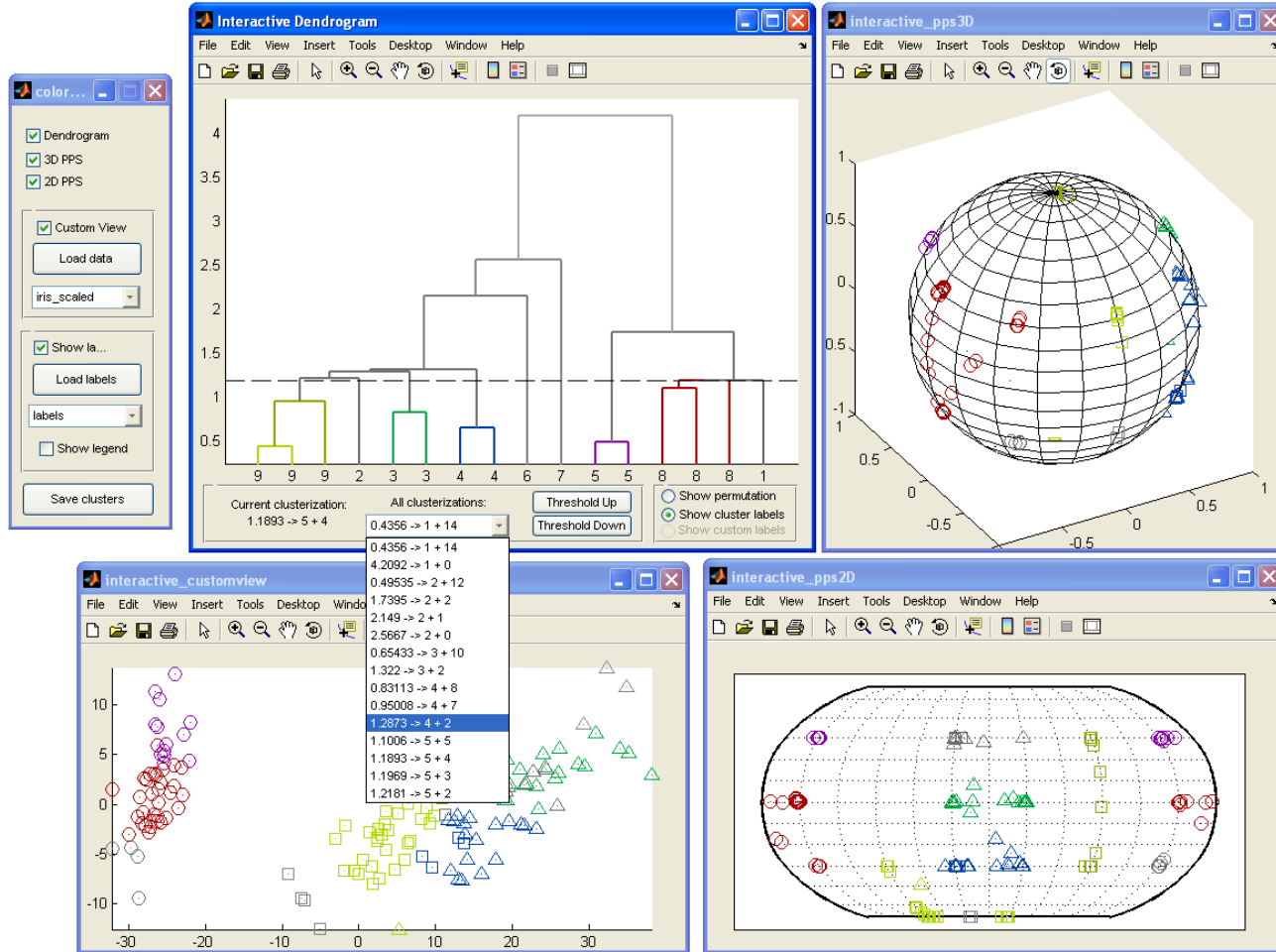
Interface



NEC toolbox



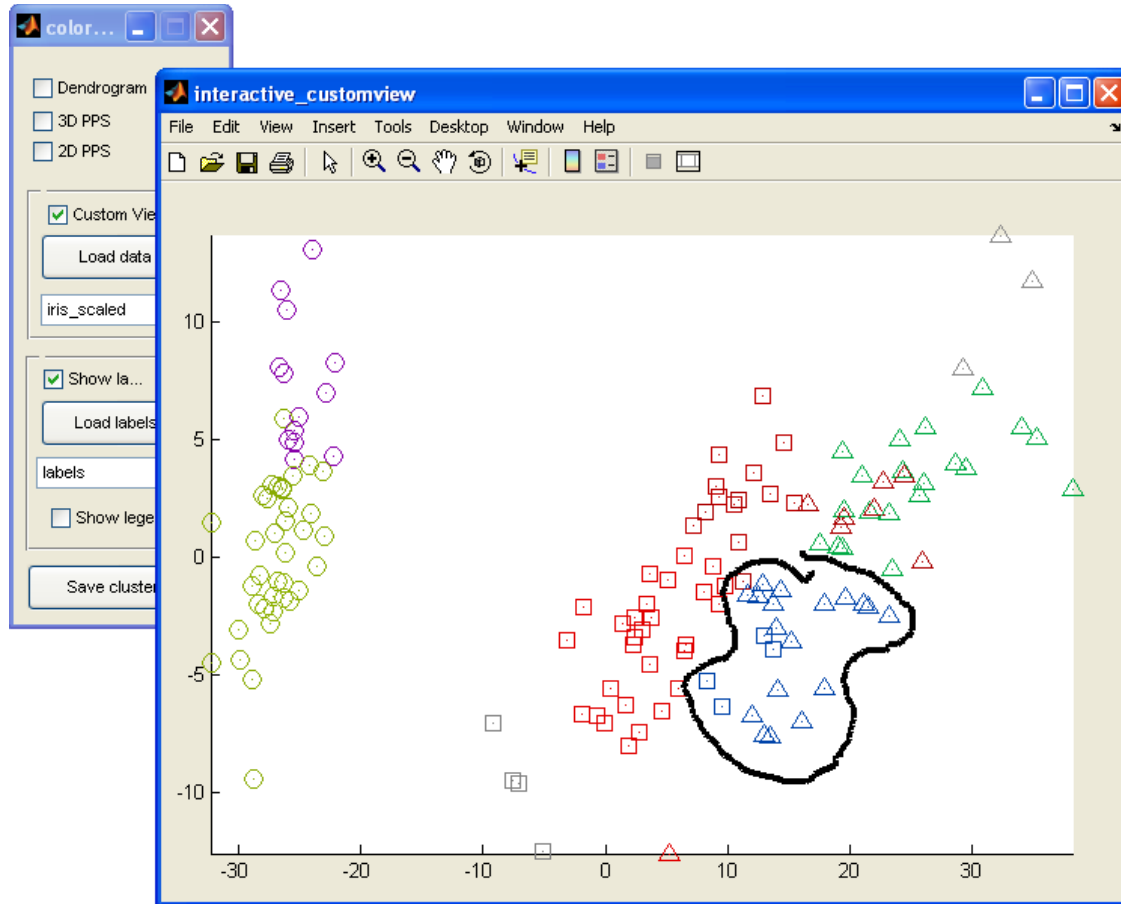
Interface



NEC toolbox



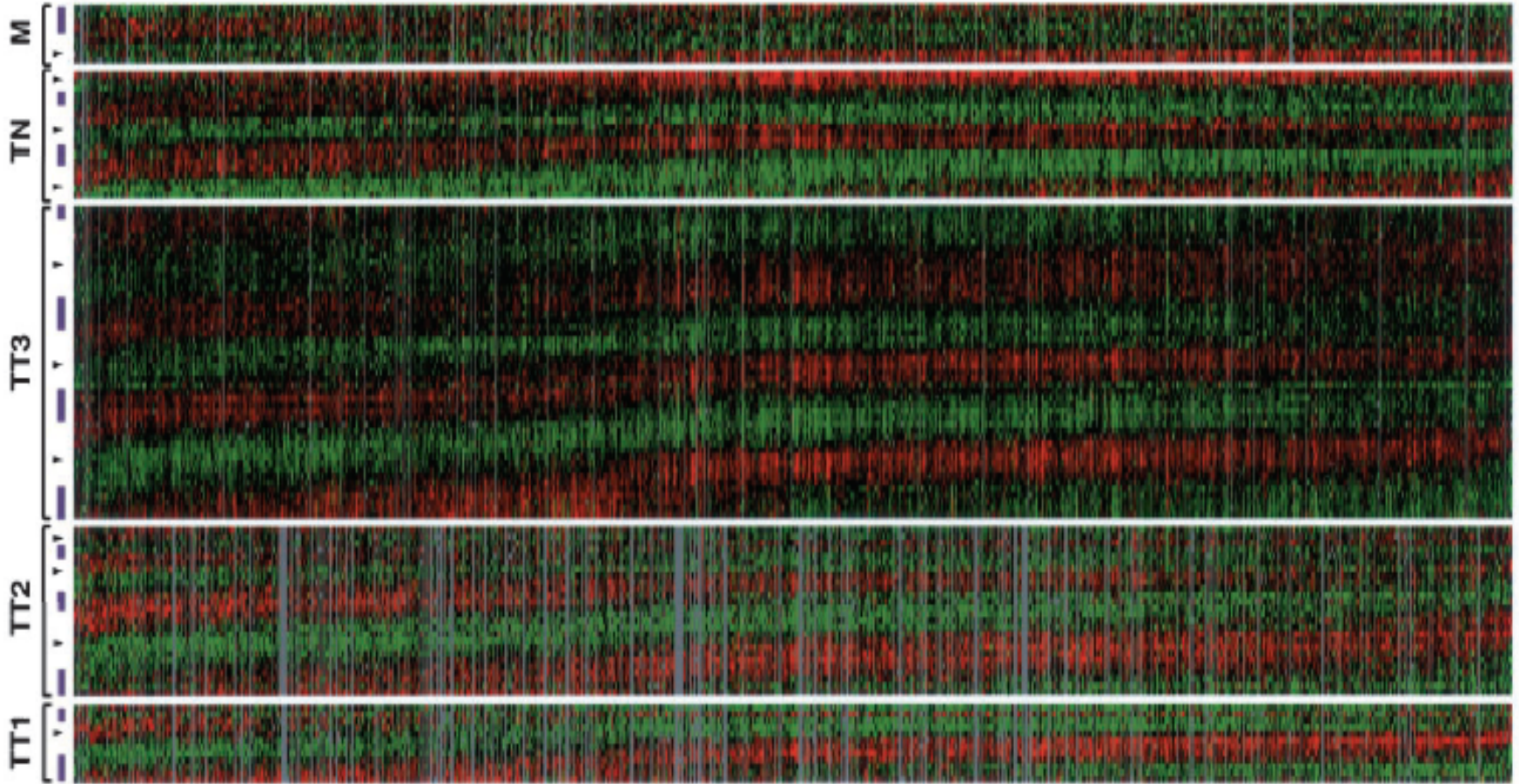
Interface



NEC toolbox



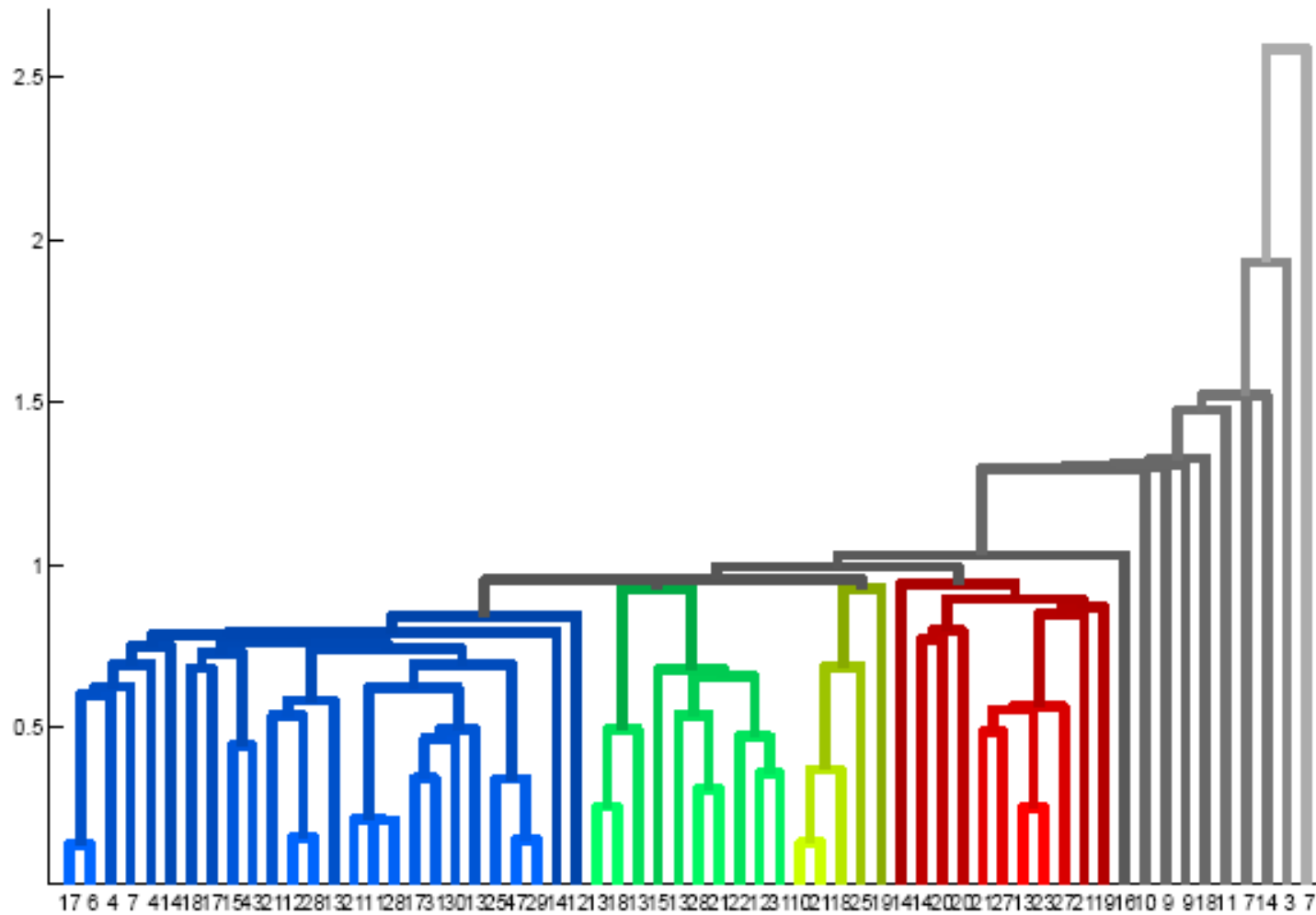
Human Cell Cycle Gene Expression Data



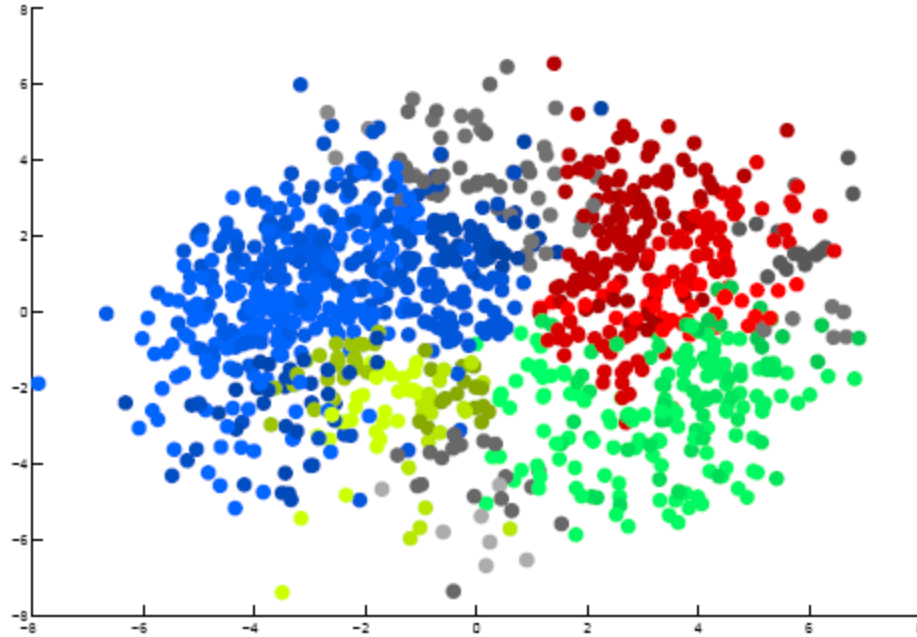
Collaboration with the Department of Physics of the University of Naples "Federico II" and Telethon Institute of Genetics and Medicine (TIGEM) of Naples



NEC dendrogram



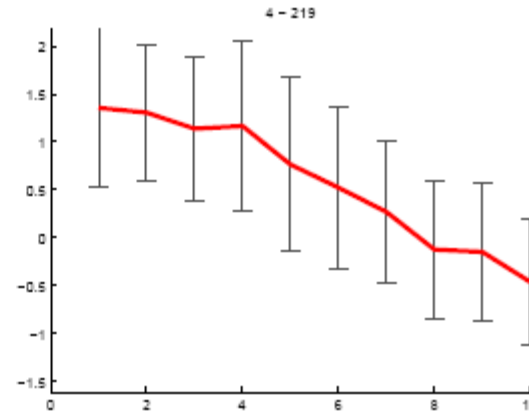
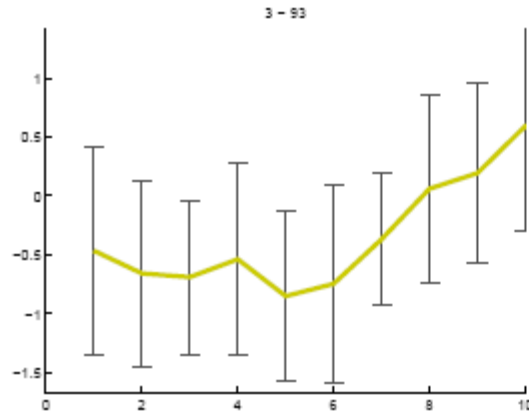
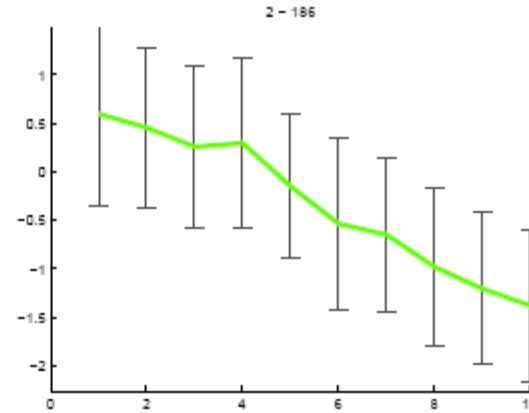
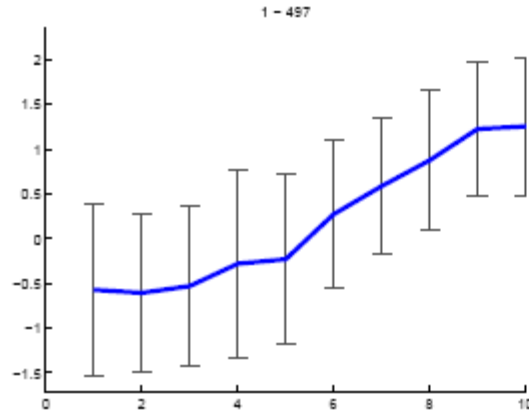
NEC dendrogram



MDS Labeling



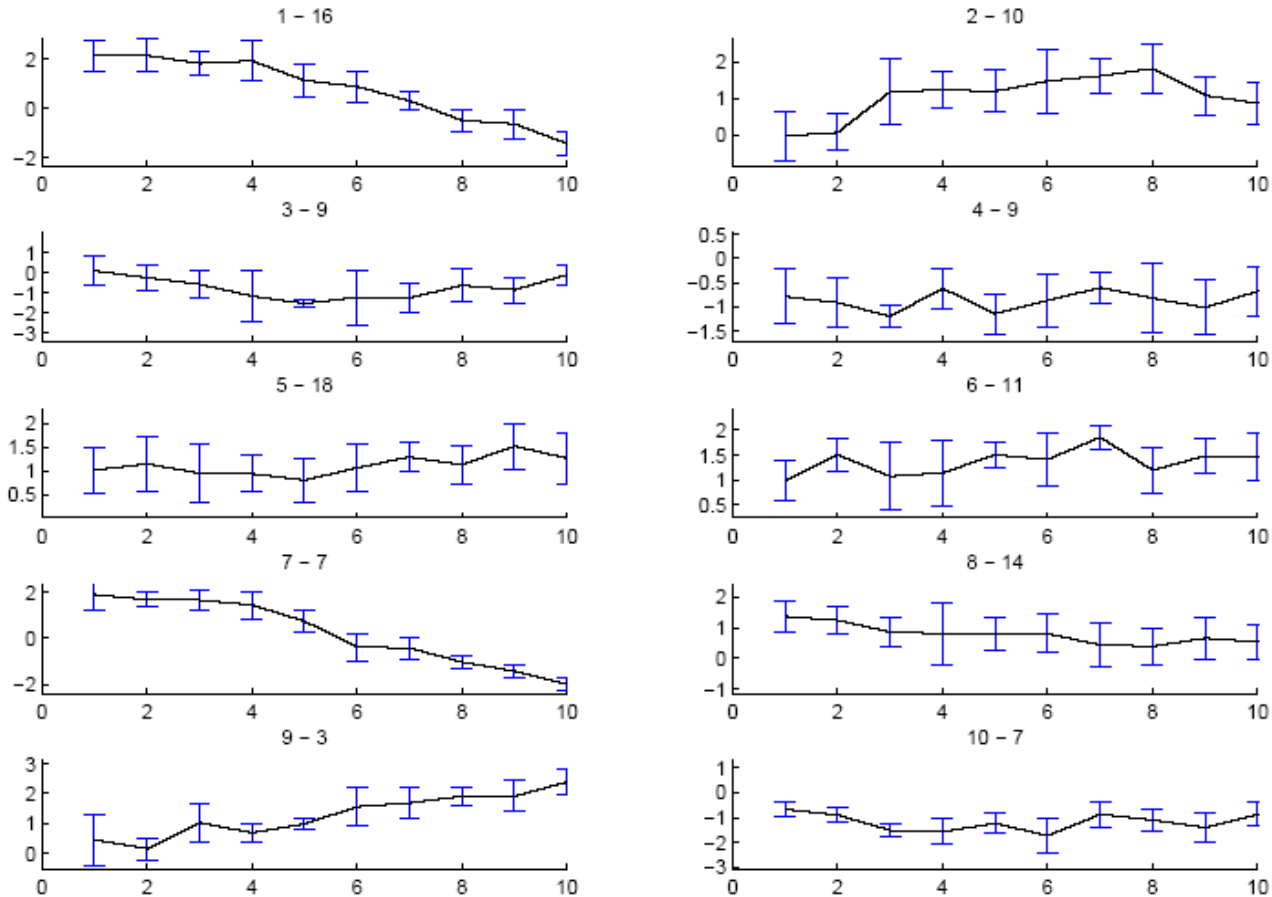
NEC dendrogram



The archetype behavior with corresponding standard deviation for the for particularly significant clusters found in our analysis



NEC dendrogram



The archetype behavior with corresponding standard deviation for the 10 outlier clusters found in our analysis.



Model selection for ensemble dispersion

- This work aims at introducing an approach to analyze the **independence between different model data in a multi-model ensemble context**
- The models are operational long-range transport and dispersion models
 - real-time **simulation of pollutant** dispersion or the accidental release of radioactive nuclides in the atmosphere
- An approach based on **the hierarchical agglomeration of distributions** of predicted radionuclide concentrations is proposed
 - two different similarity measures: **Negentropy information** and **Kullback-Leibler divergence**
- These approaches are used to analyze the data obtained during the ETEX-1 exercise
- The approach select subsets of independent models, whose performance are comparable to those from the whole ensemble

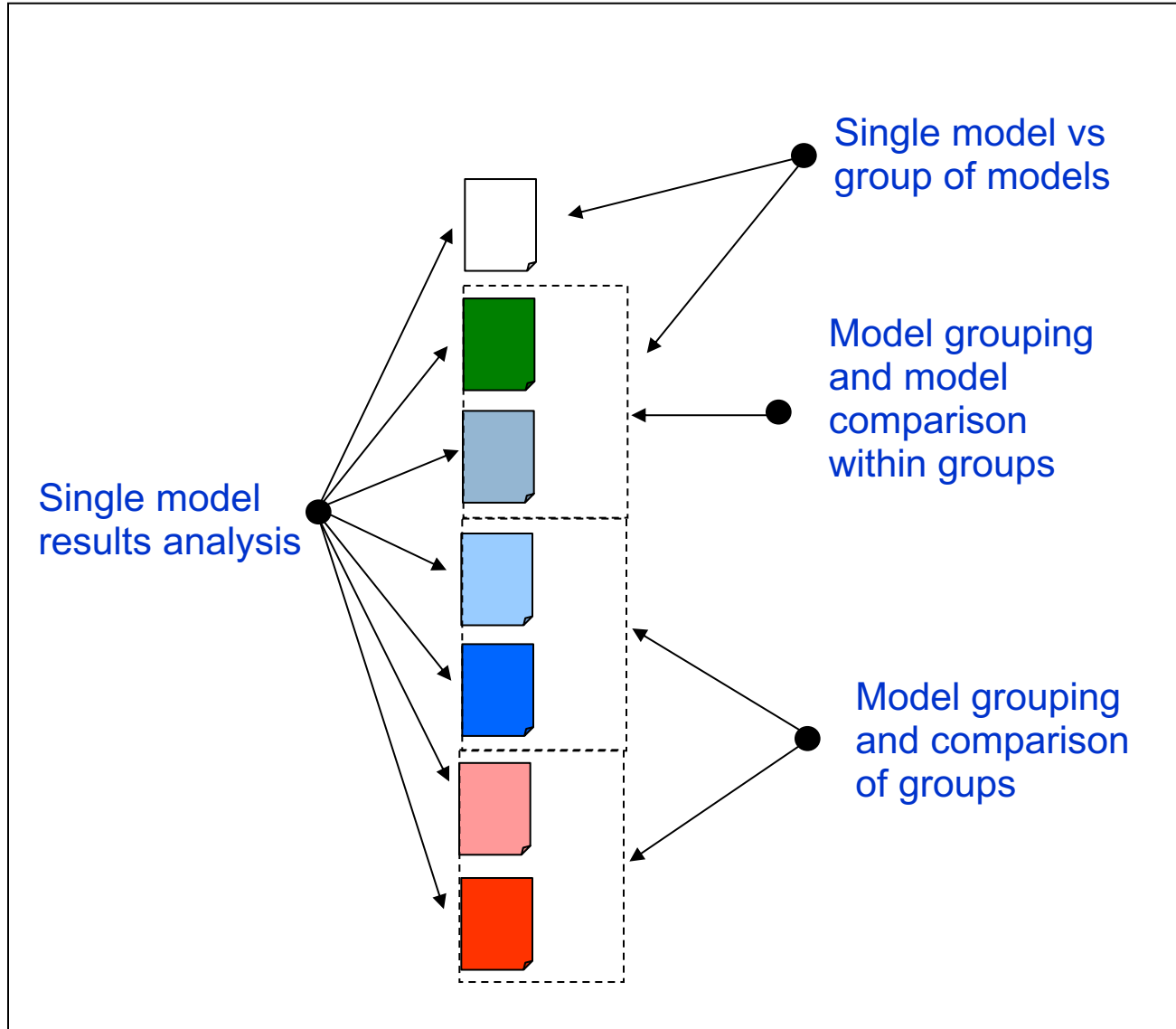
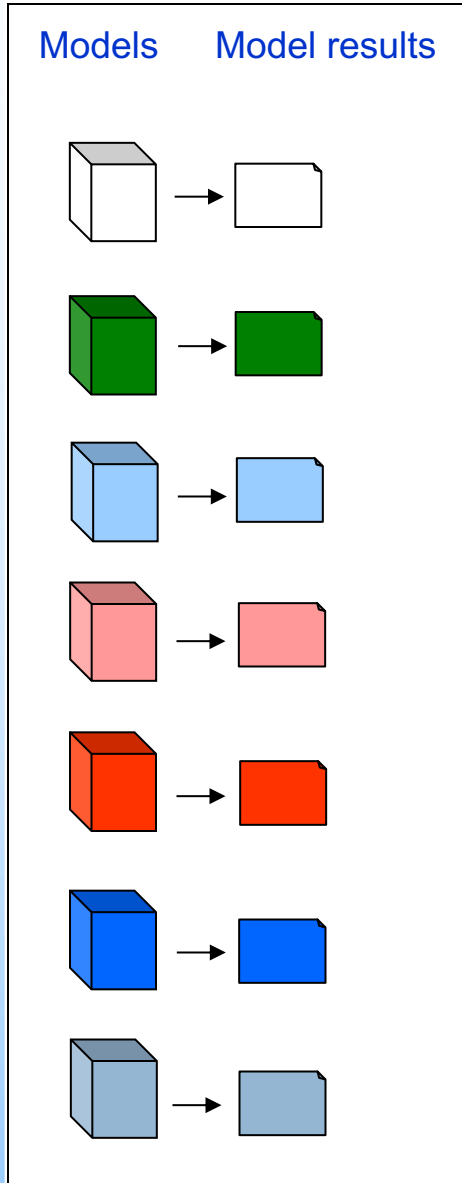


Emergency response

- **Accidental release** of radioactive material from NPP or other (i.e. Chernobyl, Algeciras, Hemel Hempstead)
- Atmospheric transport and dispersion over the continent, potential for **trans-boundary character**
 - Where is it?
 - When is getting there?
 - How much should I expect?
- At national level, met services and environmental protection agencies use long range transport and dispersion models to **forecast concentration** and deposition



Ensemble treatment - concept

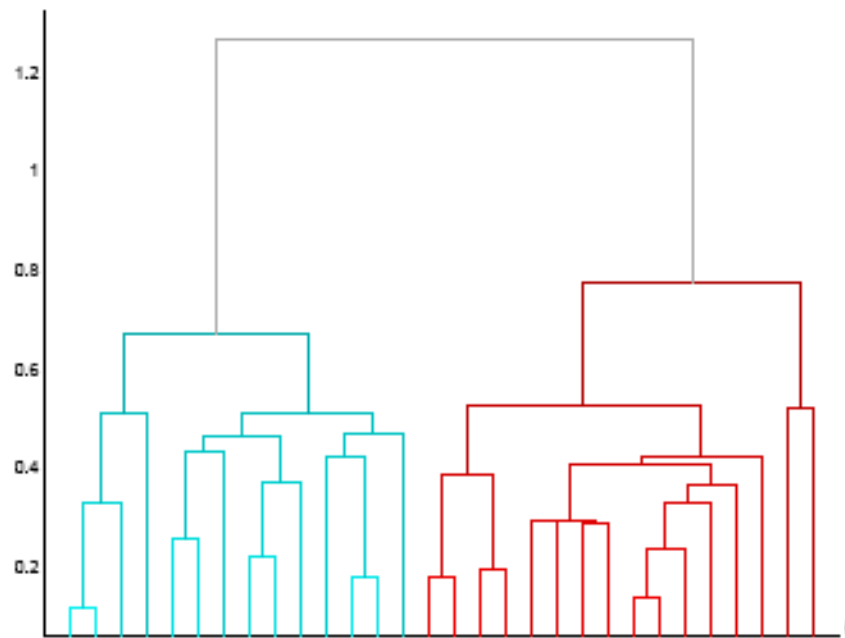


Ensemble and independence

- The **Median Model** was shown to outperform the results of any single deterministic model in reproducing the concentration of atmospheric pollutants
 - during the ETEX experiment
- A well-known statistical approach has been applied to multimodel data analysis
 - **Bayesian Model Averaging (BMA)**
 - similarities and differences between models were explored by means of correlation analysis
- **Note** - If different models are used to simulate the same phenomenon they probably will give **similar responses**
 - model ensemble results may lead to erroneous interpretations
 - this is more probable if models are strongly dependent



Model selection



Dendrogram

$$KL(\mathbf{p}||\mathbf{q}) = \sum_{i=1}^n p_i \log \left(\frac{p_i}{q_i} \right)$$

$$KL = \frac{KL(\mathbf{p}||\mathbf{q}) + KL(\mathbf{q}||\mathbf{p})}{2}$$

Kullback-Leibler

$$J_N(\mathbf{x}) = H(\mathbf{x}_{Gauss}) - H(\mathbf{x})$$

Negentropy

$$J_N(\mathbf{x}) \propto k_1 E\{G^1(\mathbf{x})\}^2 + k_2 (E\{G^2(\mathbf{x})\} - E\{G^2(v)\})^2$$



ETEX-1

- The ETEX-1 experiment concerned the release of **pseudo-radioactive material** on 23 October 1994 at 16:00 UTC from Monterfil, southeast of Rennes (France)
 - A steady westerly flow of unstable air masses was present over **central Europe**
 - Such conditions persisted for the 90 h that followed the release with frequent precipitation events over the advection area and a slow movement toward the North Sea region
- **Several independent groups** worldwide tried to forecast these observations
 - Each simulation, and therefore each ensemble member, is produced with different atmospheric dispersion models and is based on weather fields generated by (most of the time) different **Global Circulation Models (GCM)**
 - All the simulations relate to the same release conditions

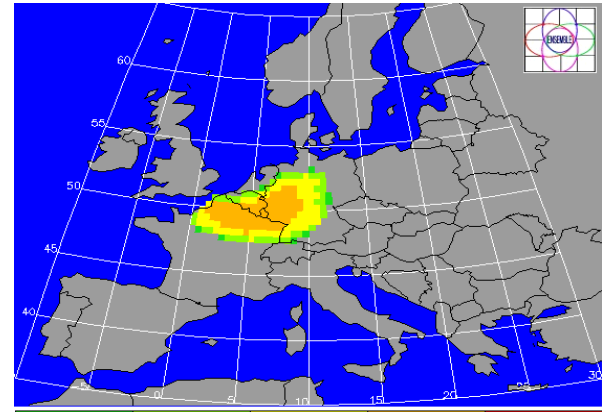
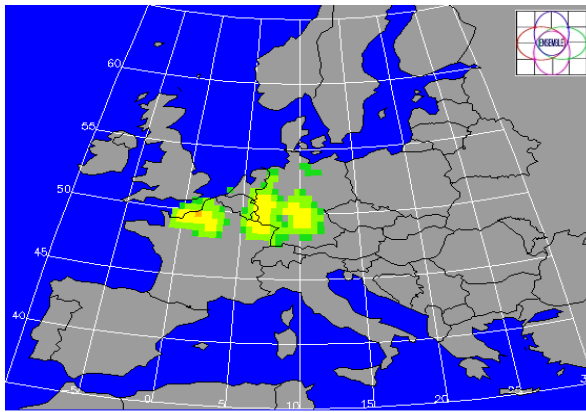
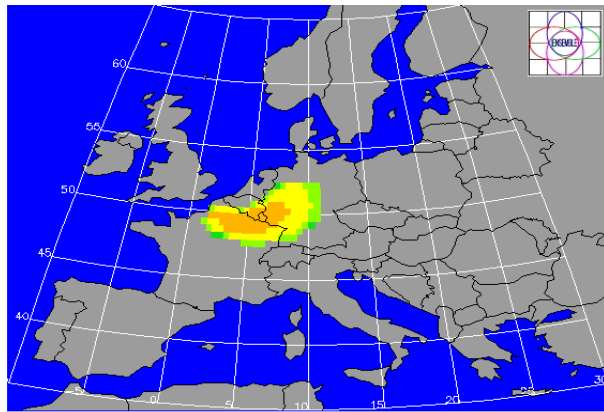


50th percentile

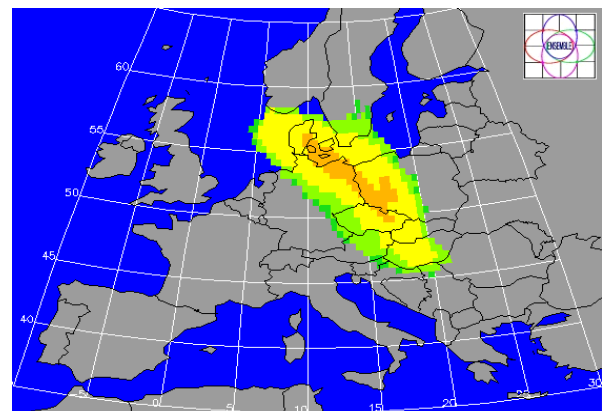
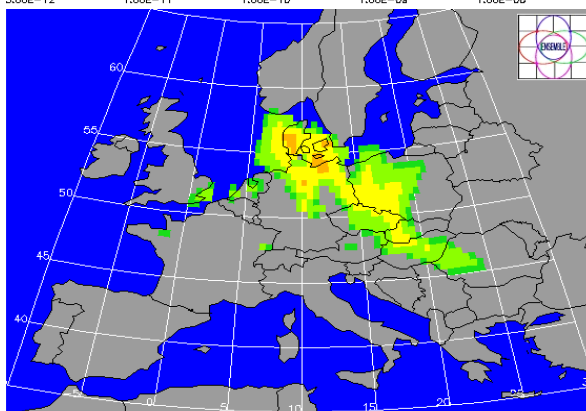
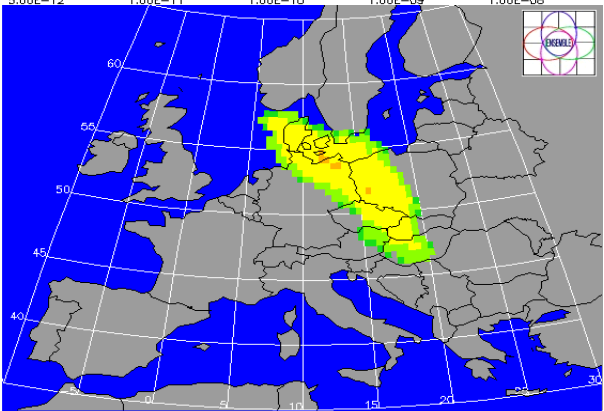
ETEX DATA

75th percentile

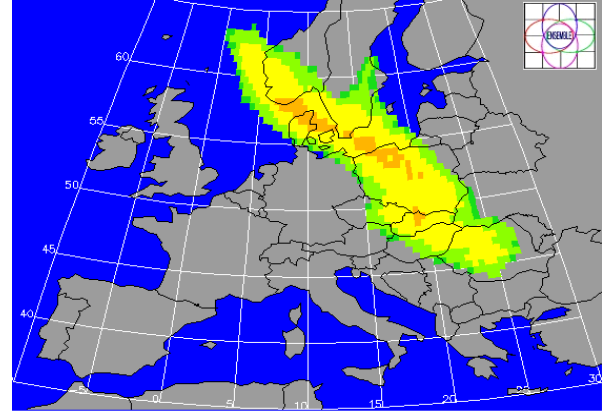
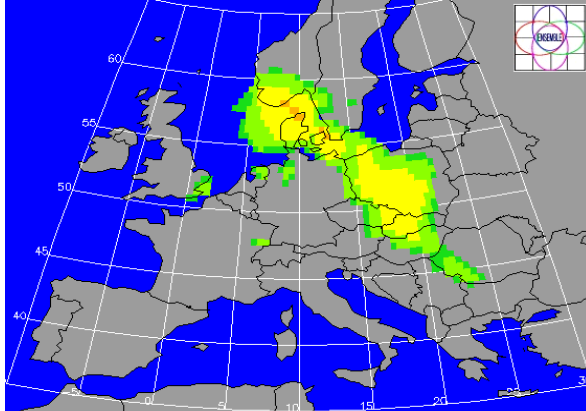
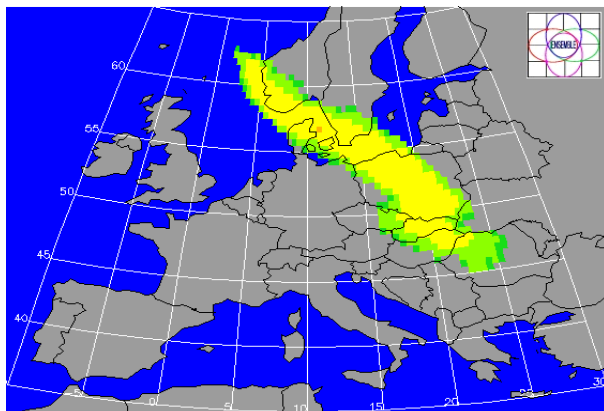
T₀+24 h



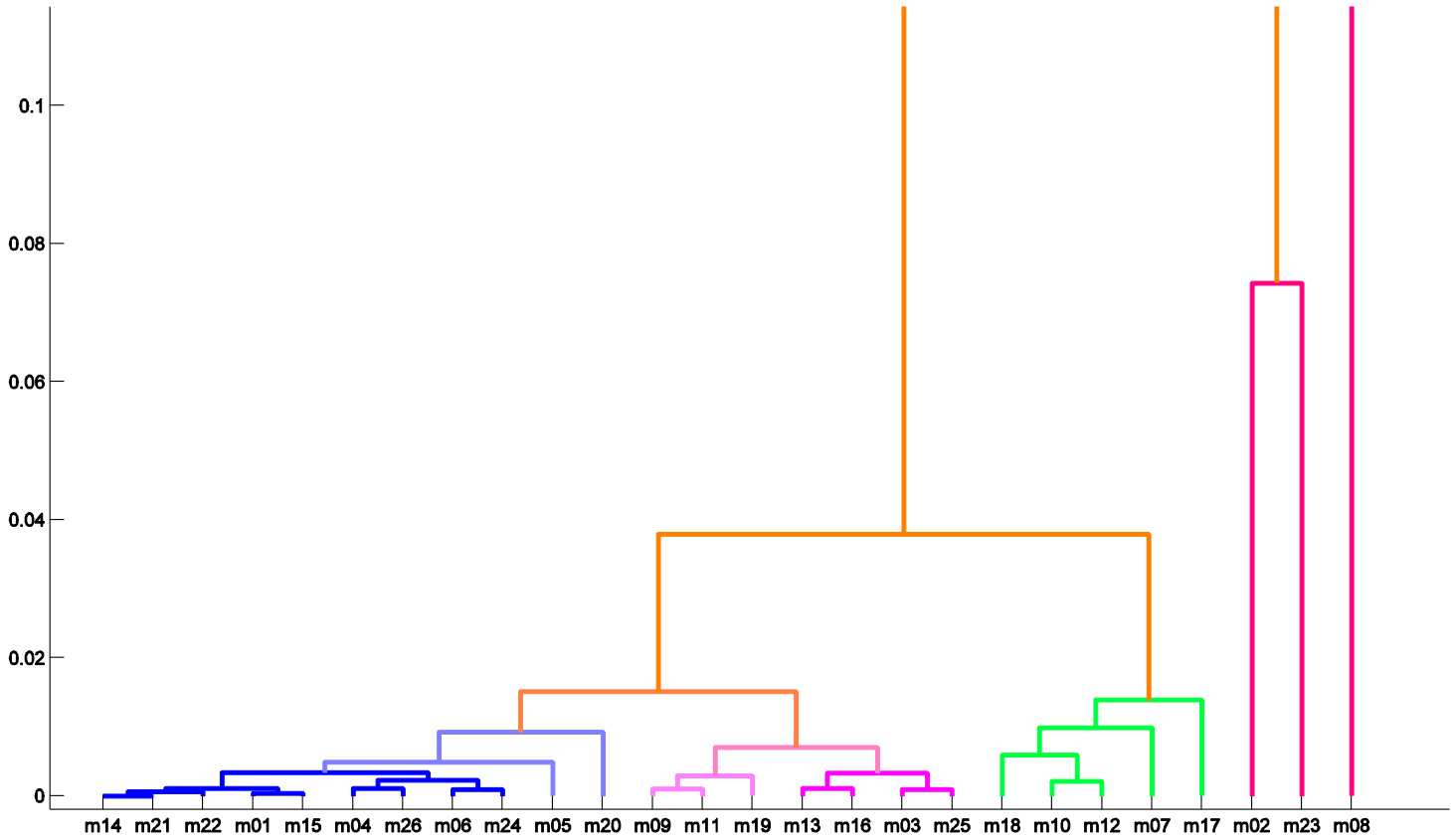
T₀+48 h



T₀+60 h



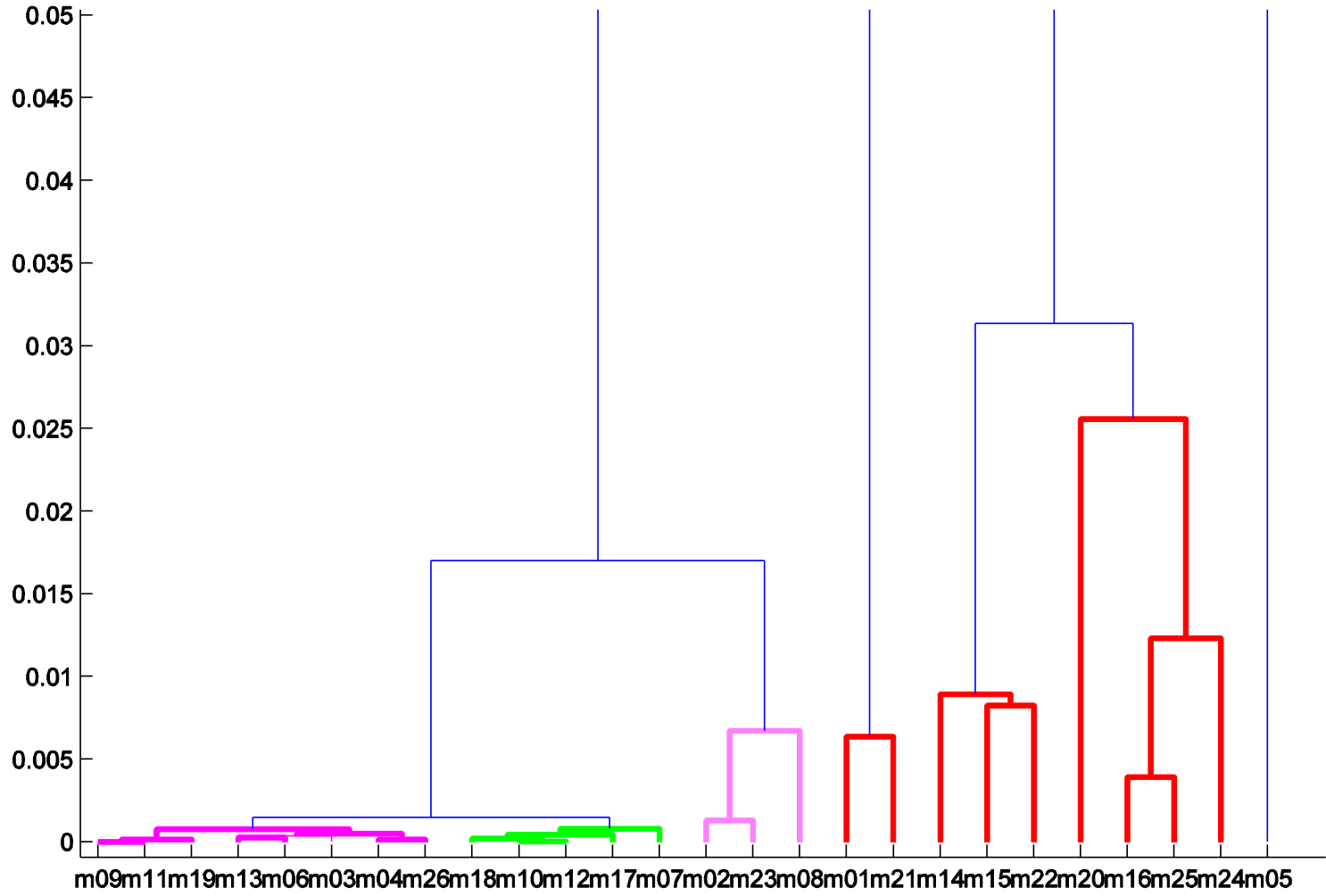
ETEX-1 results



Negentropy dendrogram



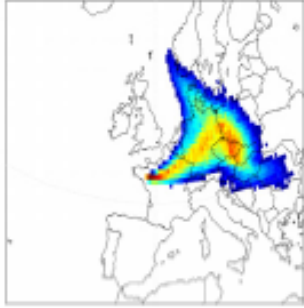
ETEX-1 results



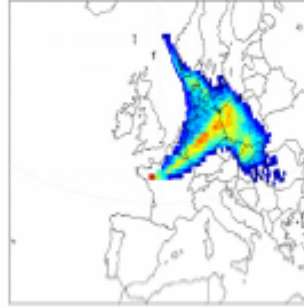
KI divergence dendrogram



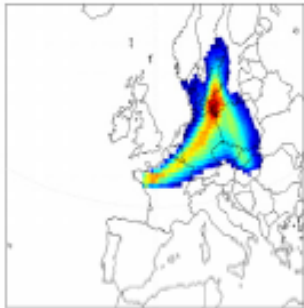
ETEX-1 results



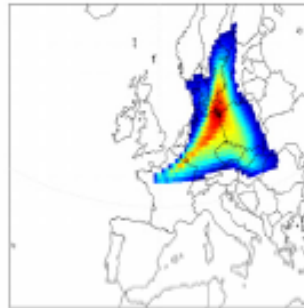
a)



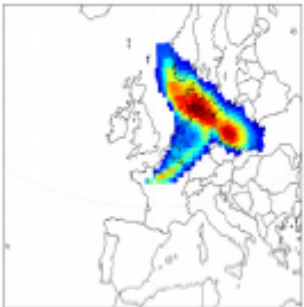
b)



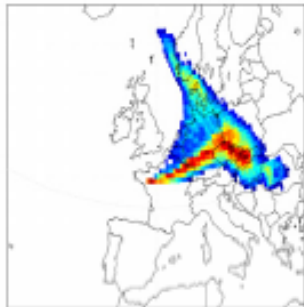
c)



d)



e)



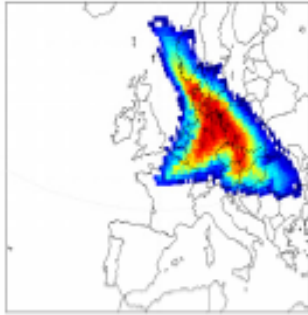
f)

blue cluster in the Negentropy dendrogram.
The visualized models are m_{14} , m_{21} , m_{01} , m_{15} , m_{06} and m_{24} , respectively

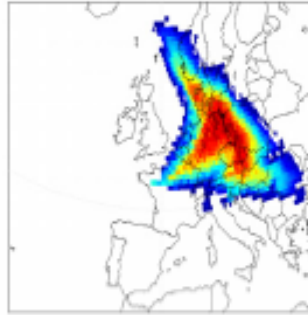
Distributions after 78 hours of the models m_{14} (a), m_{21} (b), m_{01} (c), m_{15} (d), m_{06} (e), m_{24} (f)



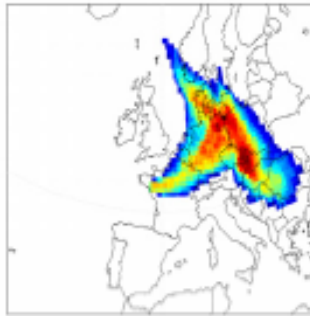
ETEX-1 results



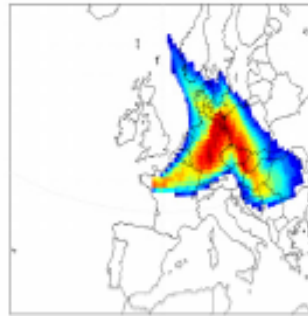
a)



b)



c)



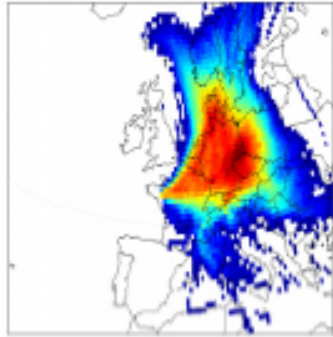
d)

Distributions after 78 hours of the models m_{09} (a), m_{11} (b), m_{13} (c), m_{16} (d)

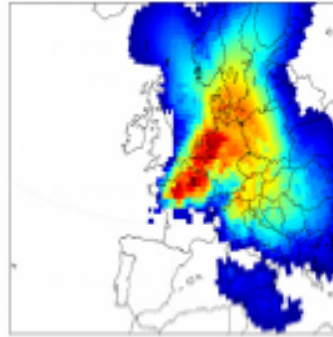
Distributions in the **magenta cluster** of the Negentropy dendrogram. In this case the models are m_{09} , m_{11} , m_{13} and m_{16}



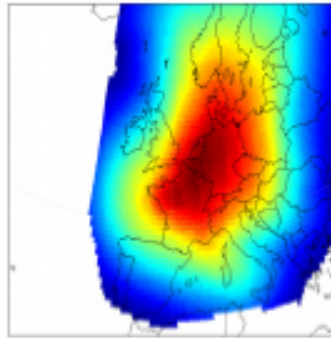
ETEX-1 results



a)



b)



c)

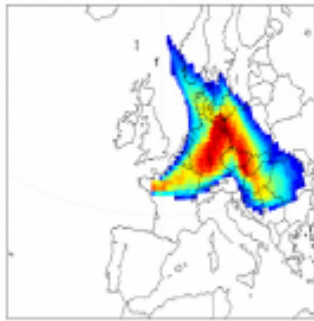
Distributions after 78 hours of the models m_{02} (a), m_{23} (b) and m_{08} (d)

Distributions in the Negentropy dendrogram. In this case the models are m_{02} , m_{23} , m_{08}

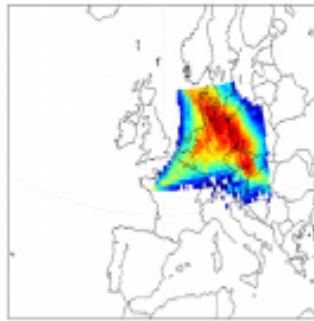
Note: the same three models are agglomerated together in the KL dendrogram but they belong to another extended cluster



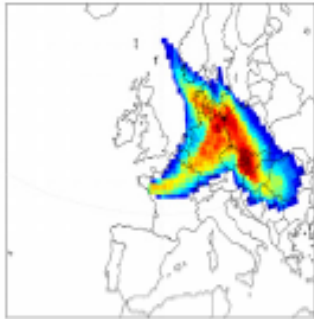
ETEX-1 results



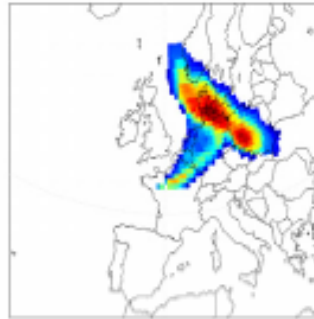
a)



b)



c)



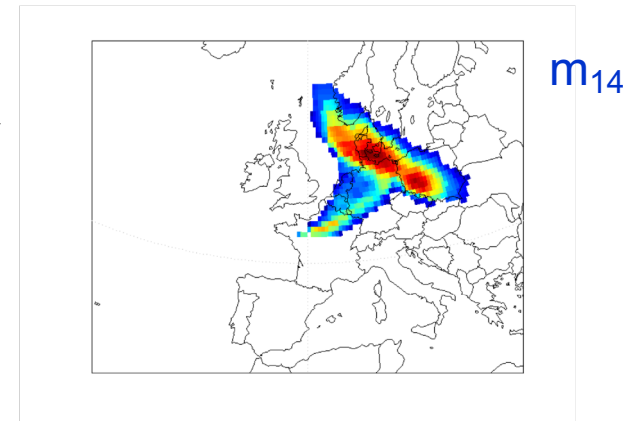
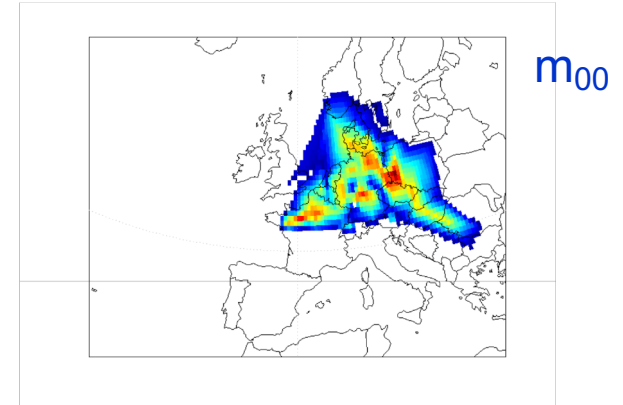
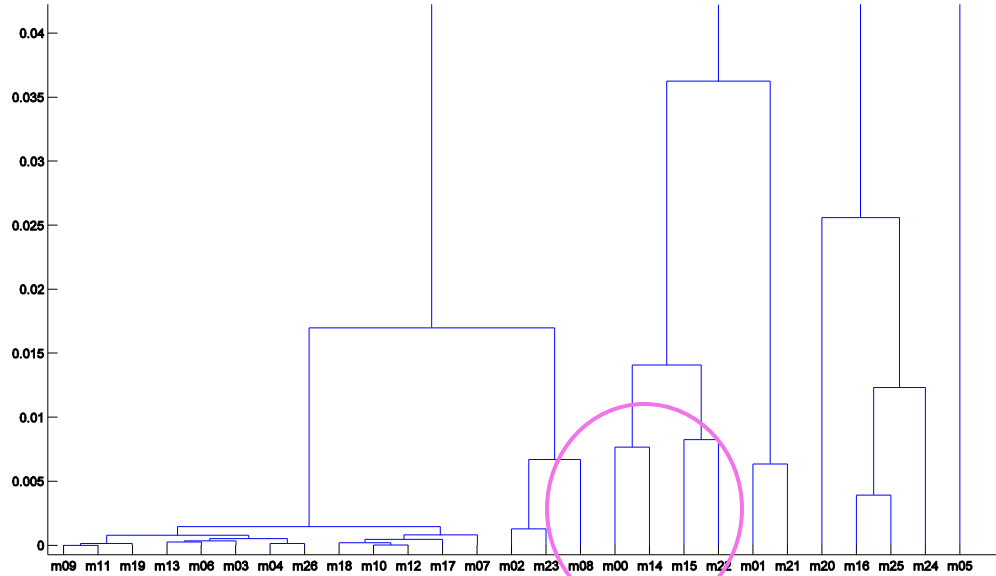
d)

Distributions after 78 hours of the models m_{16} (a), m_{25} (b), m_{13} (c) and m_{06}

In the KL dendrogram the model m_{16} is associated together with the model m_{25} but we can note that its distribution is closer to that of model m_{13} than m_{25} . In the Negentropy based dendrogram models m_{13} and m_{16} are agglomerated. Moreover model m_{13} in the KL dendrogram is agglomerated with model m_{06} , but, they have a rather different distribution



ETEX-1 results



In the KL dendrogram it is associated only with model m_{14}

